TECHNICAL UNIVERSITY OF CRETE

SCHOOL OF PRODUCTION ENGINEERING AND MANAGEMENT

Laboratory of Computational Mechanics and Optimization

PhD Thesis

'Topology optimization of an object for additive manufacturing'

by

Ioannis NTINTAKIS

Supervisor:

Dr. Georgios E. Stavroulakis, Professor, TUC

Chania, 2022

Advisory Committee

Georgios E. STAVROULAKIS - Supervisor
Professor
School of Production Engineering and Management
Technical University of Crete

Aristomenis ANTONIADIS- Advisory committee
Professor
School of Production Engineering and Management
Technical University of Crete

Nikolaos BILALIS - Advisory committee
Professor, School of Production Engineering & Management
Technical University of Crete

ΕΠΤΑΜΕΛΗΣ ΕΞΕΤΑΣΤΙΚΗ ΕΠΙΤΡΟΠΗ

Τίτλος: «Τοπολογική Βελτιστοποίηση Μοντέλου για Προσθετική Κατασκευή»

Αγγλικός τίτλος: «Topology optimization of an object for additive manufacturing»

ΔΙΔΑΚΤΟΡΙΚΗ ΔΙΑΤΡΙΒΗ

κ. Ιωάννη Ντιντάκη

ΤΡΙΜΕΛΗΣ ΣΥΜΒΟΥΛΕΥΤΙΚΗ ΕΠΙΤΡΟΠΗ:

1. Γεώργιος Σταυρουλάκης   (Επιβλέπων)
2. Αριστομένης Αντωνιάδης
3. Νικόλαος Μπιλάλης

Εγκρίθηκε από την επταμελή εξεταστική επιτροπή την: 30 / 11 / 2022   (υπογραφή)

1. **Γεώργιος Σταυρουλάκης, Καθηγητής, επιβλέπων**

   Georgios Stavroulakis
   Digitally signed by Georgios Stavroulakis
   Date: 2022.11.30 12:18:00 +02'00'

2. **Αριστομένης Αντωνιάδης, Καθηγητής**

   Digitally signed by Aristomenis Antoniadis
   Date: 2022.11.30 17:42:44 +02'00'

3. **Νικόλαος Μπιλάλης, αφυπηρετήσας Καθηγητής**

   Nikolaos Bilalis
   Digitally signed by Nikolaos Bilalis
   Date: 2022.11.30 16:51:06 +02'00'

4. **Παναγιώτης Αλευράς, Επίκουρος Καθηγητής**

   PANAGIOTIS ALEVRAS
   30.11.2022 17:56

5. **Μαρία Σταυρουλάκη, Αναπλ. Καθηγήτρια**

   MARIA STAVROULAKI
   30.11.2022 18:40

6. **Εμμανουήλ Μαραβελακης, Αναπλ. Καθηγητής**

   Emmanouil Maravelakis
   Emmanouil Maravelakis
   01.12.2022 11:12

7. **Νικόλαος Ταπόγλου, Επίκουρος Καθηγητής**

   ΝΙΚΟΛΑΟΣ ΤΑΠΟΓΛΟΥ
   Digitally signed by ΝΙΚΟΛΑΟΣ ΤΑΠΟΓΛΟΥ
   Date: 2022.12.01 12:12:43 +02'00'

<u>Summary</u>

Engineers focus on the design of new added-value products, which satisfy the human needs. The product-design process follows a base line. It starts from an idea and through 2D and 3D design, models are created for creating prototypes, which are then evaluated. During this process many design parameters and other specifications have to be taken into account.

Topology optimization is a well-known design decision tool for designers/engineers. Generative design based on topology optimization and artificial-intelligent algorithms is also a helpful design tool, especially in the early design stage of conceptual design. Topology optimization and generative design outcomes are characterized by a complex-structure shape. Often these structures are difficult, or impossible to be produced with traditional fabrication techniques. Additive manufacturing, due to its ability to fabricate any complex shape, is the appropriate method to overcome this limitation. In this thesis topology optimization and generative design are utilized for the design of a consumer product and also for the redesign of mechanical components, taking into account the limitations of the selected additive manufacturing technique. The developments of additive manufacturing in recent years and its close relevance with the results of TO and GD process are very encouraging.

Auxetic materials have enhanced dynamical properties and damping behavior, and thus they can be used in certain applications. This property is usually explained from the microstructure, although other models have been used as well, such as chiral, or mechanism-based models. Auxetic materials are used in several fields, however, optimal design towards dynamical properties is still under investigation. In this study the efficiency of auxetic materials on a dynamic loading caused by bullet penetration has been compared with non-auxetic materials.

A key factor of additive manufacturing for the fabrication of light weight structures is the selected infill structures. In the current thesis by utilizing topology optimization, new infill structures are designed with the use of the SIMP topology optimization method. The selected method predicts the material distribution in a specific and predefined domain in an accurate way, but it does not check other material properties, such us structure isotropy. In the current thesis a hybrid approach has been adopted, which combines topology optimization and the classic homogenization method to evaluate the topological optimized microstructures. Using an RVE (Representative Volume Element) the results are evaluated numerically. Then, using additive manufacturing, specimens of both microstructures are fabricated and evaluated with compression and tensile strength tests. The results agree with the numerical findings that the microstructures have anisotropic behavior.

Περίληψη

Οι μηχανικοί σχεδίασης προϊόντων αποσκοπούν στη σχεδίαση νέων, καινοτόμων προϊόντων τα οποία θα ανταποκρίνονται ισάξια τόσο στις ανάγκες των χρηστών όσο και των κατασκευαστών. Η διαδικασία σχεδίασης ενός νέου προϊόντος ακολουθεί μια διαδικασία αρκετά τυποποιημένη, που ξεκινά από τη σύλληψη της ιδέας, συνεχίζεται με τη δημιουργία δισδιάστατων και τρισδιάστατων σχεδίων και ολοκληρώνεται με τη δημιουργία πρωτοτύπων, από την αξιολόγηση των οποίων θα κριθεί η απόφαση για συνέχιση στο στάδιο της παράγωγής ή για αναθεώρηση των δεδομένων της σχεδιομελέτης. Είναι σημαντικό, να ληφθούν υπόψη όλοι οι παράγοντες που θα διαμορφώσουν τις προδιαγραφές του νέου προϊόντος και να συνεκτιμηθούν. Η διαδικασία αυτή μόνο εύκολη δεν είναι και απαιτεί χρόνο και πόρους. Σε αυτή την προσπάθεια, σύγχρονα εργαλεία που ανήκουν στο φάσμα της υπολογιστικής μηχανικής όπως η τοπολογική βελτιστοποίηση και ο γενετικός σχεδιασμός μπορούν να συμβάλλουν με κρίσιμο τρόπο στη λήψη των αποφάσεων. Παράλληλα, η αξιοποίηση της προσθετικής κατασκευής μπορεί συμβάλει αποφασιστικά όχι μόνο για τη δημιουργία πρωτοτύπων για αξιολόγηση αλλά και τελικών, έτοιμων προς χρήση, προϊόντων. Στην παρούσα διατριβή μελετάται η αξιοποίηση της τοπολογικής βελτιστοποίησης και του γενετικού σχεδιασμού σε μελέτες περίπτωσης προϊόντων ή εξαρτημάτων. Συγκεκριμένα, μελετάται η σχεδίαση ενός σχεδίου τραπεζιού από το στάδιο της ανάπτυξης των αρχικών ιδεών. Στη συνέχεια, μελετάται η βέλτιστη σχεδίαση υφιστάμενων μηχανολογικών εξαρτημάτων.

Οι σημαντικές δυνατότητες που προσφέρει η προσθετική κατασκευή, για την παραγωγή δομών υψηλής πολυπλοκότητας από μεγάλο εύρος υλικών, οδηγεί στην αξιοποίηση δομών που σε αντίθετη περίπτωση δεν θα μπορούσαν να χρησιμοποιηθούν σε εύρος παραγωγής. Χαρακτηριστικό είναι το παράδειγμα των αυξητικών υλικών οι ιδιότητες των οποίων είναι ασυνήθιστες. Ορίζονται ως αυξητικά καθώς έχουν αρνητικό λόγο Poisson. Η αυξητική συμπεριφορά προκύπτει από την ειδική δομή τους και τον τρόπου με τον οποίο παραμορφώνονται όταν φορτιστούν. Σημαντικά χαρακτηριστικά των αυξητικών υλικών είναι η αντοχή σε θραύση αλλά και σε κρούση. Στην παρούσα διατριβή ερευνάται η αξιοποίηση αυξητικών υλικών σε δυναμικό πρόβλημα κρούσης από σφαίρα. Από τα αποτελέσματα προκύπτει ευνοϊκότερη συμπεριφορά σε σύγκριση με μη αυξητική δομή.

Η ικανότητα της προσθετικής κατασκευής να χρησιμοποιείται για την κατασκευή δομών στιβαρών χαμηλού βάρους οφείλεται σε σημαντικό βαθμό στη χρήση δομών πλήρωσης. Στην παρούσα διατριβή χρησιμοποιείται μια υβριδική προσέγγιση για το σχεδιασμό νέων δομών πλήρωσης. Οι δομές προκύπτουν από

την αξιοποίηση της τοπολογικής βελτιστοποίησης. Εξαιτίας όμως, της αδυναμίας ελέγχου άλλων ιδιοτήτων της προκύπτουσας δομής πέρα από την εύρεση της βέλτιστης λύσης για την κατανομή του υλικού χρησιμοποιείται συνδυαστικά και η κλασική μέθοδος της ομογενοποίησης. Σκοπός είναι να ελεγχθεί πρώτα αριθμητικά η ισοτροπία της δομής με τον υπολογισμό του λόγου zener και του μέτρου ελαστικότητας Young. Από τα αποτελέσματα της αριθμητικής μεθόδου προκύπτει η ανισοτροπία των δομών. Στη συνέχεια, χρησιμοποιείται ένα αντιπροσωπευτικό δείγμα των μικροδομών και ελέγχονται ως υλικό πλήρωσης σε μοντέλο δοκού. Έπειτα, εκτυπώνονται τρισδιάστατες πλεγματικές δομές πλήρωσης με σκοπό την αξιολόγηση τους πειραματικά με τη διενέργεια ελέγχου σε κάμψη αλλά και εφελκυσμό. Από τα αποτελέσματα προκύπτει η επαλήθευση των αποτελεσμάτων της αριθμητικής ομογενοποίησης.

Αναλυτική Περίληψη

Σε παγκόσμιο επίπεδο είναι εμφανείς η τάση των βιομηχανικά αναπτυσσόμενων και ανεπτυγμένων χωρών να υιοθετούν προηγμένες στρατηγικές που θα οδηγήσουν στον εκσυγχρονισμό των μονάδων παραγωγής και την ανάπτυξη καινοτόμων ερευνητικών εργαλείων. Οι βιομηχανίες από την πλευρά τους επιζητούν την υιοθέτηση σύγχρονων μεθόδων παραγωγής που θα επιφέρουν αύξηση κερδών, βελτίωση της ποιότητας των παραγόμενων προϊόντων και ανάπτυξη προϊόντων υψηλής προστιθέμενης αξίας. Οι καινοτόμες αντιλήψεις παραγωγής συνηγορούν στην ικανότητα της προσθετικής κατασκευής να διαδραματίσει ένα κεντρικό ρόλο στην ανάπτυξη προηγμένων συστημάτων παραγωγής νέας γενιάς. Από την άλλη πλευρά η συνεχόμενη αύξηση της υπολογιστικής ισχύς για μαθηματική μοντελοποίηση και προσομοίωση δημιουργεί τις συνθήκες ώστε η υπολογιστική επιστήμη να συμβάλλει ουσιαστικά στην επίλυση πολύπλοκων και δυσεπίλυτων παραγωγικών διαδικασιών. Προκειμένου να εκπληρωθεί η παραπάνω επιδίωξη θα πρέπει να αναπτυχθούν σύγχρονα υπολογιστικά εργαλεία που θα επιτρέψουν στους μηχανικούς/ σχεδιαστές να αναπτύξουν και να αναλύσουν αποδοτικότερα την ανάπτυξη νέων καινοτόμων προϊόντων.

Στο πρώτο κεφάλαιο παρουσιάζεται το κίνητρο και ο σκοπός που οδήγησε στην εκπόνηση της παρούσας διατριβής . Συγκεκριμένα, καθώς η προσθετική κατασκευή αποτελεί την κατεξοχήν τεχνολογία παραγωγής προϊόντων πολύπλοκης δομής και γεωμετρίας δίνεται η δυνατότητα στους σχεδιαστές να υλοποιήσουν καινοτόμες ιδέες. Η σημαντική δυνατότητα που παρέχεται για την ανάπτυξη πρότυπου σχεδιασμού θα πρέπει να υποστηριχθεί με την ανάπτυξη κατάλληλων εργαλείων τα οποία θα ανταποκρίνονται αποτελεσματικότερα στις ιδιαιτερότητες και τους περιορισμούς της προσθετικής κατασκευής και των υλικών που χρησιμοποιούνται. Οι εξελίξεις που θα πρέπει να συντελεστούν συνοψίζονται σε τρία βασικά σημεία:

- να εξελιχθούν τα εργαλεία γενετικού σχεδιασμού και τοπολογικής βελτιστοποίησης. Σκοπός είναι, να εκτελείται η σχεδιομελέτη με τις ανάγκες της προσθετικής κατασκευής. Συγκεκριμένα, θα πρέπει να ληφθούν υπόψη χαρακτηριστικά όπως η γεωμετρία του προς μελέτη προϊόντος, οι τυπικές και λειτουργικές προδιαγραφές άλλα και οι ιδιότητες των υλικών. Κατά συνέπεια, θα πρέπει να λαμβάνεται υπόψη η ροή και η διαδικασία παραγωγής, το κόστος ανά μονάδα παραγωγής αλλά και το μέγεθος της παρτίδας παραγωγής. Συνολικά θα πρέπει να εξετάζεται ο κύκλος ζωής του προϊόντος και να αξιολογούνται οι επιπτώσεις από την αξιοποίηση της προσθετικής κατασκευής

- τα συστήματα CAD να αναδιαμορφωθούν και να είναι ποιο φιλικά προς το χρήστη. Οι υφιστάμενοι περιορισμοί, σχετικά στο σχεδιασμό παραμετρικών οριακών αναπαραστάσεων και μοντέλων στερεάς μοντελοποίησης πρέπει να ξεπεραστούν. Ιδιαίτερα για τη σχεδίαση δομών υψηλής πολυπλοκότητας
- τα διαθέσιμα εργαλεία υπολογιστικής μηχανικής για την προσομοίωση και τη βελτιστοποίηση των δομών θα πρέπει να εξελιχθούν. Σκοπός είναι να είναι σε θέση να ανταποκρίνονται αποτελεσματικά στους κατασκευαστικούς περιορισμούς και τις ιδιαίτερες συνθήκες των τεχνικών της προσθετικής κατασκευής

Στο δεύτερο κεφάλαιο παρουσιάζεται η βιβλιογραφική επισκόπηση που πραγματοποιήθηκε στη θεματική περιοχή της διατριβής όπως ο γενετικός σχεδιασμός με έμφαση στην εφαρμογή λύσεων για τον αποτελεσματικό σχεδιασμό προϊόντων για την παραγωγή. Η βιβλιογραφική έρευνα εστιάζει επίσης, στην υπολογιστική μηχανική. Η υπολογιστική μηχανική αποτελεί την επιστημονική περιοχή που χρησιμοποιεί αριθμητικές μεθόδους για την επίλυση προβλημάτων της μηχανικής. Παραδοσιακά τα προβλήματα της μηχανικής λύνονταν είτε αναλυτικά είτε πειραματικά δηλαδή κάνοντας μετρήσεις σε κάποιο μοντέλο του προβλήματος που μας ενδιαφέρει. Η υπολογιστική μηχανική είναι ο τρίτος δρόμος. Η ανάπτυξη των ηλεκτρονικών υπολογιστών τις τελευταίες δεκαετίες έδωσε τη δυνατότητα να επιλύονται προβλήματα τα οποία ήταν αδύνατον να επιλυθούν στο παρελθόν, είτε λόγω του μεγάλου μεγέθους, είτε λόγω του μεγάλου απαιτούμενου υπολογιστικού χρόνου. Η υπολογιστική μηχανική μειώνει σημαντικά τον απαιτούμενο αριθμό πειραμάτων. Αυτό το χαρακτηριστικό αποτελεί ιδιαίτερο πλεονέκτημα καθώς μειώνεται ο χρόνος ανάπτυξης του προϊόντος. Επιπλέον, οδηγεί σε μείωση του κόστους ανάπτυξης του προϊόντος, προσφέροντας παράλληλα τη δυνατότητα συντομότερης εισόδου του προϊόντος στην αγορά. Επιπροσθέτως, η δυνατότητα υπολογισμού μεγάλου όγκου δεδομένων, δίνει τη δυνατότητα στον μελετητή να εξετάσει τη συμπεριφορά διάφορων υλικών. Είναι εφικτός ο ορισμός περισσότερων περιορισμών, μειώνοντας έτσι τη πιθανότητα αστοχίας ή μη ορθής λειτουργίας.

Η δομική βελτιστοποίηση αναφέρεται στη βιβλιογραφία από τις αρχές του 20ου αιώνα. Συγκεκριμένα, το 1904 όταν ο Michell διατύπωσε την αναλυτική λύση για την ελαχιστοποίηση δεδομένων περιορισμών κατά τη διαδικασία του σχεδιασμού κατασκευών. Εκ τότε οι 'δομές Michell', όπως καθιερώθηκαν, αξιοποιούνται για το σχεδιασμό δομών που διακρίνονταν για την ελάχιστη ενδοτικότητα τους. Ενώ, το 1988 διεξήχθη η πρώτη εφαρμογή βελτιστοποίησης με τη λογική της ύπαρξης ή μη υλικού σε μια δεδομένη περιοχή σχεδίασης. Το 1989 δημιουργείται η μέθοδος βελτιστοποίησης που σήμερα είναι γνωστή ως SIMP (Solid Isotropic Material with Penalization) που σημαίνει ποινικοποίηση των

ενδιάμεσων τιμών ώστε, η δομή να αναπαρασταθεί σε σχέδιο όπου θα υπάρχει ή όχι υλικό. Ο ορισμός του προβλήματος της βελτιστοποίησης, αποτελεί ένα συνδυασμό πολλών παραμέτρων, που αφορούν την μελέτη του δομικού σχεδιασμού μιας κατασκευής ή ενός αντικειμένου. Σκοπός είναι, να ευρεθεί η βέλτιστη λύση δομικού σχεδιασμού εντός ενός προκαθορισμένου χώρου. Για την επίλυση του προβλήματος, δεδομένα αποτελούν, ο όγκος του μοντέλου, οι συνθήκες φόρτισης, οι δομές στήριξης-πάκτωσης του μοντέλου. Επιπλέον, πρόσθετοι περιορισμοί που αφορούν το μέγεθος και η θέση οπών-ανοιγμάτων, ή την ύπαρξη υλικού. Το αποτέλεσμα της βελτιστοποίησης ως προς το μέγεθος, το σχήμα και δομή που θα αποκτήσει το μοντέλο παραμένει άγνωστο.

Για την επίλυση ενός κλασικού προβλήματος δομικής βελτιστοποίησης θα πρέπει να εξεταστεί μια πληθώρα συνδυασμών από περιορισμούς ώστε να επιτευχθεί ο επιθυμητός σκοπός. Αποσκοπώντας στην ικανοποίηση των περιορισμών, η δομική βελτιστοποίηση διαχωρίζεται σε τρεις κατηγορίες. Με κριτήριο την πολυπλοκότητα επίλυσης οι τρεις κατηγορίες ταξινομούνται ως ακολούθως:

- βελτιστοποίηση μεγέθους (size optimization). Η βελτιστοποίηση μεγέθους αποτελεί την απλούστερη μορφή της δομικής βελτιστοποίησης. Το σχήμα της δομής, είναι γνωστό και στόχο αποτελεί να βελτιστοποιηθεί η κατασκευή προσαρμόζοντας τις διαστάσεις των επιμέρους στοιχείων. Το πάχος της κατασκευής παραμένει σταθερό, όπως και η τοπολογία του μοντέλου. Έτσι, βελτιώνεται η μηχανική συμπεριφορά του μοντέλου, όπως προκύπτει έπειτα από την ανάλυση τάσεων που ακολουθεί

- βελτιστοποίηση σχήματος (shape optimization). Στη βελτιστοποίηση σχήματος, στόχο αποτελεί ο καθορισμός του βέλτιστου σχήματος σε μία προκαθορισμένη περιοχή. Σε αυτή την περίπτωση οι μεταβλητές του σχεδιασμού μπορεί να είναι το πάχος του υλικού, η διάμετρος των οπών, η τιμή των ακτινών σε στρογγυλεύσεις ακμών και γενικότερα στοιχεία της κατασκευής που είναι μετρήσιμα

- βελτιστοποίηση τοπολογίας (topology optimization). Η βελτιστοποίηση της τοπολογίας αποτελεί ένα ιδιαίτερα ισχυρό εργαλείο στο χώρο του σχεδιασμού προϊόντων, στον υπολογισμό μηχανισμών και αλλού

Επιπλέον, στο δεύτερο κεφάλαιο γίνεται αναφορά στη διαδικασία σχεδίασης ενός νέου προϊόντος με την αξιοποίηση σύγχρονων εργαλείων. Κύριο σημείο αναφοράς αποτελεί η τοπολογική βελτιστοποίηση εκφραζόμενη από τις βασικές τεχνικές εφαρμογής. Η τοπολογική βελτιστοποίηση, ορίζεται ως μια μαθηματική διαδικασία η οποία βελτιστοποιεί την κατανομή του υλικού μέσα σε ένα προκαθορισμένο χώρο ώστε να ικανοποιούνται οι οριακές συνθήκες και οι σχεδιαστικοί περιορισμοί. Χρησιμοποιώντας τη βελτιστοποίηση τοπολογίας, οι

σχεδιαστές - μηχανικοί είναι σε θέση να προσδιορίσουν το βέλτιστο σχέδιο που να ικανοποιεί τις απαιτήσεις της μελέτης. Η κεντρική ιδέα στη βελτιστοποίηση μίας δομής, είναι η χρήση μικρότερης ποσότητας υλικού, από ότι προηγουμένως, διατηρώντας παράλληλα την ίδια, ή ακόμα και καλύτερη μηχανική συμπεριφορά, στις οριζόμενες οριακές συνθήκες. Σε αντίθεση με τη βελτιστοποίηση μεγέθους και σχήματος, δεν είναι γνωστό το σχήμα ή ο αριθμός των οπών, καθώς και των υπολοίπων γεωμετρικών χαρακτηριστικών. Για ένα δεδομένο σχεδιαστικό χωρίο, το ζητούμενο είναι να υπολογιστεί η βέλτιστη κατανομή του υλικού, ώστε να καθοριστεί η ύπαρξη υλικού ή η δημιουργία κενού. Για την επίλυση του προβλήματος, θα πρέπει να χρησιμοποιηθεί η μέθοδος των πεπερασμένων στοιχείων, ώστε, η σχεδιαστική περιοχή να κατατμηθεί σε πολύ μικρές διακριτές περιοχές πλέγματος (mesh). Ουσιαστικά, πρόκειται για την επίλυση προβλήματος 0-1 υποδηλώνοντας την ύπαρξη ή όχι στοιχείων στη δεδομένη περιοχή του πλέγματος.

Συχνά, η προκύπτουσα δομή έπειτα από την τοπολογική βελτιστοποίηση, είναι εξαιρετικά δύσκολο ή οικονομικά ασύμφορο να παραχθεί με τη χρήση παραδοσιακών μεθόδων παραγωγής, όπως είναι οι αφαιρετικές. Σε αυτές και, όχι μόνο τις περιπτώσεις, κρίνεται χρήσιμη και αποτελεσματική η χρήση τεχνολογιών προσθετικής κατασκευής, όπου ουσιαστικά είναι εφικτή η δημιουργία οποιασδήποτε δομής ανεξαρτήτου βαθμού πολυπλοκότητας. Άλλωστε, οι οικονομικές αναλύσεις καταδεικνύουν με τον πλέον σαφή τρόπο το οικονομικό όφελος που προκύπτει από τη χρήση τεχνολογιών προσθετικής κατασκευής. Ιδιαίτερα, για την παραγωγή αντικειμένων πολύπλοκης δομής σε μικρές έως μεσαίες παρτίδες παραγωγής. Λαμβάνοντας υπόψη τη διαρκή και ολοένα αυξανόμενη ανάγκη για τη δημιουργία δομών μικρού βάρους, η τοπολογική βελτιστοποίηση προσφέρεται ως το ιδανικό μέσο για τη μελέτη και τον προσδιορισμό της ποσότητας του υλικού που θα απαιτηθεί. Συμπερασματικά, οδηγεί σε πολύ σημαντικά οφέλη στο σχεδιασμό προϊόντων όπως τα ακόλουθα:

- δημιουργία δομών χαμηλού βάρους
- δημιουργία έτοιμών δομών για συναρμολόγηση ή έτοιμα προϊόντα
- ελαχιστοποιεί την ποσότητα των πρώτων υλών
- συμβάλει σημαντικά στην εξοικονόμηση ενέργειας
- ελαχιστοποιεί την ανάγκη παραγωγής φυσικών πρωτοτύπων
- μειώνει σημαντικά την ανάγκη διενέργειας πειραμάτων
- μειώνει σημαντικά το χρόνο εισαγωγής νέων προϊόντων στην αγορά

Η λειτουργία του αλγορίθμου τοπολογικής βελτιστοποίησης λειτουργεί με σκοπό τη μεταβολή της πυκνότητας των στοιχείων στην περιοχή σχεδίασης. Σκοπός είναι να ευρεθεί ο κατάλληλος συνδυασμός των τιμών που θα ικανοποιούν με βέλτιστο τρόπο τους περιορισμούς που έχουν οριστεί. Στο πρώτο στάδιο της βελτιστοποίησης, διατυπώνονται οι αρχικές ιδέες για την πιθανή γεωμετρία του αντικειμένου. Για τον ορισμό των προδιαγραφών εξετάζονται διάφορα υλικά και μέθοδοι κατασκευής. Μελετώνται οι εσωτερικοί και οι εξωτερικοί περιορισμοί καθώς και οι απρόβλεπτοι παράγοντες. Με βάση τα δεδομένα που προκύπτουν από τα αποτελέσματα του πρώτου σταδίου, προκύπτει η αρχική γεωμετρία του μοντέλου, προσδιορίζεται ο στόχος της βελτιστοποίησης, ορίζονται οι περιορισμοί και οι παράμετροι σχεδίασης. Στο τρίτο στάδιο, ελέγχεται από τον αλγόριθμο το πλήθος των δεδομένων, με οδηγό την ικανοποίηση της αντικειμενικής συνάρτησης. Αν ικανοποιούνται οι σχεδιαστικοί περιορισμοί η διαδικασία τερματίζεται και εξάγονται τα αποτελέσματα. Αν όχι, η διαδικασία επαναλαμβάνεται, προχωρώντας σε τροποποιήσεις των παραμέτρων της σχεδίασης και το στάδιο της βελτιστοποίησης εκτελείται ξανά. Οι βασικότερες μέθοδοι βελτιστοποίησης διακρίνονται σε τρεις κατηγορίες:

- μαθηματικές τεχνικές, οι οποίες χρησιμοποιούνται για την εύρεση του ελαχίστου συναρτήσεων αρκετών μεταβλητών με περιορισμούς
- στοχαστικές μέθοδοι, οι οποίες χρησιμοποιούνται για την ανάλυση προβλημάτων τυχαίων μεταβλητών με καθορισμένη κατανομή
- στατιστικές μέθοδοι, χρησιμοποιούνται για τη δημιουργία εμπειρικών μοντέλων από πειραματικά στοιχεία

Οι μέθοδοι τοπολογικής βελτιστοποίησης αποτελούν τη βασική αρχή για τον προσδιορισμό του ιδεατού σχήματος και τοπολογίας σε μια κατασκευή. Η αρχιτεκτονική που ακολουθείτε σε κάθε μία από τις μεθόδους τοπολογικής βελτιστοποίησης οριοθετεί και τη μεθοδολογία σχεδίασης της κατασκευής. Οι τεχνικές βελτιστοποίησης, αναζητούν εκείνες τις τιμές των μεταβλητών που ελαχιστοποιούν την αντικειμενική συνάρτηση κάτω από ένα σύνολο περιορισμών με τη μορφή ανισοτήτων. Οι λεγόμενες συνθήκες Kuhn – Tucker (K-T), αποτελούν τις αναγκαίες πρώτης τάξης συνθήκες για τον υπολογισμό του ακρότατου σημείου σε προβλήματα ελαχιστοποίησης με περιορισμούς ανισοτήτων και ισοτήτων. Οι συνθήκες Kuhn–Tucker, είναι κατάλληλες για ελαχιστοποίηση αν η αντικειμενική συνάρτηση είναι κυρτή και το σύνολο των περιορισμών κυρτό.

Στην βιβλιογραφική επισκόπηση εμπεριέχεται και η μελέτη των αυξητικών υλικών. Τα αυξητικά υλικά έχουν ως βασικό χαρακτηριστικό τον αρνητικό λόγο Poisson ($v<0$) και αποτελούν μια ξεχωριστή κατηγορία υλικών με ιδιαίτερες και ασυνήθιστες ιδιότητες. Η ασυνήθιστη συμπεριφορά, αποτυπώνεται στη ιδιότητα τους όταν επιμηκύνονται προς μία κατεύθυνση να

διογκώνεται το υλικό στην κάθετη κατεύθυνση, αντί να λεπταίνει όπως κάνουν τα γνωστά υλικά. Και όταν συμπιέζεται στη μία διάσταση, να συρρικνώνεται στην άλλη αντί να διαστέλλεται. Το όνομα τους προέρχεται από την ελληνική λέξη 'αυξητικός' που σημαίνει 'αυτό που τείνει να αυξάνεται' . Τα αυξητικά υλικά δεν οφείλουν τις μοναδικές ιδιότητες τους στη σύσταση τους αλλά στη μορφή της δομής τους και ανήκουν στη ομάδα των μεταϋλικών. Ως μετα-υλικά χαρακτηρίζονται τα υλικά εκείνα των οποίων οι ιδιότητες τους δε συναντώνται σε φυσικά υλικά. Το όνομα τους προέρχεται από την ελληνική λέξη 'μετα' που σημαίνει 'πέρα από᾽ και τη λατινική λέξη 'materia' που σημαίνει υλικό. Τα πεδία χρήσης των αυξητικών υλικών ποικίλουν και σημειώνουν μια διαρκή αύξηση.

Το τρίτο κεφάλαιο εστιάζει στην προσθετική κατασκευή. Με την αξιοποίηση της προσθετικής κατασκευής, οι μηχανικοί και οι σχεδιαστές προϊόντων έχουν τη δυνατότητα παραγωγής φυσικών πρωτοτύπων. Η αξιοποίηση της τοπολογική βελτιστοποίηση στη σχεδιομελέτη του προϊόντος αποτελεί ένα πρόσθετο εργαλείο για το σχεδιαστή. Ιδιαιτέρως σημαντική είναι η συμβολή της προσθετικής κατασκευής, στην παραγωγή δομών χαμηλού βάρους και υψηλής πολυπλοκότητα όπως είναι οι πλεγματικές δομές. Συχνά, παρόμοιες δομές είναι εμπνευσμένες από τη φύση, και απώτερος σκοπός από τη χρήση τους αποτελεί η βέλτιστη κατανομή του υλικού σε δεδομένο χωρίο με σκοπό την επίτευξη μέγιστης αντοχής με παράλληλη μείωση του υλικού. Τα πλέον κατάλληλα εργαλεία για το σχεδιασμό πλεγματικών δομών αποτελούν η τοπολογική βελτιστοποίηση και ο γενετικός σχεδιασμός.

Η μετεξέλιξη της τεχνολογίας της πρωτοτυποποίησης σε τεχνολογία προσθετικής κατασκευής αναπόφευκτα επηρεάζει το σχεδιασμό των βιομηχανικών προϊόντων. Η προσθετική κατασκευή είναι ικανή να προσφέρει λύσεις σε ένα πλήθος σχεδιαστικών προβλημάτων που αφορούν ένα σημαντικό φάσμα της βιομηχανικής παραγωγής. Οι κατασκευαστές αποσκοπούν στο να δημιουργήσουν στιβαρές δομές χαμηλού βάρους, οι οποίες θα αντέχουν κατά τη χρήση τους χωρίς να αστοχούν. Τα πλεονεκτήματα που προσφέρει η προσθετική κατασκευή, δεν περιορίζονται μόνο στις ανάγκες των κατασκευαστών αλλά σε οποιονδήποτε διαθέτει πρόσβαση σε τρισδιάστατο εκτυπωτή. Όμως, η απουσία γνώσεων υπολογιστικής μηχανικής συχνά αποτελεί αιτία αστοχιών κατά την εκτύπωση, ή σε σπατάλη περίσσιου υλικού εκτύπωσης λόγω υπερ ή υπό-διαστασιολόγησης της δομής.

Η δομή του εκτυπωμένου μοντέλου διαθέτει δύο ειδών υποστηρικτικά, τα εσωτερικά και τα εξωτερικά υποστηρικτικά. Τα εσωτερικά υποστηρικτικά είναι μόνιμα και συμβάλλουν όχι μόνο στη συνοχή της δομής του μοντέλου κατά την εκτύπωση αλλά ενισχύουν και την αντοχή του φυσικού μοντέλου. Αντιθέτως, τα εξωτερικά υποστηρικτικά είναι προσωρινά, συμβάλλουν στην αυτό-υποστήριξη του μοντέλου κατά την εκτύπωση και στη συνέχεια αφαιρούνται. Η προσθήκη υποστηρικτικών οδηγεί αναπόφευκτα σε αύξηση του κόστος παραγωγής.

Αναμφισβήτητα το κόστος των υποστηρικτών θα πρέπει να ληφθεί σοβαρά υπόψη κατά το σχεδιασμό της εσωτερικής, αλλά, και της εξωτερικής δομής του μοντέλου. Ο απλούστερος τύπος πλήρωσης μιας εσωτερικής κοιλότητας είναι η χρήση 2Δ δομών στήριξης. Όμως, οι εκτυπώσιμες δομές χαρακτηρίζονται από μειωμένη μηχανική αντοχή. Οι 3Δ δομές πλήρωσης επαναλαμβάνονται προς όλες τις διευθύνσεις και αποτελούν μια σημαντική κατηγορία δομών με ισοτροπική συμπεριφορά. Συνήθως, οι συγκεκριμένες δομές είναι γνωστές ως κυβικές, εξαιτίας του χαρακτηριστικού γνωρίσματος της όμοιας συμμετρίας προς τις τρείς διευθύνσεις. Σε αντίθεση με τις δισδιάστατες, οι τρισδιάστατες δομές χαρακτηρίζονται από γεωμετρία υψηλής πολυπλοκότητας γεγονός που δυσχεραίνει την εκτύπωση τους. Η τρίτη κατηγορία δομών πλήρωσης δε χαρακτηρίζεται ούτε από 2Δ σχήματα ούτε από 3Δ γεωμετρία. Ουσιαστικά πρόκειται για βελτιστοποιημένες δομές, με χαρακτηριστικό γνώρισμα το μη περιοδικό σχήμα. Εσωτερικά, μπορεί να υπάρχουν κενά με βαθμωτή πλήρωση ή εσωτερικές δομές με επαναλαμβανόμενες βελτιστοποιημένες δομές πλέγματος. Συχνά, παρουσιάζουν διαφορετικές χωρικές ιδιότητες ή ιδιαίτερες ελαστικές ιδιότητες και μεταβαλλόμενο λόγο Poisson. Οι εξωτερικές μη-μόνιμες υποστηρικτικές δομές θα πρέπει μετά την εκτύπωση να αφαιρεθούν. Ο τρόπος απομάκρυνσης τους ποικίλει ανάλογα με το υλικό που έχουν δημιουργηθεί. Η βελτιστοποιημένη χρήση των υποστηρικτικών είναι σημαντική ώστε να μειωθεί η χρήση υλικού, που θα απαιτηθεί, για τη δημιουργία τους και παράλληλα να μειωθεί ο χρόνος που απαιτείται για την απομάκρυνση τους.

Η ικανότητα παραγωγής πλεγματικών δομών χαμηλού βάρους αποτελεί ένα βασικό χαρακτηριστικό της προθετικής κατασκευής και οφείλετε στην ικανότητα δημιουργίας δομών οι οποίες εσωτερικά είτε είναι κενές, είτε χαρακτηρίζονται από πλεγματικές δομές, ενώ το εξωτερικό τμήμα περιβάλλεται από ένα συμπαγές κέλυφος. Συνεπώς, ο τύπος πλήρωσης της εσωτερικής κοιλότητας (infill), που συνήθως χαρακτηρίζεται από μια επαναληπτική γεωμετρία, αποτελεί μια κρίσιμη παράμετρος από την οποία καθορίζεται σε σημαντικό βαθμό ο χρόνος και το κόστος της εκτύπωσης αλλά και η στιβαρότητα της εκτυπωμένης δομής.

Από την αλληλεπίδραση του βιομηχανικού σχεδιασμού με την προσθετική κατασκευή κατά τη διαδικασία σχεδίασης / ανάπτυξης ενός νέου προϊόντος προκύπτουν μια σειρά από οφέλη. Σκοπός είναι, από τη σχεδιαστική λειτουργικότητα να οδηγηθούμε στην παραγωγή του προϊόντος. Τα οφέλη αυτά ενισχύονται σημαντικά από την υιοθέτηση της τοπολογικής βελτιστοποίησης κατά τη σχεδιομελέτη του προϊόντος. Τα σπουδαιότερα οφέλη είναι τα εξής:

- σχεδιαστική ελευθερία, η προκύπτουσα μορφή του αντικειμένου δεν περιορίζεται από τη φαντασία του σχεδιαστή. Παράλληλα, βασικό χαρακτηριστικό της προσθετικής κατασκευής αποτελεί η δυνατότητα παραγωγής οποιασδήποτε μορφής σχεδόν χωρίς κανένα περιορισμό
- μειούμενος χρόνος ανάπτυξης και εξέλιξης νέων ιδεών, η τοπολογική βελτιστοποίηση παράγει αποτελέσματα σχεδόν αυτοματοποιημένα και ιδιαίτερα γρήγορα. Αντίστοιχα και η προσθετική κατασκευή διακρίνεται για το χαμηλό χρόνο παραγωγής εξαιτίας της έλλειψης εργαλείων, καλουπιών ενώ ανταποκρίνεται ιδιαίτερα καλά στην κατά παραγγελία παραγωγή
- προσαρμοστικότητα στην παραγωγή, η τοπολογική βελτιστοποίηση συμβάλει σημαντικά στην προσαρμογή του σχεδίου σε συγκεκριμένες απαιτήσεις. Ενώ, με την προσθετική κατασκευή είναι εφικτή η παραγωγή αντικειμένων διαφορετικής μορφής στην ίδια φάση παραγωγής

Στο τέταρτο κεφάλαιο μελετάται η συμπεριφορά αυξητικής δομής, σχήματος αστεριού, σε πρόβλημα κρούσης. Η ιδιαίτερη και ασυνήθιστη μηχανική των αυξητικών υλικών συμβάλει έτσι ώστε να χρησιμοποιούνται με πολύ θετικά αποτελέσματα σε πλήθος εφαρμογών. Στην παρούσα διατριβή μελετάται η χρήση των αυξητικών υλικών σε πλάκες θωράκισης. Σκοπός της μελέτης είναι η συγκριτική αξιολόγηση της συμπεριφοράς πλακών θωράκισης με τη χρήση αυξητικών και μη αυξητικών υλικών. Στην πλάκα από αυξητικό υλικό χρησιμοποιείται κλασική αυξητική δομή αστεριού ενώ η μη αυξητική δομή αποτελείται από κυψελοειδές σχήμα. Το υλικό των πλακών είναι το αλουμίνιο 5052-Η34. Από τα αποτελέσματα των δοκιμών με τη χρήση FE Analysis προκύπτει ότι η αυξητική δομή ανταποκρίνεται αποτελεσματικότερα στη μελέτη διάτρησης σε σχέση με την κλασική δομή. Συγκεκριμένα, η αυξητική δομή παρουσιάζει μικρότερη συνολική μετατόπιση όπως και επιβαλλόμενη τάση.

Στο πέμπτο κεφάλαιο παρουσιάζεται αναλυτικά η εκτέλεση μελέτης γενετικού σχεδιασμού, που αφορά, το σχεδιασμό ενός νέου προϊόντος (τραπεζιού), από το στάδιο της αρχικής ιδέας έως τον τελικό σχεδιασμό. Για την εκπόνηση της μελέτης, χρησιμοποιήθηκαν τα εργαστηριακά αποτελέσματα που προέκυψαν από πειράματα σε θλίψη εκτυπωμένων πρωτοτύπων. Αρχικά, εκτελέστηκε μελέτη τοπολογικής βελτιστοποίησης με σκοπό τον ανασχεδιασμό της βασικής άνω επιφάνειας του μοντέλου. Η αξιολόγηση των αποτελεσμάτων οδήγησε στην εκπόνηση νέας μελέτης γενετικού σχεδιασμού, που αυτή τη φορά, περιλαμβάνει όλο το μοντέλο. Οι οριακές συνθήκες και οι σχεδιαστικοί περιορισμοί διατηρήθηκαν ίδιοι. Οι πιθανές σχεδιαστικές λύσεις που προέκυψαν αξιολογήθηκαν. Τα προβλήματα που εντοπίστηκαν αντιμετωπίστηκαν με την επιβολή πρόσθετων σχεδιαστικών περιορισμών, με σκοπό, να ικανοποιηθούν οι προδιαγραφές του προϊόντος αποτελεσματικότερα. Οι νέες προτεινόμενες

σχεδιαστικές λύσεις αξιολογήθηκαν με τη χρήση της μεθόδου των πεπερασμένων στοιχείων. Από τα αποτελέσματα των αναλύσεων, προέκυψαν οι περιοχές του μοντέλου που έπρεπε να ανασχεδιαστούν ώστε να βελτιωθεί η μηχανική του συμπεριφορά. Το αναθεωρημένο μοντέλο μελετήθηκε ξανά, με τη χρήση των πεπερασμένων στοιχείων και προέκυψε η τελική βελτιστοποιημένη δομή .

Στο κεφάλαιο 6 μελετήθηκε ο ανασχεδιασμός υφιστάμενων μηχανολογικών εξαρτημάτων με τη χρήση του γενετικού σχεδιασμού. Σκοπός του ανασχεδιασμού ήταν η μείωση της μάζας των εξαρτημάτων με ταυτόχρονη ικανοποίηση των περιορισμών της επιλεγμένων τεχνικών της προσθετικής κατασκευής. Επιλέχθηκε ο ανασχεδιασμός των βάσεων έδρασης πνευματικού κυλίνδρου βιομηχανικής χρήσης με διάμετρο 32 χιλιοστά. Με τη χρήση του γενετικού σχεδιασμού μελετήθηκαν τρείς από τις ποιο κοινές βάσεις έδρασης, η Pivot bracket with rigid bearing AB7, η βάση Clevis bracket MP2 και η βάση Clevis bracket MP4. Το υλικό κατασκευής των στηριγμάτων είναι από αλουμίνιο. Για κάθε εξάρτημα προέκυψε ένα πλήθος σχεδιαστικών λύσεων οι οποίες αξιολογήθηκαν. Οι τεχνικές προσθετικής κατασκευής που λήφθηκαν υπόψη ήταν η Fused Filament Fabrication (FFF) και η Wire Laser Metal Deposition (W-LMD). Για κάθε τεχνική λήφθηκε υπόψη διαφορετικός υπολογισμός της γωνίας κρέμασης. Για την τεχνική FFF μελετήθηκαν σχεδιαστικές λύσεις με μέγιστη γωνία κρέμασης τις 45°. Για τη τεχνική W-LMD τα αποτελέσματα μελετήθηκαν με μέγιστη γωνία κρέμασης τις 20°. Από τα αποτελέσματα προέκυψε ότι, είναι εφικτή η μείωση της μάζας περίπου κατά 60% χωρίς να επηρεάζεται σημαντικά ο συντελεστής ασφαλείας. Στις βελτιστοποιημένες δομές, η τάση Von Misses δεν αυξήθηκε πάνω από 15% ενώ η αύξηση της συνολικής μετατόπισης δε ξεπέρασε το 20%.

Στο έβδομο κεφάλαιο παρουσιάζεται αναλυτικά ο σχεδιασμός νέων πλεγματικών μικροδομών με σκοπό την αξιοποίηση τους ως εσωτερικές δομές πλήρωσης σε τεχνικές προσθετικής κατασκευής. Οι μικροδομές προέκυψαν με τη χρήση της τοπολογικής βελτιστοποίησης και συγκεκριμένα με την αξιοποίηση της μεθόδου Solid Isotropic Material with Penalization (SIMP). Η εκτέλεσης της μελέτης εκκινείτε με τη χρήση ενός στερεού μοντέλου σε σχήμα κύβου με διαστάσεις 15x15x15χιλ. Για τη εκτέλεση της μελέτης τοπολογικής βελτιστοποίησης χρησιμοποιήθηκε το 'topology optimization' block στο σύστημα υπολογιστικής μηχανικής nTopology. Συνολικά εκτελέστηκαν δύο μελέτες τοπολογικής βελτιστοποίησης και προέκυψαν ισάριθμες δομές. Οι οριακές συνθήκες (boundary conditions) που εφαρμόστηκαν και στις δύο δομές είναι όμοιες. Συγκεκριμένα, στη βάση του κύβου εφαρμόστηκε περιορισμός συγκράτησης με αποκλεισμό όλων των βαθμών ελευθερίας. Κατά τη διαδικασία

της διακριτοποίησης δημιουργήθηκε ένα στερεό μοντέλο που αποτελούνταν από 25.781 τετράεδρα στοιχεία με μήκος ακμής 1 χιλ. Η αντικειμενική συνάρτηση έχει οριστεί έτσι ώστε να ζητείται η ελαχιστοποίηση της μάζας του υλικού εντός του προκαθορισμένου σχεδιαστικού χωρίου. Καθοριστικό ρόλο στη διαμόρφωση του βελτιστοποιημένου μοντέλου, κατέχει η ικανοποίηση του περιορισμού του κλασματικού όγκου. Η τιμή του περιορισμού μπορεί να κυμανθεί από 0 έως 1, ενώ ο βελτιστοποιημένος όγκος ικανοποιεί τον περιορισμό όταν αποκτήσει ίση ή μικρότερη τιμή. Η δημιουργία διαφορετικών δομών προκύπτει από τη διαφορετικό τρόπο επιβολής των φορτίσεων οι οποίες και στις δύο περιπτώσεις είναι 300Ν. Έπειτα από την αξιολόγηση των αποτελεσμάτων της τοπολογικής βελτιστοποίησης ακολουθεί το στάδιο της δημιουργίας του μοναδιαίου κυττάρου για κάθε μικροδομή.

Η τοπολογική βελτιστοποίηση λύνει το βασικό πρόβλημα εύρεσης της καλύτερης κατανομής του υλικού σε ένα προκαθορισμένο σχεδιαστικό χωρίο. Όμως, δεν εξετάζονται άλλες ιδιότητες της βελτιστοποιημένης δομής όπως η ισοτροπία. Λαμβάνοντας ένα αντιπροσωπευτικό δείγμα της μικροδομής, εκτελέστηκε η διαδικασία της ομογενοποίησης με σκοπό, να εξεταστεί η ισοτροπία των δομών. Με τη αξιοποίηση του 'homogenization unit cell' block του συστήματος nTopology προέκυψαν οι ομεγοποιημένες δομές, οι οποίες μπορούν πλέον να αξιοποιηθούν ως υλικά. Η αξιολόγηση των υλικών πραγματοποιήθηκε με τη μέθοδο των πεπερασμένων στοιχείων ως υλικό πλήρωσης σε φορέα δοκού. Επιπλέον, υπολογίστηκε η σχετική πυκνότητα των νέων υλικών για διαφορετικές τιμές κλασματικού όγκου αλλά και οι αντίστοιχες τιμές του λόγου Zener. Από τη διαδικασία της ομογενοποίησης προέκυψε η ανισοτροπική συμπεριφορά των μικροδομών. Για την αξιολόγηση των νέων υλικών πλήρωσης εκτελέστηκαν δοκιμές με τη χρήση της μεθόδου των πεπερασμένων στοιχείων σε φορέα δοκού. Από τα αποτελέσματα των δοκιμών προέκυψε η αυξημένη ελαστικότητα αλλά και αισθητά χαμηλότερες τάσεις στο φορέα με τη χρήση των πλεγματικών μικροδομών σε σχέση με τη χρήση συμπαγούς υλικού.

Στο τελευταίο μέρος του εβδόμου κεφαλαίου παρουσιάζεται η πειραματική αξιολόγηση των νέων μικροδομών με τη κατασκευή δειγμάτων με τις νέες πλεγματικές δομές σε τρισδιάστατο εκτυπωτή. Με τη χρήση εκτυπωτή που υποστηρίζει την τεχνική εκτύπωσης FFF παράχθηκαν δείγματα για δοκιμές σε θλίψη και σε εφελκυσμό. Από τα αποτελέσματα επαληθεύτηκε η ανισότροπη συμπεριφορά των μικροδομών. Επιπλέον, από την πειραματική μελέτη προέκυψε στιβαρή μηχανική συμπεριφορά της μικροδομής#1 που ενδείκνυται ως υλικό πλήρωσης σε απαιτητικές και υψηλών τάσεων εφαρμογές. Ενώ, η μικροδομή#2 εμφάνισε μικρότερη μηχανική αντοχή άλλα με πολύ μικρότερη σχετική πυκνότητα σε σχέση με την πρώτη μικροδομή και συστήνεται ως υλικό πλήρωσης σε εφαρμογές με χαμηλότερες απαιτήσεις σε φορτίσεις.

Στο κεφάλαιο οκτώ παρουσιάζονται τα συμπεράσματα της διατριβής, η συμβολή της παρούσας έρευνας καθώς και προτεινόμενες μελλοντικές κατευθύνσεις επέκτασης της έρευνας. Στο τέλος του κειμένου παρατίθεται η βιβλιογραφία που αξιοποιήθηκε για την εκπόνηση της παρούσας διατριβής.

<u>Acknowledgements</u>

First and foremost, I am extremely grateful to my supervisor Prof. Georgios Stavroulakis. His guidance helped me in all stages of the research and writing of this thesis. I could not imagine a better supervisor and mentor. Besides my advisor, I would like to thank the rest of my advisory thesis committee: Prof. Aristomenis Antoniadis and Prof. Nikolaos Bilalis. I would like to express my thanks to Prof. Kavoulakis Georgios for his help and support. Also, I would like to thank my parents for their continuing support all these years. Last but not least, I would like to thank my wife, Nikoletta and my kids Tilemachos and Dominikos for their patience, understanding and support.

Table of Contents

LIST of FIGURES

Contents   xvii

Contents _____ xvii

LIST of TABLES

CHAPTER **1**

INTRODUCTION

1.1 Motivation

During the last decades there is a clear tendency to adopt advanced strategies that will lead to the modernization of production units and develop innovative research tools. Industries seek to utilize modern production methods that will increase their profit, improve their product quality, and develop new high-added-value products. Based on the recent advantages, Additive Manufacturing (AM) can play a keystone role in this issue. The increased advances in computational power helps engineers to solve complex production problems. The modern computational tools allow engineers/designers to utilize the advances of Additive Manufacturing in manufacturing processing.

Additive manufacturing is the leading production technology for the fabrication of high-complexity structures. This advance enables designers to implement innovative ideas during the product design process. This ability should be supported by the appropriate computational and design tools, which will respond more effectively to the features of the additive manufacturing techniques and materials used. The developments that should be carried out are summarized below:

- Topology optimization and Generative Design systems to be improved based on the specific product specifications
- Utilizing Application Programming Interface (API) in order for engineers/ designers to control better the influence of each design constraint to the potential design solutions
- Overcome the limitations of commercial Computer Aided Design (CAD) systems in order to design structures with high complexity more easily

- Utilizing topology optimization to create improved 3d infill structures for additive manufacturing
- The computational mechanics tools have to be improved in order to meet the limitations and special requirements of each additive manufacturing technique

Solving an optimization problem is a complicated study. There are many individual design parameters which must be taken into account. The potential design solution cannot be predicted easily. To take a decision how a material amount shall be distributed within a volume is not easy. The boundary conditions, the shape and size of voids areas, the solid, or semi-solid areas, the support structures and the infill structure are the design constraints. A general flow chart of optimization problem is presented in figure 1.1. The mathematical expression of the optimization problem is defined as the minimization of the objective function, which is subject to a set of constraints and is expressed as follows (Rao, 1996):

$$\text{Finding of x=} \begin{Bmatrix} \chi_1 \\ \chi_2 \\ \cdot \\ \cdot \\ x_n \end{Bmatrix} \text{which minimize } f(x) \qquad (1.1)$$

$$\text{Where } g_i(x) \leq 0, i=1,2,....,m \text{ and,}$$

$$h_j(x) = 0, j=1,2,...,n$$

f(x) is defined as the objective function, or cost function, essentially is a criterion for comparing acceptable solutions, in order to select the optimal design. An objective goal is to minimize f(x).

The functions $g_i(x)$ and $h_j(x)$ express equalities and inequalities respectively that determine the problem parameters. Points on the constraint surface with a value $g_i(x)=0$ meet the constraint limits. The design domain is divided into two complementary parts. The first part refers to permissible points, thus $g_i(x)< 0$. The second part refers to unacceptable points and implies $g_i(x)> 0$.

The design domain is defined as an n-dimensional Cartesian coordinate space, where each axis corresponds to a variable. Where x is the vector of design variables that the design solution satisfies in order to be adopted (Ntintakis and Stavroulakis, 2020). Two categories of restrictions are mentioned:

- Functional constraints, which refer to system limitations
- Geometric constraints, which refer to physical constraints

$$\text{Minimize} \quad f(\mathbf{x})$$
$$\text{Subject to} \quad g(\mathbf{x}) \le 0$$
$$h(\mathbf{x}) = 0$$

START — Determine an initial design (x_0)

Improve Design   Computer Simulation — Evaluate f(x), g(x), h(x)

Change x

Converge ? — Does your design meet a termination criterion?

N

Y

END
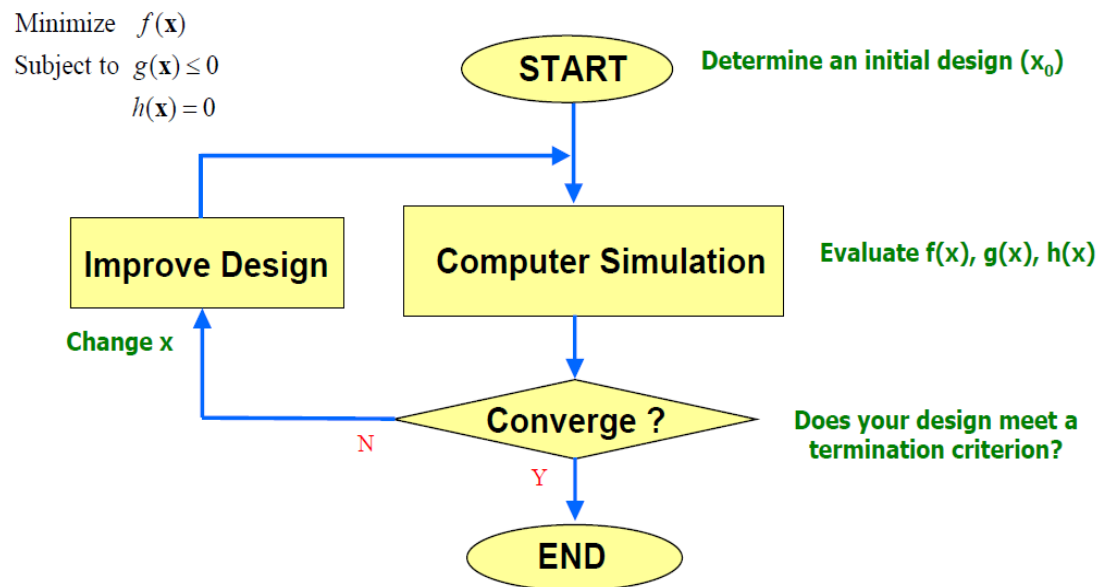
Figure 1.1 General workflow of an optimization algorithm

In recent years, the combination of Additive Manufacturing and Topology Optimization is rapidly advancing. The outcome-optimized structures are often complicated, and most times they cannot be fabricated with the use of traditional manufacturing methods. More and more researchers develop new methods and algorithms to improve these methods. Most of them try to evolve new algorithms and techniques that are usually based on the most well-known methods of Solid Isotropic Material with Penalization (SIMP), Bi-Directional Evolutionary Structural Optimization (BESO), and Level Set method. Anisotropy is not easily integrated into the general topological optimization algorithms, so evaluating the homogenization of the topology-optimized structures is an appropriate step (Ntintakis and Stavroulakis, 2022).

1.2 Purpose and approach

Additive Manufacturing (AM) is a well-known and rapidly advancing method, especially in the manufacturing of high-strength and lightweight microstructures. Utilizing AM, it is possible to fabricate any structure, no matter how complicated it is. At the same time, Topology Optimization (TO) is an appropriate method which allows engineers to create high-strength and mass optimized microstructure lattices.

The most well-known topology optimization methods, like the Solid Isotropic Material with Penalization (SIMP), or the Bi-Directional Evolutionary Structural Optimization (BESO), predict the optimal material distribution within a given design domain. Except the prediction of material distribution, another question that arises is whether other structurable characteristics have to be taken into account. In this question the answer is negative. TO methods do not check other characteristics of the structure, such as anisotropy. In the current thesis, in order to evaluate and characterize the optimized microstructure, a general purpose homogenization method is utilized to calculate the Zener ratio and the elastic modulus. Using the Fused Filament Fabrication (FFF) technique, which is a material-extrusion 3D printing method, lattice structure samples are fabricated and tested in compression and tensile strength tests.

A critical parameter for an efficient and cost-effective printing process is the infill material. The infill structures shape vary from 2D shapes, to high-complexity 3d structures. In the present thesis utilizing the SIMP method, new 3d topological optimized structures are derived and checked experimentally. The new infill structures design start from a solid cubic volume of 15×15 mm. With different boundary conditions and relative density, two new infill structures are created.

1.3 Thesis outline

The thesis is organized as follows: Chapter 2 presents the literature on the topics of topology-optimization, generative design, additive manufacturing techniques, homogenization and auxetic materials. Chapter 3 presents the different types of infills for additive manufacturing. In this chapter we start from the 2d shapes, and continue to 3D infills with isotropic behavior. Then, we turn to gyroid infills and finally to optimized infills, with non-periodic structure. Chapter 4 refers to auxetic materials under dynamic response. The purpose of this thesis is the comparative evaluation of the behavior of shield armor plates consisting of auxetic and non-auxetic materials in a dynamic bullet penetration problem in armor plates. Inject Binder technique, Fused Filament Fabrication (FFF) and Wire Laser Metal Deposition (W-LMD) are presented analytically. Chapter 5 presents a case study of a product design process, where topology optimization, generative design and additive manufacturing have been utilized. The contribution of optimized methods in the early design stage of concept design is investigated. Chapter 6 presents a case study about the contribution of generative design during the redesign process of mechanical components. The main objective of this chapter is the design of lightweight structures which are fully

compatible with Fused Filament Fabrication (FFF) and Wire Laser Metal Deposition (W-LMD) additive manufacturing techniques.

Chapter 7 presents the results for topological optimized 3d infill structure for additive manufacturing. The mechanical behavior of the proposed infills has been verified using modern CAD/CAE software. The evaluation of the new infills using a homogenization method was done experimentally. Chapter 8 summarizes the novel results of this thesis. Promising proposals for future work are presented as possible topics for further research.

CHAPTER **2**

LITERATURE REVIEW

2.1 Computational Mechanics

Computational mechanics is the scientific area that uses numerical methods to approximate the solution of engineering problems. Traditionally, the problems of engineering are solved either analytically, or experimentally. In addition, more complicated structures may be examined using computational mechanics, which provides an alternative way to approach this problem. The development of computers over the last few decades has enabled engineers to approach problems that were impossible to solve in the past, either because of the large computational load. Computational mechanics complements analytical solutions and significantly reduces the number of required experiments. The present work focuses on structural optimization, which is a significant tool during the design process and especially in the design of lightweight structures under specific design constraints.

There are three different types of structural optimization:

- size optimization, which is the simplest implementation of structural optimization. The objective of sizing optimization is to adjust the dimensions of the individual structure components as their shape remain constant (see figure 2.1a). The mechanical behavior of the model is improved as the thickness and topology of the structure remain the same (Stava et al., 2012)

- shape optimization, where the goal is to determine the optimal shape in a predefined design domain (Haslinger and Mäkinen, 2003). In this case, the design variables can be the thickness of the material, the diameter of the holes, and generally measurable elements of the structure (see figure 2.1b)

- topology optimization is the third and more complicated form of structural optimization, where the shape and size of structure elements change. Topology optimization is a mathematical method which spatially optimizes the distribution

of material within a fixed and predefined design domain. The objective is to find the optimal design solution so that boundary conditions and design constrains are satisfied. Compared with size and shape optimization, the final shape, or the size of voids are unpredictable. Topology optimization methods can be based on simplified Optimality Criteria iterative reanalysis methods, Heuretics, and optimization techniques (see figure 2.1c)

a.

b.

c.
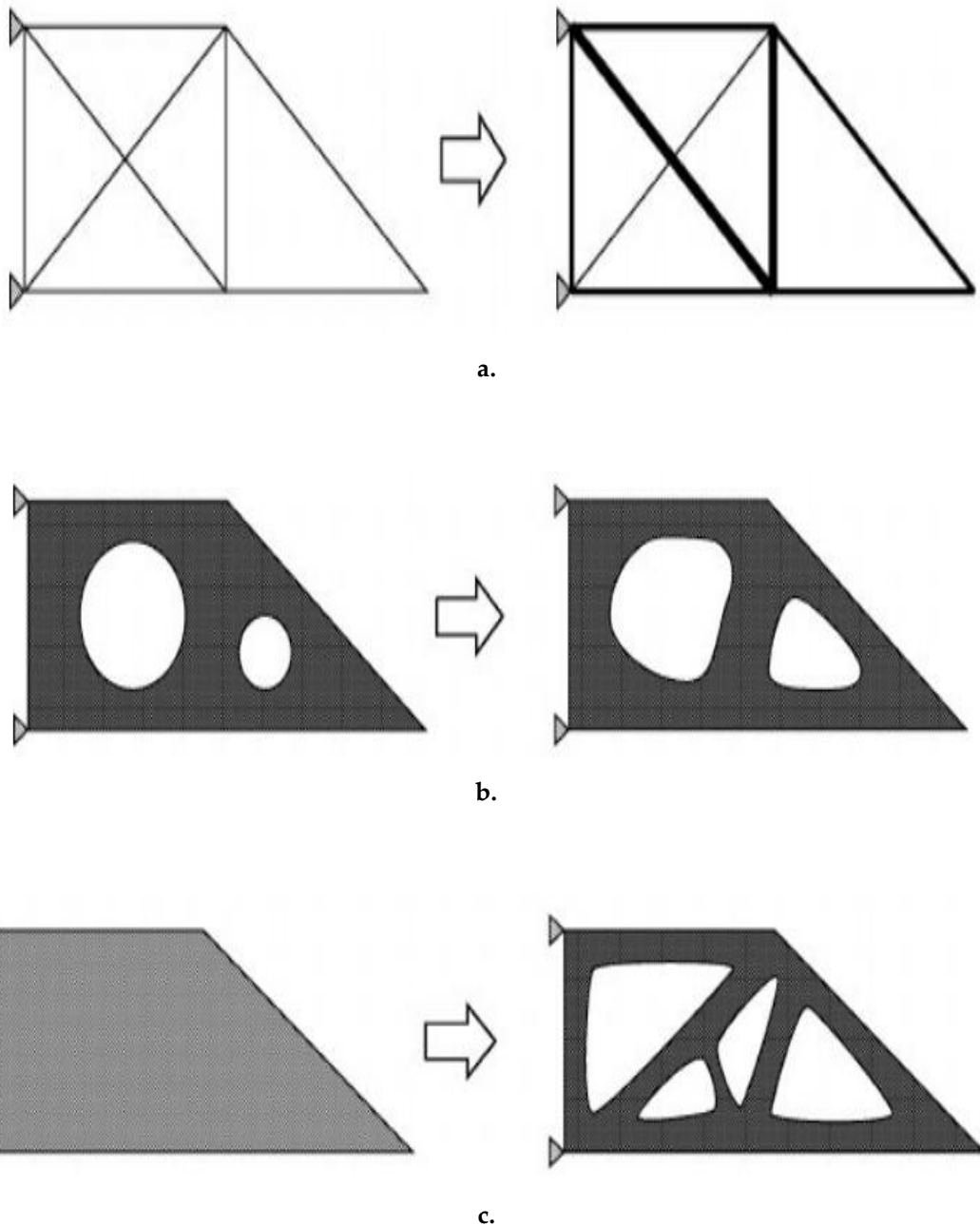
Figure 2.1 Structural optimization categories, a) size optimization example, b) shape optimization example and c) topology optimization example

2.2 From traditional Design Methodologies to Design for Additive Manufacturing (DFAM)

In the late 19th and early 20th centuries, architects and designers believed that building and product design should reflect their use. The American architect Louis Sullivan was the strongest supporter of this principle, as he analyzed in his article titled 'The Tall Office Building Artistically Considered'. The ancient Roman architect Marcus Vitruvius Pollio shared this view. Prior to WWII the modernist architects dissented from the above principle. They regarded decorate elements -which architects call ornaments- as superfluous in modern buildings. Sullivan did not question this theory, although the building he designed was characterized by Art Nouveau and Celtic decorative features. Meanwhile, there was a disagreement about product design whether it should comply with market demands, or whether it should focus on product functionality. For example, the American auto industry put an end to the introduction of aerodynamic forms to mass production. Some car resellers claimed that the aerodynamic shape would end up to a certain shape very similar for all vehicles and thus automobile sales would drop (Ntintakis et al., 2020; Tucker and Meikle, 1982).

After WWII and up until the Oxford conference on Design Methods in 1963 design was considered to be a more cohesive work than a scientific procedure with distinct staying. The methodology that designers adopt during the designing procedure has been the subject of investigation over the last six decades. Initially, the aspect that designers should follow a certain designing process through formalized procedures, or designing methods prevailed. However, this led many designers to believe that the adoption of a specific process will limit their creativity and imagination. This obstacle was overcome after the integration of brainstorming into the design process. Due to the development of the designing methods, a main concern came up; the connection of design methodology to computer science as a prerequisite to thoroughly understanding and defining design (Gutman, 2017). In the 70's Bill Hiller developed a new designing method, according to which the experience gained from local designing problems could be useful for addressing layer–scale issues (Hillier and Leaman, 1974) . This is the first and foremost feature of this early period of design methodology. Moreover, the design problem was not clearly defined to adopt an optional solution. During this period the researchers were opposed to the development of design methods – albeit they changed their opinion over the next years (Alexander, 1971). This can be attributed to the fact that the design methods were rapidly developed and recognized by the researchers of this period (Checkland, 1981; Ntintakis et al., 2020). The last decade's product development

process follows a more specific process with distinct stages (figure 2.2). Through this process, designers must ensure that the new product is well designed. In the first stage, product specifications have to be defined according to the needs of the users. Next is the stage which includes concept design, and then initial 3d models, and the final 3d model. The third stage is the prototype phase in which designers must produce functional physical models to evaluate their ideas and to check ergonomics, functionality, and product stability. Prototypes are fully functional and end users can use them to give efficient feedback (Babalis et al., 2013). In the last decade, more and more designers and engineers have been adapting 3D printing techniques to create prototypes (Bose and Bandyopadhyay, 2019) (Wong and Hernandez, 2012) (Sauerwein et al., 2019) (Ntintakis et al., 2020).
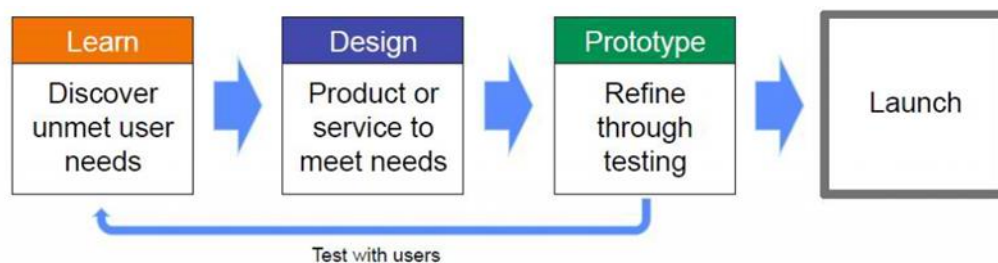
Figure 2.2 Product design process

To support the prototyping stage various three-dimensional printing techniques have been well developed, with each of them having strengths and weaknesses. Differences are based on how the individual layers have been spread to create various components, such as material melting, melt deposition, or the use of liquid materials through different technological processes. Mainly, the discussion is related to the issues of speed, cost of prototype and 3D printers, choice and cost of materials, and the ability for multicolor prototype (Kechagias et al., 2014).

The second stage of this process is the conceptual design stage. Conceptual design and 3D Computer Aided Design (CAD) are two distinguished phases (figure 2.2). In conceptual design, CAD is rarely used and primarily utilized later to analyze, validate, and fabricate the design (Kazi et al., 2017). In recent years this trend changed gradually and the role of computer science in the field of design is increasing. Especially, utilizing artificial intelligence and design simulation, through the Generative Design (GD) process, designers/engineers can evaluate a large number of potential design solutions (Umetani et al., 2012). This modern design approach is becoming a more and more popular solution in the early design stage of conceptual

design. The core synthesis of commercial generative design systems is based on Topology Optimization (TO) techniques. These techniques are mathematical methods that optimize the material distribution within a predefined design space.

The limitations of traditional CAD systems are reduced with the integration of GD with Artificial Intelligent (AL) algorithms. This synergy offers great opportunities to designers/engineers to move away from the traditional design process and leads to new design strategies and manufacturing capabilities. It is a great challenge for designers and engineers to develop rigorous and robust models which take into account many aspects of product design such as aesthetics, manufacturability, production cost, engineering performance, etc. New design tools describe an initial combination of a generative design and an associative modeling system using XML models (Shea et al., 2005). A new approach for GD is the combination with Deep Learning (DL). Relative work presents the need and effectiveness of adopting deep learning for the generative design research area. An AI system based on deep generative design can generate numerous design options, which are not only aesthetic, but are also optimized for engineering performance (Ntintakis et al., 2022; Oh et al., 2019).

2.3 Topology Optimization (TO)

Topology Optimization has its roots in the study of Michel trusses and the use of a ground-structure approach. A dense truss simulates the continuum, and in the course of some structural optimization process regarding the cross sections of the bars, unloaded elements are eliminated and the optimal topology arises. TO can solve the problem of finding the proper distribution for a limited volume of material within a specific design domain (Ntintakis and Stavroulakis, 2022).

Topology Optimization is a significant tool for the product design process. Depending on the desired result a suitably defined objective function can be maximized, or minimized (Gebisa and Lemu, 2017). The advantages of TO are:

- creation of lightweight structures
- generation of a ready-to-build part/assembly
- minimization of the amount of raw material
- energy saving
- less need for natural prototypes
- reduction of physical prototypes and tests
- reduction of the entry time of a product into the market

In the domain of an optimized model, the material's elastic properties compared with the density may vary so the material can be removed permanently (Querin, 2017). Often the optimized structure is extremely difficult to be produced by using traditional manufacturing methods like lathe or milling and usually additive manufacturing is the appropriate production method. According to the literature, there are several articles where topology optimization is utilized in the product design process (Ganesh Rajkumar et al., 2021). During the TO study, all boundary conditions have to be defined.

Topology Optimization is the mathematical method that can optimize the material distribution within a specific design domain. The objective is the system performance maximization for a given set of loads. There are several TO implementations, like Solid Isotropic Material with Penalization (SIMP), Level Set (LS) method, and Bi-Directional Evolutionary Structural Optimization (BESO). TO calculates the element's relative density distribution in the design domain (Sigmund and Maute, 2013; Tang et al., 2015; Wang et al., 2003). Some of the topologies are limited in additive manufacturing like the truss-like cellular structures in the functionally graded modeling method. There are only a few isotropic cellular structures when the established TO methods are calculated for isotropic materials. Topology Optimization and Additive Manufacturing are coupled in an efficient manner and can make the most of their potential, in order to allow for wide application prospects in modern manufacturing (Ntintakis et al., 2020; Zhu et al., 2021).

2.3.1 Volume Based / Solid Isotropic Material with Penalization (SIMP) method

Volume- based is known as SIMP - Solid Isotropic Material with Penalization- method and is widespread in CAE software. The process starts by defining a linear block of voxels. The density of each voxel is defined between zero to one. If the value is equal to unity, then in this specific voxel the material is completely dense. If it is zero, then in this voxel there is no need for material. Any other value indicates that the material in this voxel does not have to be solid for the enforced loads. These values are very useful in FEA models for topology optimization analysis (Bendsøe and Sigmund, 2004; Ntintakis et al., 2020). In figure 2.3 a typical topology optimization volume-based problem is presented (Bendsøe, 1989).
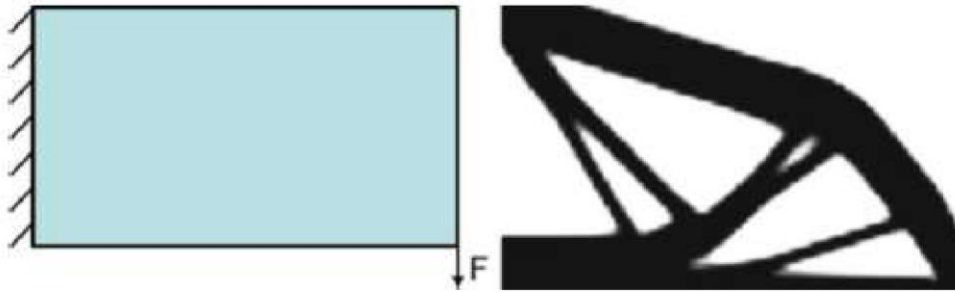
Figure 2.3 A typical optimization problem.

The history of SIMP takes us back to the 1980s when Bendsoe first conceived the idea of parameterizing the design domain and not proceeding to the solution of an on-off problem, the TO. It was until the 1990s that this method was highlighted. The SIMP method is able to maintain a fixed FE mesh and associate each of the Finite Elements with a density function ϱ(x) whose values range from 0 (void) to 1 (solid). As presented by Rozvany et al., an artificial material that can also be conceived as a mesostructured material with holes can be created by the intermediate values. The last design solution has black regions (indicating solid regions), white regions (indicating voids), and grey regions (indicating intermediate densities). The grey areas cannot be fabricated and have to be eliminated(Eschenauer and Olhoff, 2001; Rozvany, 2009; Rozvany et al., 1995; Sokół and Rozvany, 2013). According to the SIMP method, the formula for the stiffness matrix of the optimized structure is:

$$K_{SIMP\,(\rho)} = \sum_{e=1}^{N} \ [\rho_{min} + (1 - \rho_{min})\rho_e^p]K_e$$

where:
K_e are the elements of the stiffness matrix
ρ_{min} is the minimum penalty factor
N is the number of total elements in the design domain

During the TO study, the main goal is to maximize the stiffness of a structure or minimize its compliance with a given amount of the total mass, usually defined as a percentage of the available design area. The total compliance is equal to the cumulative deformation energy of the elements. Minimizing the total compliance, C, is equivalent to maximizing the overall stiffness. The optimization algorithm, through an iterative process, seeks to solve the element densities that minimize the overall compliance of the structure (Ntintakis and Stavroulakis, 2022).

The mathematical formula which expresses C is:

$$C(\{\rho\}) = \sum_{e=1}^{N} (\rho_e)^p [U_e]^T [K_e] [U_e]$$

where:
(U_e) is the displacement vector of element e
(K_e) is the stiffness of element e
$\{\rho\}$ is the vector which consists of the relative density of the ϱe elements.

2.3.2 Truss Based TO Method

The truss-based, or ground-structure approach is based on a large number of elements relating to a grid of beams between a set of nodes in a given volume. The method initially detects which supports are necessary for the structure and determines their size. Then the method removes the beams that do not meet the study requirements. In the results, the necessary beams are represented with bold lines and dark blue color. The less necessary beams denoted with less dark blue colors and the unnecessary beams appear without change in their thickness (see figure 2.4), (Perez and Behdinan, 2007). Extension to multi objective optimization has been tried by (Stavroulakis et al., 2009, 2008). This approach is, historically, the first method of topology optimization (Ntintakis et al., 2020).
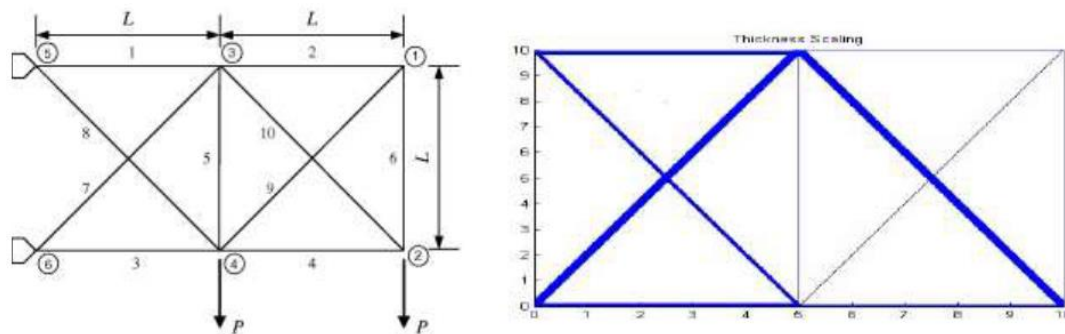
Figure 2.4 The results of design domain and the TO study.

2.3.3 The Level Set Method (LSM)

The LSM is a numerical technique for tracking interfaces and shapes. The level-set method makes it easy to follow shapes that change topology when a shape splits in two, develops holes, or the reverse of these operations. With LSM level-set model numerical computations can be performed without having to parameterize these objects, which is called the Eulerian approach (Osher and Sethian, 1988). The LSM tries to minimize the objective function with the compliance of constraints for the volume of used material (Ntintakis et al., 2022).

The mathematical formulation of LSM is described as:

$$min_x \quad : \quad c(x) = U^T K U = \sum_{e=1}^{N} u_e^T k_e u_e = \sum_{e=1}^{N} x_e u_e^T k_l u_e$$

$$subject \; to \quad : \quad \begin{aligned} & V(x) = V_{req} \\ & KU = F \\ & \left. \begin{aligned} x_e &= 0 \\ x_e &= 1 \end{aligned} \right\} \forall e = 1, \ldots, N \end{aligned}$$

where:

$x = (x1, \ldots, xN)$ is the vector of element densities, with entries of xe = 0 for a void element and xe = 1 for a solid element, where e is the element index

c(x) is the compliance objective function

F and U are the global force and displacement vectors, respectively

K is the global stiffness matrix

u_e and k_e are the element displacement vectors and the element stiffness matrix for element e

k_l is the element stiffness matrix corresponding to a solid element

N is the total number of elements in the design domain

V(x) is the total volume of material within all solid elements

V_{req} is the allowable material used

2.4 Generative Design (GD)

During the design process a designer/engineer has to take decisions for product shape, ergonomic design, material selection, product stiffness and durability, and so on. The combination of these parameters creates a complex problem. Designers must take this decision very fast and in an accurate way. In this effort, advanced systems like generative design, topology optimization, and additive manufacturing are very helpful. Generative Design (GD) has become more and more popular in recent years. Quite generally GD mimics nature by using algorithms inspired by the way in which bones grow in animals. A basic outcome of this algorithm is to add material where it is necessary and to remove it from the design domain where it is not necessary (Ntintakis and Stavroulakis, 2020). By adopting the Generative Design (GD) methodology, the designer can now design, in less time, an object with better results and produce optimized products that take into account various constraints, such as the production method, the material, and the cost. The need for a guiding theoretical framework for generative design is widely recognized, especially the link with topology optimization (Caldas and Duarte, 2004; Chase, 2005).

The iteration is repeated. Within each iteration, the GD tests the outcome structure and learns from each step output. The total number of iterations depends on the specified constraints and the final forms are designed in a unique organic shape (McKnight, 2017).

Generative Design (GD) is an iterative design process that will generate a certain number of outputs design solutions that meet certain constraints. A designer will fine-tune the feasible region by selecting specific output or changing input values, ranges, and distribution. Recent research efforts on generative design utilizes topology optimization as a design generator instead of design parameterization and develops the methods to generate numerous designs in parallel with cloud computing (Ntintakis et al., 2022). The characteristics of GD include:

- a significant tool for the concept design stage
- an appropriate tool for mass reduction and lightweight structures
- fully compatible models for Additive Manufacturing
- artificial Intelligent (AI) algorithms
- structure Topology Optimization (TO)
- generated models that meet certain constraints and boundary conditions
- potential design solutions
- human-machine design methodology
- a minimized timetable for ready to use products.

At the early stages of GD this method was used in architecture and civil engineering. Nowadays it is growing up rapidly in mechanical design. GD is a repetitive method which gives us a set of potential design solutions. Designers can change the inputs in a way to choose the best solution. It is therefore a fast method of exploring design possibilities that are used in various design fields. As a process, generative design can be analyzed as shown in figure 2.5 (Bohnacker et al., 2012). As a first step, the user has to define the design constrains in the algorithm. Then a sketch or a general 3D model is used. Finally, the rules are defined, and the algorithm starts to formalize the rules in parameters, in order to output potential solutions. Each time the algorithm offers several potential design solutions. Designers/engineers judge the outcomes and modify the input rules to take more accurate solutions. The process

stops when the designer judges that one of the potential solutions is the appropriate (Ntintakis and Stavroulakis, 2020). Therefore, the algorithmic method transforms the requirements into a 3D structure. This new design approach provides significantly more mass reduction and parts consolidation opportunities that cannot be achieved through traditional design optimization methods.

Nowadays GD is based on cloud systems, where much more computer power is available. Another reason is that generative designs are not able to be manufactured with traditional manufacturing methods. The enormous development of additive manufacturing techniques in recent years gives the opportunity to make ready-to-use complex and lightweight structures.
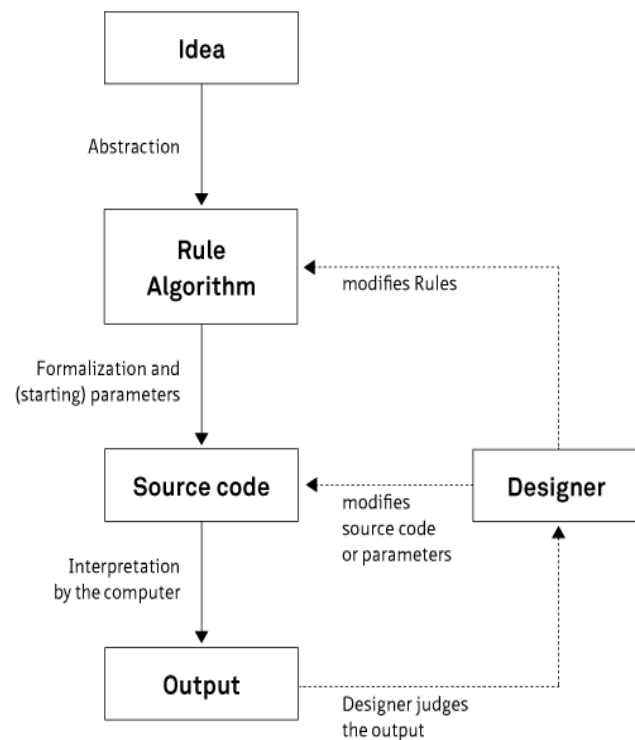
Figure 2.5 The overall process of the Generative system

The GD approach simplifies the work of designers/engineers. Utilizing GD, the required time to design a new product is reduced. The system provides a variety of solutions that, most likely, the designer could not think of. GD enables engineers-

designers to focus on the "WHAT?" of their work instead of the "HOW?"(see figure 2.6) (Tsavdaridis et al., 2015). The use of GD is closely linked to the use of topology optimization (Ntintakis et al., 2022).
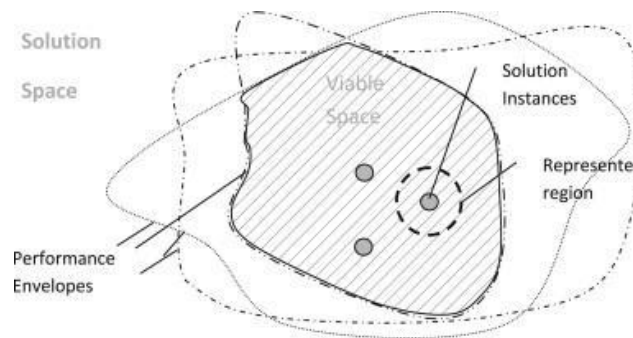
Figure 2.6 Potential solution space

2.4.1 Generative Design Algorithms

Generative Design process, with several notable differences, is quite similar to the Topology Optimization process. The conceptual design phase consists of exploring alternatives based on design requirements, and then the output population is ranked during a preparatory analysis to select the most appropriate design solution. The simplicity of the process and the compliance of the alternatives with the design requirements or the customer's preferences is a critical and time-consuming task for designers. Even though generic algorithms are used in most generative design systems, the need for fine-tuning input parameters becomes is not helpful for most designers.

2.4.1.1 Jaya Algorithm

Jaya algorithm is suitable for generative design systems because it does not require the tuning of specific parameters (Khan and Awan, 2018). The process requires only the controlling of basic parameters like the size of the population (p) and the number of solutions (s) (Eiben et al., 1999). During the process, the algorithm compares the proposed solutions and keeps the best one. In case of a solution is better than the previous one, it is accepted, instead, the previous one kept (see figure 2.7). For example, let us consider a problem that has n design parameters (j= 1, 2, …, n) and s population numbers (k=1, 2, …, s). The value of the jth parameter for a kth solution during the ith iteration is symbolized as X_{jki} and this value is calculated from the equation:

$$X'_jk_i = X_jk_i + r_1k_i(X_jb_{esti} - |X_jk_i|) - r_2k_i(X_{jworsti} - |X_jk_i|),$$

where: X_{jbesti}, $X_{jworsti}$ are the updated values of the parameter j, for the best and worst value, respectively X'_jk_i is the updated value of X_jk_i. Finally, r_1k_i, r_2k_i are two random numbers in the range (0,1).
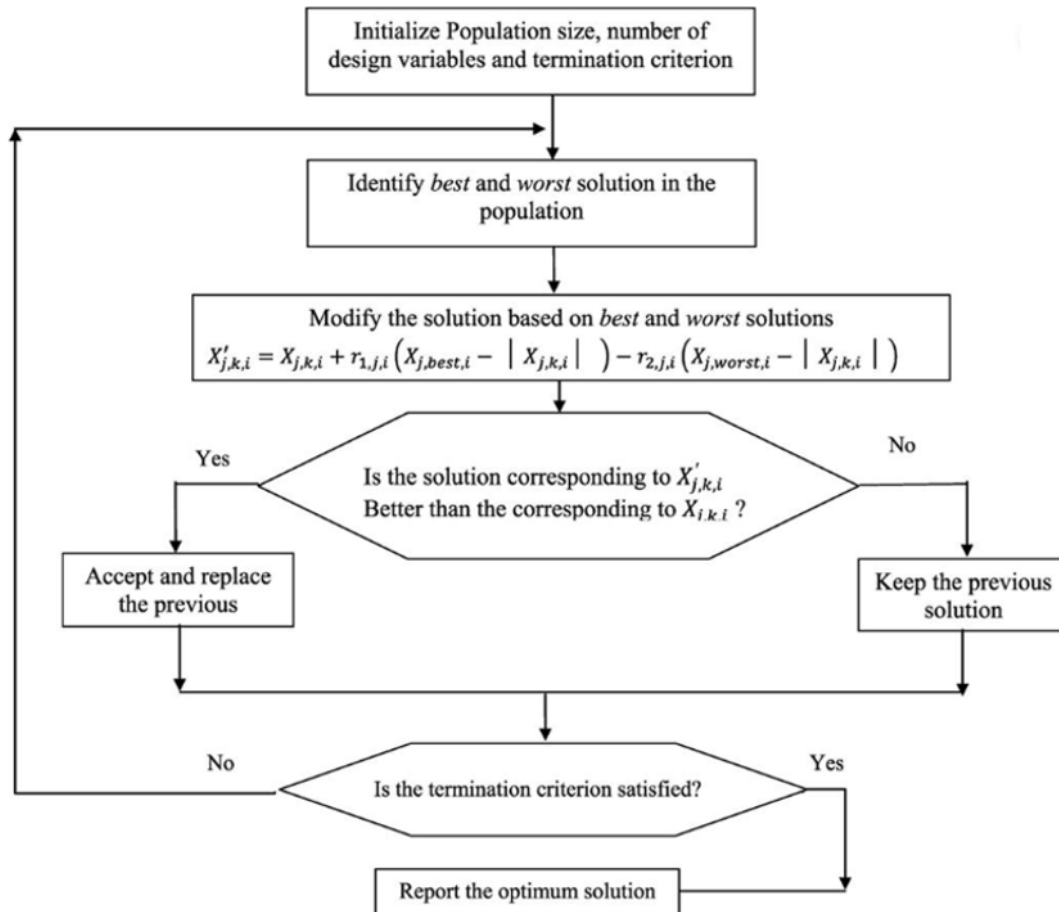
Figure 2.7 Jaya algorithm flowchart

2.4.1.2 Space-Filling (SF) technique

A CAD model (*m*) can be approved by *n* numbers of design parameters (x_{m1}, x_{m2}, …, x_{mn}), and each of these takes an area in a design domain (Khan and Awan, 2018). The limits (j= 1, 2, …, n) of the design domain are specified from the upper and lower limits [x_m$_j$^u] and [x_m$_j$^l] respectively) of each parameter. For the calculation of

optimized solutions, for each set of N potential solutions the space-filling $U1(B)$ of the design domain is calculated from the equation:

$$U_1(B) = \sum_{p=1}^{N-1} \quad \sum_{q=p+1}^{N} \quad \frac{1}{L_{pq}^2}$$

and
$$L_{pq} = \sqrt{\sum_{j=1}^{n} \quad (\underline{x_{pj}} - \underline{x_{qj}})^2}$$

where L_{pq} is the appropriate distance between the designs p and q and x_{pj}, x_{qj} are scalar values of the jth design domain dimensions in the range of 0,1. Finally N is the number of potential design solutions.

2.4.1.3 Weight Grid Search Technique

This technique tests the outcome design solutions controlling the boundary limits of the design domain. Criteria which have not been satisfied by the algorithm have to be fulfilled. In this technique a new term of U2(B) for non-collapsing is introduced in the cost function, which is proposed by the function:

$$U_2(B) = a \times \sum_{p=1}^{N-1} \quad \sum_{q=p+1}^{N} \quad \sum_{j=1}^{n} \quad f(y_{pj}, y_{qj})$$

$$f(y_{pj}, y_{qj}) = \{1 \quad if \ y_{pj} = y_{qj} \ 0 \qquad otherwise$$

$$\{if \ x_{pj}{}^{e} \leq x_{pj} < x_{pj}{}^{e+1} \quad then \quad y_{pj} = e \ if \ x_{pj}{}^{e} \leq x_{pj} < x_{pj}{}^{e+1} \quad then \quad y_{pj} = e$$

where α, is a parameter defined by the user and y_{pj}, y_{qj} are the corresponding integer coordinate, for x_{pj}, x_{qj} in the jth dimension.

2.4.2 Generative Design in Industry

Generative design has been applied in consumer products and in mechanical synthesis to pursue performance-driven design (Buonamici et al., 2020). GD is entering rapidly into the product and parts manufacturing industry. Several GD methods are available like the Generative Design Method (GDM), which is a comprehensive CAD-based generative design exploration method designed to work at all stages of the design development process-spanning, from conceptual to detailed design (Krish, 2011).

In 2019 the company Kartell produced the first commercial chair made using generative design, in collaboration with Autodesk and with the famous designer Philippe Starck (see figure 2.8). As Starck said '*We ask from intelligent system to carry the body chair with the least amount of material*'.

In the aerospace industry, generative design is a well-know technology. Recently NASA worked with Autodesk to create a space-lander prototype that can withstand the temperatures and pressures of outer space. The main goal was to create the lightest possible structure, in order for the final prototype to look like a spider. Also, the RUAG Sentil satellite was optimized topologically and Additive Manufacturing (AM) was used for the antenna bracket construction. The used material was the EOS Aluminum AlSi10Mg, which has high strength and resists to dynamic stress. The optimization goal was not only the lightweight structure, but also the minimization of undesired vibration from rocket high speed. The antenna bracket weight reduction was over 40%, from 1.6 kg to 0.94 kg.

Figure 2.8 The 'A.I. chair', the first commercial generative design chair.

In the automotive sector in 2018 General Motors started to develop new car components using GD. One of them is a new seat bracket which is 40% lighter and 20% stiffer than the previous one. The potential solutions were chosen from about 150 potential design solutions (see figure 2.9). The generative component consolidates eight different components into one 3D-printed part. Audi used AM to produce the water connection for the W12 engine and Porsche made the gearstick for the 959 model. BMW produced more than 25,000 prototypes helping the design process. Also, Ford, did not have the need to produce tools for prototypes, saving a huge cost in the product development process (Jauhar et al., 2012; Ntintakis and Stavroulakis, 2020).

(a)   b)
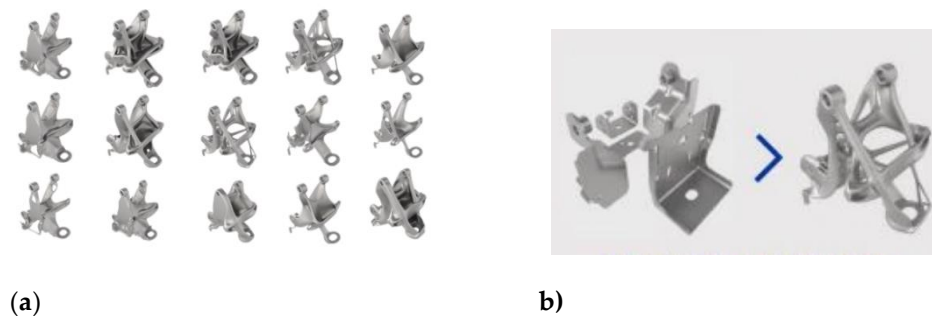
Figure 2.9 a) Potential generative models b) The component before and after GD.

In the aviation industry, the Airbus group has performed analytical studies about the reduction of CO2 emission by about 40% from weight minimization. For this purpose, they redesign with TO the toll of the Airbus A320 nacelle hinge bracket, using the direct metal laser sintering AM technology, instead of the traditional casting methods (Tomlin and Meyer, 2011). In 2015 Airbus got the award 'German Future Awards' for focusing on modern production processes, such as additive layer manufacturing and advanced materials. One of the developed materials, especially designed for use in AM, is 'Scalmalloy', which is a second-generation aluminum-magnesium-scandium alloy created by APWorks, an Airbus subsidiary. This material offers outstanding mechanical properties, meaning it can undergo significant stress and stretching before breaking. This is the first time it has been used on a large scale inside an aircraft component. Generative design is a priority for Airbus, Peter Sander of Emerging Technologies and Concepts at Airbus says, "*It isn't as simple as copying nature,*" and "*Successful bionics depends on establishing a deep understanding of natural materials and then working out how to apply that knowledge in the industrial world*".

For the development of new products, it is of great importance to find the best possible topology for given design objectives and constraints at an early stage of the design process. In industrial practice, the product quality and durability have to be improved at a relatively low cost. Due to the results of the GD study, the optimum topology and layout design have to be defined. This process is commonly known as Structural Optimization which, is a new tool in the area of Computer-Aided Engineering and belongs to the broader field of computational mechanics.

Often there is a misunderstanding between Generative Design and Topology Optimization (TO). TO creates only one design that has been optimized for structural integrity based on existing criteria and GD creates multiple designs in an evolutionary way. Topology Optimization is suitable when you have a set space and overall idea and just need the algorithm to make it as lightweight as possible. On the other hand,

GD is mainly used when the whole shape is unknown so that the program will give us a lot of potential solutions, taking into consideration constraints like the desired material and manufacturing method. Certain similarities with repeated use of topology optimization driven by a nature-inspired optimization technique has been studied already (Kaminakis and Stavroulakis, 2012; Ntintakis et al., 2022).

2.5 Homogenization

In most research manuscripts, the researchers present new methods and algorithms based on well-known TO methods to predict the material distribution more accurately and cost-effectively. However, in most cases, the proposed methods do not evaluate other characteristics of the optimized structures, such as isotropy. In the current thesis, the isotropy of the optimized lightweight structures was checked, and a general homogenization method was used.

A microscale study is necessary to understand the behavior of the new proposed structures on a global scale. Plenty of studies have been developed to specify the behavior of cellular and heterogeneous structures (Chatzigeorgiou et al., 2022; Drosopoulos and Stavroulakis, 2022). Often, cellular materials are characterized by a high design complexity, which limits the manufacturability process. Additive manufacturing overcomes these issues, and lattice structures can be fabricated precisely and with lower production costs (Rehme and Emmelmann, 2006). The keystone of the homogenization is the properties of a heterogenous material to represented in a small fraction of that. Represented Volume Element (RVE) is defined as the limited fraction of the whole heterogenous material. Then, the characteristics of the heterogonous material are applied as the boundary conditions in the whole design volume (Somnic and Jo, 2022a). For a square unit cell, the RVE method is applied as in figure 2.10. Furthermore, homogenization methods are used in order to produce a quickly infilling gradient microstructure (Lee et al., 2021; Ntintakis and Stavroulakis, 2022).
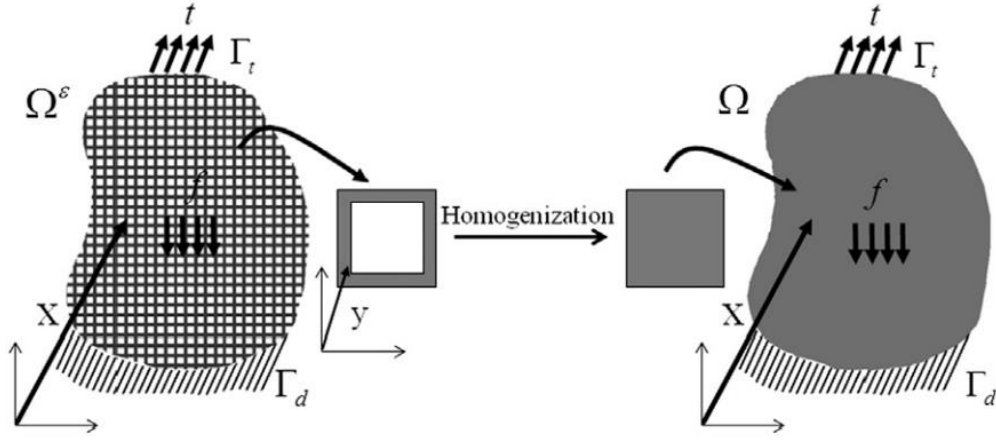
Figure 2.10 Represented Volume Element for a square unit cell.

The behavior of a lattice structure can be described using the generalized Hooke's law: $\sigma_{ij} = c_{ijkl}\varepsilon_{kl}$. The anisotropic form of Hooke's law can be expressed by the stiffness matric [c]:

$$\begin{bmatrix} C_{11} & C_{12} & C_{13} & C_{14} & C_{15} & C_{16} \\ C_{12} & C_{22} & C_{23} & C_{24} & C_{25} & C_{26} \\ C_{13} & C_{23} & C_{33} & C_{34} & C_{35} & C_{36} \\ C_{14} & C_{24} & C_{34} & C_{44} & C_{45} & C_{46} \\ C_{15} & C_{25} & C_{35} & C_{45} & C_{55} & C_{56} \\ C_{16} & C_{26} & C_{36} & C_{46} & C_{56} & C_{66} \end{bmatrix}$$

In homogenization study Zener ratio can be calculated. The Zener ratio is a dimensionless number that is used to quantify the anisotropy for cubic structures (Zener and Siegel, 1949). Conceptually, it quantifies how far a material is from being isotropic (where the value is equal to unit, it means that this material has isotropic behavior) (Ntintakis and Stavroulakis, 2022). The calculation of the Zener ratio is derived from the mathematical formula:

$$A = \frac{2C_{44}}{C_{11} - C_{12}}$$

2.6 Auxetic materials

Most of materials which exist in the nature, tend to get thinner to the direction of loading, or excitation, when stretched. In other words, as for elastic loadings, shrinkage usually appears in the direction which is perpendicular to the applied load. This behavior results in the reduction of the cross-sectional area of the structure. In case of

compressive loadings, the exactly opposite effect appears and the cross-sectional area increases. The change of the length of the elastic material in the perpendicular direction with respect to the applied load, is given by the Poisson's ratio, which is usually a positive number taking values in the interval (0, 0.5). This ratio is defined as the negative fraction of transverse strain $\Delta y/ly$ over the axial strain $\Delta x/lx$ (Wan et al., 2004). However, there are materials which present exactly the opposite behavior. These materials, featuring a negative Poisson's ratio, are called auxetic materials and can be conceived as microstructures, which become thicker in the perpendicular direction to the one of the applied tensile loadings. This is because of artificial joints inside the microstructure, which, in turn, help flexing to occur (K. E. Evans, 1991; Theocaris et al., 1997). This attribute provides the auxetic behavior to these materials. The main reason for this unusual characteristic is due to their specific internal structure. This property is usually explained from the microstructure (star-shaped frames or inclusions), although other models have been used, as well (chiral, perforated, or mechanism-based) (Tairidis et al., 2022).

A key feature of the auxetic materials is the negative Poisson's ratio ($v < 0$). They form a particular category of materials characterized by special and unusual mechanical properties. The auxetic materials are characterized by indentation resistance, fracture toughness and impact resistance. Due to their special and unusual mechanical response, these present positive results in many applications. In current thesis was studied the behavior of the auxetic star shape materials in dynamic bullet penetration problems. Their unusual behavior lies in the fact that once stretched in one direction, the material gets thicker in the perpendicular direction, unlike common materials which present thinness. In addition, when part of the material is being squeezed, the rest of it tends to shrink, rather than expand and it gets denser in the process.

Their name derives from the Greek word "αυξητικός", which means "who which going to be increased" (Ken E Evans, 1991). The auxetic materials are considered interesting because they exhibit improved mechanical properties, such as shear strength, resistance to strain and strength against fracture (Evans, 1990; Lakes, 1987). The auxetic materials belong to the group of metamaterials and owe their unique properties not to their composition, but to the form of their structure. Metamaterials are materials whose properties are not found in natural materials. Their name derives from the Greek word "μετά" which means "beyond" and from the Latin word "materia", which means material. The fields of use of auxetic materials vary and are constantly increasing.

An interesting application of auxetic materials is in the domain of protection equipment. Additive manufacturing has a significant contribution to the construction of armors. The construction of the auxetic structures using conventional production

methods is often unfeasible as these characterized by geometry of high complexity. Yang studied the potential uses of the re-entrant hexagon and arrowhead type printed auxetic structures made from common polymers in order to be used in body protection (Hitesh D Vora and Young Chang, n.d.). Imbalzano studied the blast resistance of hybrid sandwich panels (Gabriele Imbalzano, n.d.; Imbalzano et al., 2017, 2016). Han created two structures of auxetic materials for high absorption of energy (Dae SeungKang, n.d.). Alomarah studied the in-plane mechanical properties of auxetic structures subjected to dynamic compression numerically and experimentally (Alomarah et al., 2020). The effectiveness of sandwich structures with auxetic 3D re-entrant lattice core and semi-auxetic braided composite face sheets subjected to high-velocity impact have been investigated (Madke and Chowdhury, 2020). The auxetic behavior of materials in engineering applications is still have being discussed (Stavroulakis, 2005; Tairidis et al., 2022).

The modern approach to design auxetics is based on topology optimization methods. For example, a topology optimized architecture with programmable Poisson's ratio over large deformations is presented and discussed in (Clausen et al., 2015). From the mathematical point of view, the optimization goal is defined as the minimization of the error between the actual and the pre-defined value of Poisson's ratio over a range of discrete, nominal strain values. The topology optimized structures are designed and printed with programmable Poisson's ratios ranging from −0.8 to 0.8 over large deformations of 20 % or more. Additionally, it is shown that from the combination of topology optimization and additive manufacturing, it is possible to design the new materials with the desired properties. A suitable topology optimization procedure for the optimum design of compliant mechanisms, using evolutionary-hybrid algorithms, for the design of auxetic materials has been proposed in (Kaminakis et al., 2015; Kaminakis and Stavroulakis, 2012; Tairidis et al., 2022).

CHAPTER **3**

Additive Manufacturing

3.1 Utilizing additive manufacturing and topology optimization

The evolution of rapid prototyping to additive manufacturing offers manufacturers a new beneficial production method. Manufacturers, whose objective is to produce robust and low-weight structures obtain a strong production advance. Additive manufacturing can offer this ability giving solutions to several production problems that concern a significant range of industrial manufacturing. The advances of additive manufacturing are not limited to manufacturers, but also affect the designers and engineers, encouraging design freedom and creativity. But the lack of use of computational mechanics tools leads to unsuccessful printing attempts, or the waste of excess printing material due to over-dimensioning.

Coupling additive manufacturing with topology optimization and generative design designers/engineers obtain a strong advance from the early stage of design process until the prototyping and the final production process (see figure 3.1). Design parameters are considered as constraints and satisfied during TO and GD study. The advances of this coupling can be classified as:

- the design freedom, designers can create complex topologies and shapes thanks to the design freedom provided by TO. Moreover, the topological optimized structures are extremely difficult to be fabricated with traditional production process

- the design of durable structures, material distribution in a predefined design can be predicted with the use of TO algorithms regarding to the material stiffness matrix. The results of the proposed optimized structures are evaluated though FE analysis and can be fabricated with AM techniques for further evaluation

- the minimization of time to market, the ability to create quickly accurate and functional prototypes is very helpful during product design process

- the production flexibility, TO contributes significantly in design process in order specific design constrains to be adopted in the final design. Utilizing additive manufacturing, it is possible to produce objects with different shapes in the same production stage
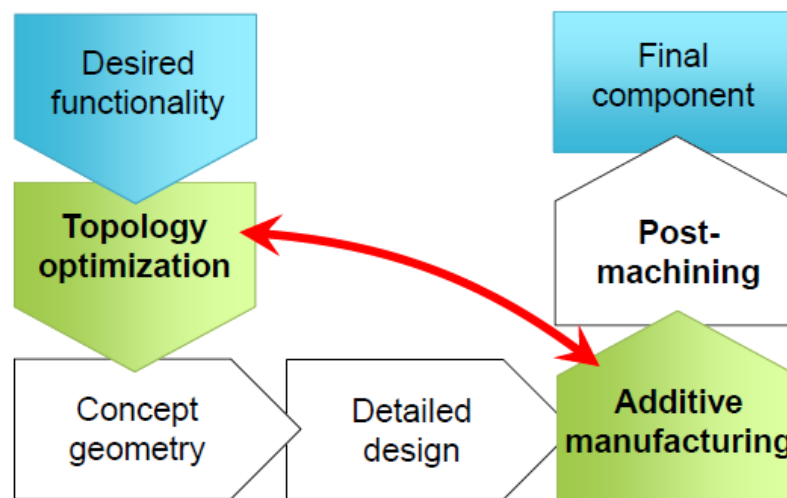
Figure 3.1 Coupling of topology optimization and additive manufacturing during the product design process

Designers are able to create complex topologies and shapes, thanks to the design freedom provided by Additive Manufacturing (AM) (Bikas et al., 2016; Hajare and Gajbhiye, 2022). In our days, the design manufacturing procedures have been expanded to conventional manufacturing processes, although Design for Additive Manufacturing (DfAM) methods have to be further elaborated (Suárez et al., 2022; Vaneker et al., 2020; Veiga et al., 2021; Wiberg et al., 2019). Many of these methods help engineers to utilize the properties that are enabled by AM. Such methodologies are, Topology Optimization (TO), the AM manufacturability analysis, and cellular structures. Cellular structures are observed in nature such as in plant stems or in bamboo microstructures (Ghazlan et al., 2020; Gong et al., 2020; Li et al., 2019). These structures present an incline and can proceed toward better material distribution for performance optimization. The design of artificial cellular structures, making them suitable for processes such as energy absorption, or heat transfer (Ntintakis and Stavroulakis, 2022).

3.2 Additive manufacturing technologies

Additive manufacturing technologies according to the materials which use can be divided into three categories:

- techniques that melt or soften materials
- techniques which use liquid materials
- techniques with use powdered materials

Material extrusion is an AM technique which is belongs to the first category. During the printing process a continuous filament of thermoplastic material deposited layer by layer. FDM (Fused Deposition Modeling) technology was developed by Scott Crump, founder of Stratasys Ltd in 1980. Other well-known familiar technique is FFF (Fused Filament Fabrication). Although it is not as accurate or fast as other additive manufacturing techniques, is widely used. The main characteristics of FDM/FFF technique characteristics are:

- it is the most widespread technology
- it is distinguished by the ease of application and the friendliness of the environment
- it is possible to create complex structures
- the need of support structure depending on overhang angle
- the high strength of printed parts

Inject Binder is one of the most well-known technology which use powder as raw material. Is a high-speed process and produces objects with relatively harsh finish. The raw material is plaster type powder, the granules of the powder are homogeneous in size and shape, showing only limited variation with respect to their size. As the particles are smaller as the quality of printed part is better (Suwanprateeb et al., 2010). The process requires the use of powder as a feedstock and adhesive to achieve the agglomeration of powder grains. The printing process part involves two stages. In the first stage a slicer program divides the object geometry into number of layers and powder is speeded in each single layer. Each powder layer is sprayed selectively with an adhesive. Then a layer of fresh powder is deposited, and the process repeated until all layers to printed. In the post processing stage, the printed model is removed from the container and with the use of compressed air is cleaned from the excess powder. Then, the printed part is sprayed with cyanoacrylate or other substances to improve part stability and surface finish (Ntintakis et al., 2020; Varotsis, 2018; Zhang et al., 2018). The advantages of inject binder technique are:

- the lack of support structure during printing process
- the ability to print multiple objects simultaneously
- there is no need to use a heat source that can create residual stresses in the parts
- is more cost-effective to print bigger parts in inject binder printer than other printer type
- the printing of multi-color parts

In current thesis the required specimens were printed in Z-450 from Z-Corp which is ideal for the production of architecture and product design prototypes. The used raw material in inject binder technique is a plaster-based powder (zp151) which is sprayed with a water-based binder with 2-Pyrrolidone (zb63).

3.3 Types of infills in AM

An advantage of AM techniques is the ability to reduce the necessary manufacturing material when producing a part and the weight of the part itself, thanks to its nature (Jiang and Ma, 2020; Plocher and Panesar, 2019; Seharing et al., 2020). AM can manufacture lightweight parts characterized by a sparse internal infill and an external skin. Regarding to the fabrication process, the type of the infill is a crucial parameter. The most reliable and fast printing infills are made by printing the same pattern for every layer. These are the 2D infills, and they are characterized by a vertical cross-section, which creates a geometry fertile to anisotropic structural properties (Feng et al., 2018).

Another type of infills, that present an isotropic behavior, are the 3D infills. In particular, the infills that have a cubical symmetry are called "cubic infills", and they repeat in all three directions. Another type of strong and fast printing 3D infill is the mathematically based "gyroid infill", which can simplify the designing process. The disadvantage that comes along with 3D infills is that they are not easy to be printed and show a high complexity (Bean et al., 2022; Podroužek et al., 2019).

The final type of infills is those that cannot be characterized either as 2D infills or as 3D infills. Due to process optimization, they have a non-periodical nature, which allows them to be rich in forms. They may have internal structures containing voids, using grad-ed infills, or internal structures with repeating optimized lattice structures. These can show differing spatial properties, or particular elastic properties. In an effort to stimulate the general orthotopic properties, Poisson's ratio and elastic moduli tuning, many researchers have used Topology Optimization (Hoang et al., 2020; Liu et al., 2018; Ntintakis and Stavroulakis, 2022; Wu et al., 2016).

CHAPTER **4**

Auxetic materials in dynamic response

4.1 Design of auxetic structures

Mechanical metamaterials with a negative Poisson's ratio are called auxetic materials, or simply auxetics. Auxetic materials have enhanced dynamical properties and damping behavior, and thus they can be used in certain applications. This property is usually explained from the microstructure (e.g. , star-shaped frames, or inclusions), although other models have been used as well, such as chiral, or mechanism-based models (Wu et al., 2019). Auxetic materials are used in several fields; however, optimal design towards dynamical properties is still under investigation. The modern approach to design auxetics is based on topology optimization methods. Nevertheless, even classical auxetic microstructures may be used, possibly after tuning, for certain applications. A first attempt to review the effect of auxetic metamaterials in applications with dynamic loadings is attempted in the present thesis. The design of auxetic materials in the laboratory can be based on optimal design for the definition, or fine-tuning of the auxetic microstructure. The effectiveness of these materials, as well as their response and adaptiveness to nonlinearities, can be verified by applying numerical homogenization tools and CAD/CAE software. A body, which exhibits an auxetic behavior, can consist of recurring patterns of identical microstructures, as is usually the case in homogenization. Each microstructure consists of a monolithic body with specific geometry and a predefined deformation, which integrates all the features of a compliant mechanism. In figure 4.1, the behavior of a conventional and an auxetic material, based on their microstructure, is shown (Tairidis et al., 2022).
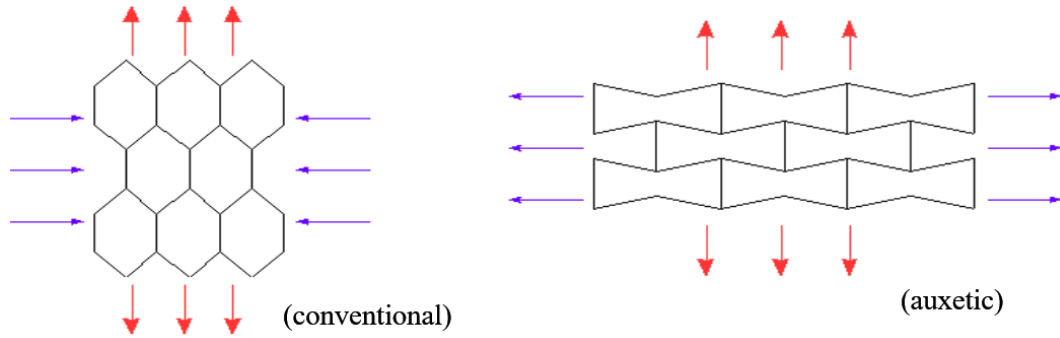
Figure 4.1 Auxetic materials, in comparison with conventional materials.

According to Gibson and Ashby (1988), who proposed the properties of the cell based on the beam theory, a unitary cell of a cellular structure can be used for the prediction of the behavior of the sandwich panel (Gibson and Ashby, 1997). The parameters of the unit cell are the height of the cell (h), the length of the cell wall (l), the depth of the cell wall (d) and the angle between the horizontal and the leaning cell wall. Moreover, the height ratio, and the depth ratio can be also calculated. For the conventional cell the angle is given as $\theta = 30°$ and the ratio $\alpha = 1$, while for the auxetic one the angle is given as $\theta = -30$ and $\alpha = 2$. The selection of the parameters of the auxetic cell has not been made arbitrarily, but in a in such a way that the behavior of the auxetic simulates the function of a conventional cell, since the active coefficient is the same at the two vertical directions (Tairidis et al., 2022).

The overall dimensions of the conventional unit cell are given by:

$$L_c = 2l \cos \theta$$

$$H_c = 2(h + l \sin \theta)$$

where L_c is the total length and H_c is the total height of the conventional unit cell.

Similarly, the total dimensions of the auxetic unit cell are given by:

$$L_a = 2l \cos \theta$$

$$H_a = 2(h - l \sin \theta) \text{ ,}$$

where L_a is the total length and H_a is the total height of the auxetic unit cell.

4.2 Design and Finite Element Analysis - Bullet Penetration test

Ashby and Gibson proposed the properties of the cell based on the beam theory and also discovered that a unitary cell of a cellular structure can be used as a prediction tool for the behavior of the sandwich panel.

Figure 4.2 shows the unitary cell of both the conventional and the auxetic structure, along with the parameters that define the geometry of the cell. The main design parameters of the cell size are the height of the cell, the length and the thickness of the cell wall and the angle between the cell wall and the horizontal axis.

The first structure is characterized by a honeycomb structure without presenting any auxetic behavior. The structure consists of a set of cells in a 2 x 6 layout with dimensions 43.95 x 20.27 x 30 mm. The shape of the auxetic structure is characterized by the star shape, which has been chosen for the negative Poisson's ratio and consequently, its auxetic behavior. This particular structure was chosen because of its relatively simple shape that helps in its production with the utilization of additive manufacturing. The whole structure consists of a set of cells in a 2 x 7 arrangement, the dimensions being 43.53 x 11.93 x 30 mm. In both models, the sandwich panel is created by adding a front and a back panel of 0.5 mm thickness (Tairidis et al., 2022).
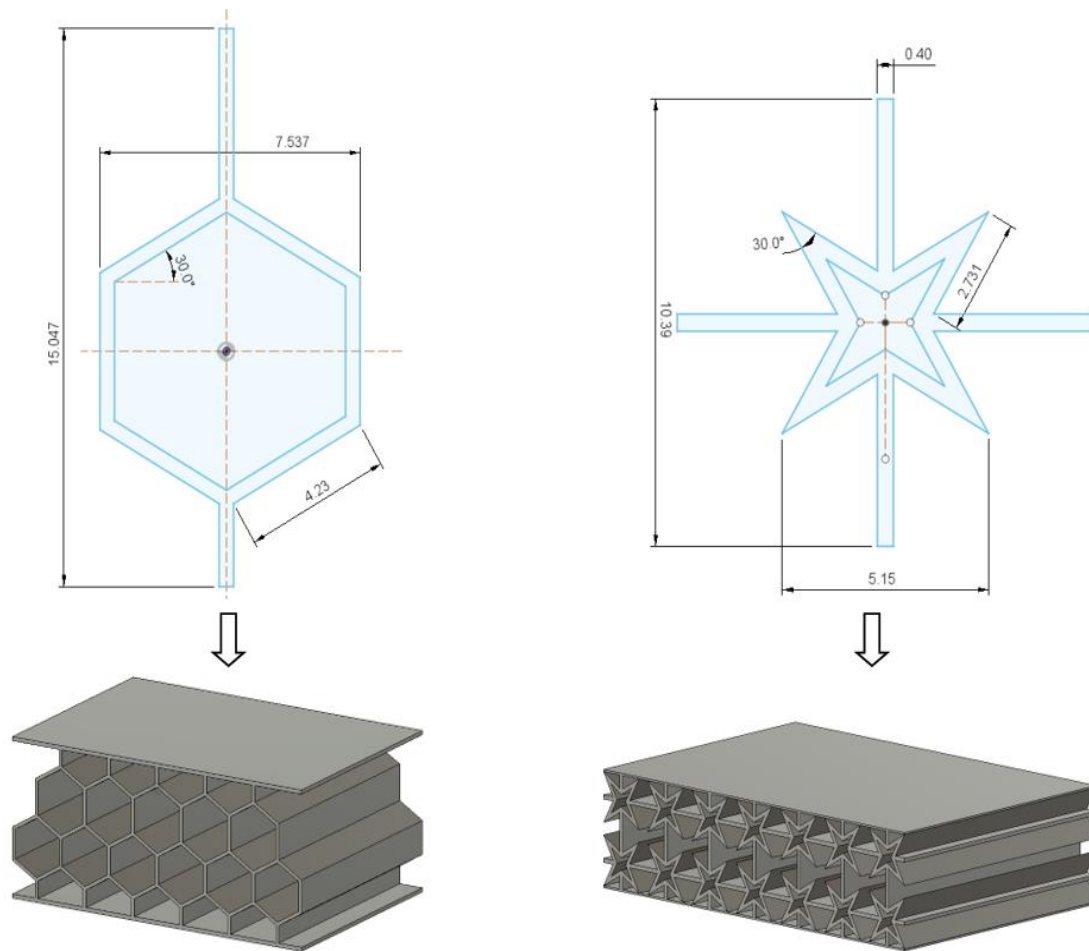
Figure 4.2 Non auxetic honeycomb structure and star-shaped auxetic structure.

In both FEA studies a 9 mm diameter bullet at speed of 830 m/sec was used. The total duration of each study was 1 ms (see figure 4.3). The proper displacement restraint has been determined on the lateral surfaces of the two structures (symmetrically). Aluminum alloy A5052-H34 was used as study material of the cellular structure due to its high stiffness. Table 4.1 shows the properties of the material used.

Young's Modulus (GPa)	Poisson's Ratio	Yield Strength (MPa)	Tensile Strength (MPa)	Shear Modulus (GPa)	Density (kg/mm^3)
70.33	0.36	213.7	262	25924,2	2.68E-06

Table 4.1 Properties of Aluminum 5052–H34.

There are 40.991 FE nodes, and the elements of the model are 20.614; the number of time steps of simulation is 25. Also, the finite elements are of the tetrahedral type. Finite Element Analysis (FEA) was performed using the Autodesk explicit analysis algorithm. The parametric model has been generated with the use of Autodesk Fusion 360 platform. In order to specify the effect of impact force on each structure, the maximum stress (Von Misses) and maximum displacement have been calculated. Figure 4.4 shows the maximum stress on auxetic and conventional structure (Tairidis et al., 2022). The maximum displacement on conventional and auxetic structure respectively, is shown in figure 4.5.

time period: 0.2 ms   time period: 0.6 ms

time period: 0.8 ms   time period: 1 ms

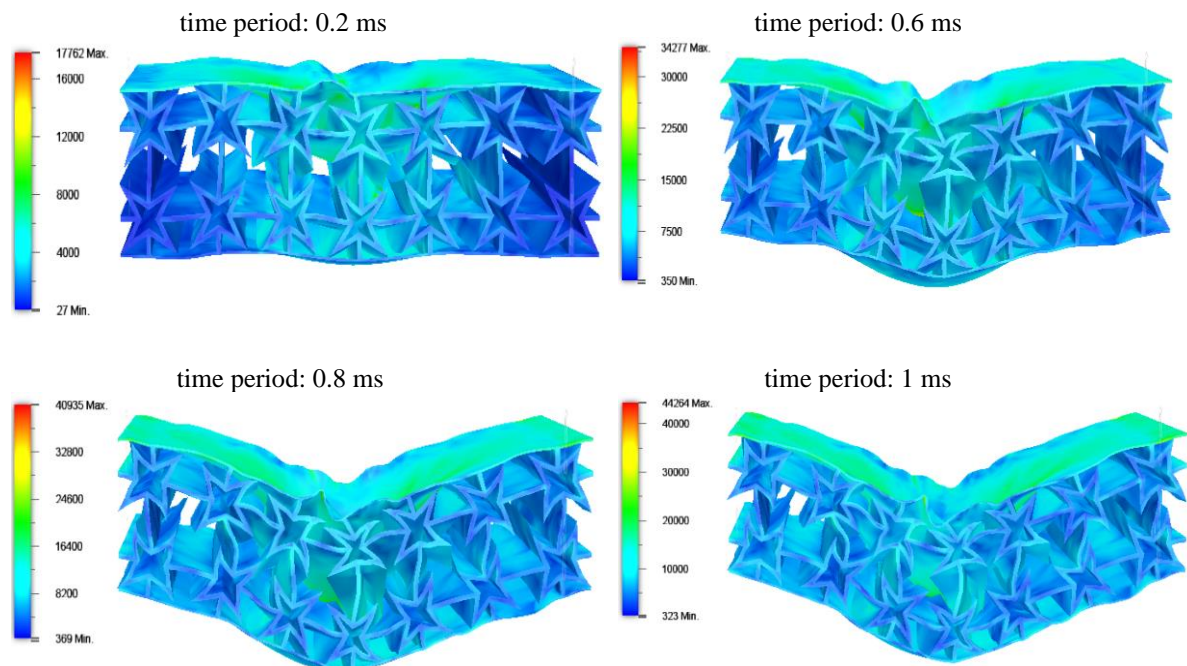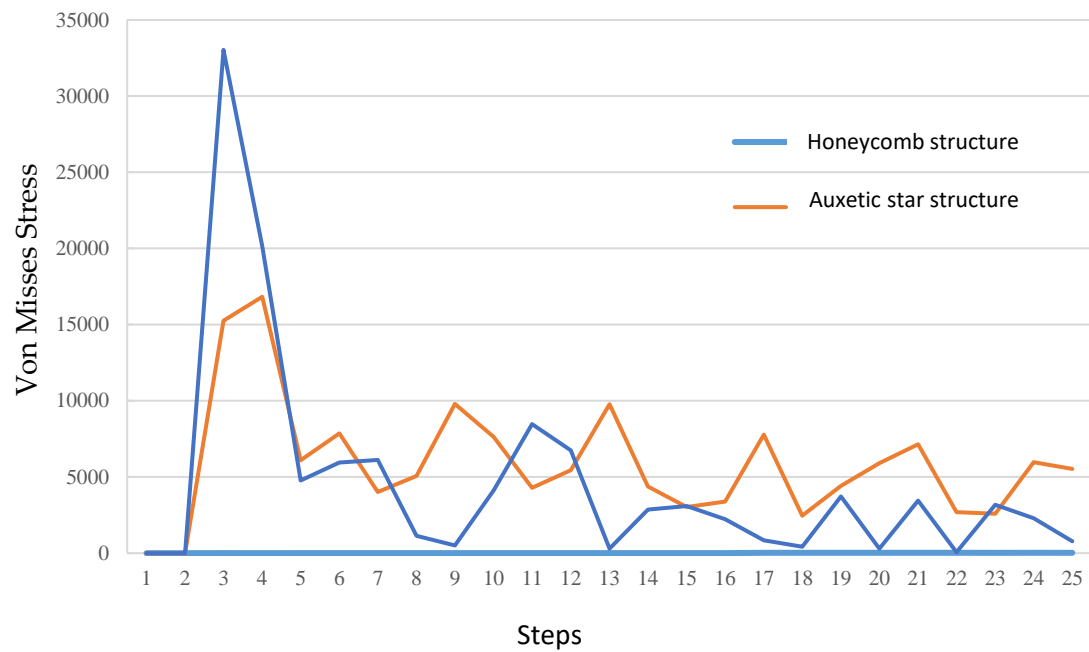Figure 4.3 Bullet impact on the baseline auxetic star-shape sandwich panel.

Figure 4.4 The impact von Misses stress of the upper surface of conventional honeycomb structure and auxetic star shape structure. The total stress on conventional structure is double compared with star shape structure.
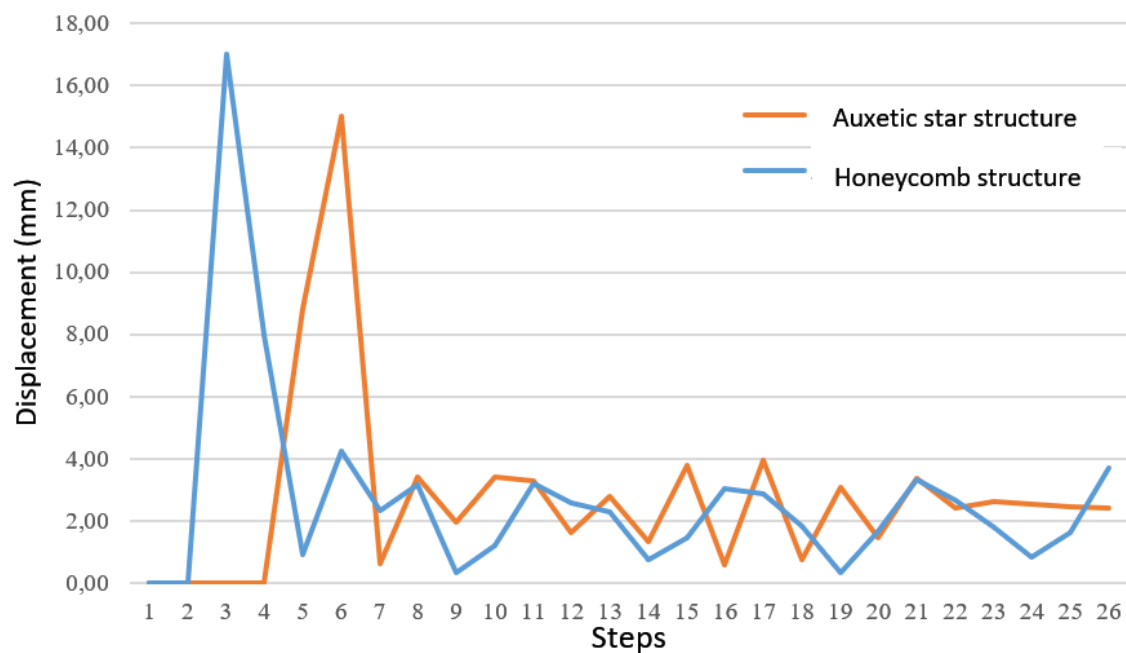
Figure 4.5 Displacement of the upper surface of conventional honeycomb structure and auxetic star shape structure.

For each structure, the stress on the top surface is higher than the bottom surface during the impact load period. After releasing the impact load, the stresses on the bottom surfaces were reduced for both the honeycomb and the star-shaped auxetic structure. During the dynamic test the material behavior is in the elastic region.

From the numerical experiments of the present investigation, it was shown that auxetic materials have unique mechanical behavior, which is based on negative Poisson ratio of the cell structures. The results showed that even if the structure was subjected to extremely high impact loads, the auxetic materials maintained a very good behavior. According to the results, on the front surface of the auxetic structure the movement is smaller and on the back surface the movement value is lower related with to the maximum values. Thus, it is noted, that the rate of the vibration damping is smoother in the auxetic structure, compared to the non-auxetic, where a constant movement is present during the analysis. It was also shown that a significantly higher Von Mises stresses are measured at the non-auxetic structure (Tairidis et al., 2022).

CHAPTER 5

Utilizing Topology Optimization, Generative Design and Additive Manufacturing to product design process

5.1 Generative design framework

A generative design study is a set of data that describes a design problem. Several design constraints can be added which describe a specific design objective. These constraints include functional, manufacturing, and mechanical requirements. Also, material type and performance criteria have to be defined. Once the study setup is defined, a set of potential design solutions, that meet these requirements, are suggested.

Define Objectives

Optimization objectives and limits must be defined, to specify additional requirements that the outcomes should satisfy. The solver tries to achieve the limits, through a number of iterations. Maximizing stiffness and minimizing mass are the basic objectives. If the desired result is to achieve the maximum possible stiffness of the design for a given mass, then maximization of stiffness has to be selected, specifying the value of the mass target. On the other hand, the objective of mass minimization gives the minimum possible mass of the design.

Define manufacturing methods and materials

It is possible for a single GD study to generate design solutions for several manufacturing methods and materials. Multiple options are available; for each

selected method several protentional design solutions are generated. The manufacturing cost estimation for a specific production volume is available. Materials with different properties for each manufacturing method can be defined. It is possible to select several materials for all manufacturing methods. At least one material for each activated manufacturing method has to be defined.

Preserve geometry

Preserve geometry should represent the minimum geometry that is needed in the final shape of a design. It should include sections of geometry that are essential for the performance and functionality of your design. A preserve geometry can include:

- a connection to attach a body to other objects, like bolt holes
- a body that interacts with objects like handles or handlebars
- geometries, where loads and constraints are applied, must be defined as preserved geometry
- Areas that ensure that the design is suitable for use in its intended environment

Obstacle geometry

Obstacle geometries are often used when the geometry attaches to other objects, to prevent the body from extending into and interfering with, other objects. When other objects attach to an obstacle geometry, they are moving. Obstacle geometries are often used at connection points. For example, to keep the hole for a bolt free of material, or to represent the freedom of movement to enable placing the bolt into the hole freely. Bodies assigned an obstacle geometry are displayed in red on the canvas. They represent empty spaces where the material is not created during the generation of outcomes.

Starting shape

Starting shape is defined as an initial geometry type in the design space. A body is assigned as starting shape to optimize an existing design or influence the shape of the generated design. A body is defined as starting shape in the initial stage of the design process. It is determined by all important points given in the definition of the design problem. The outcome generation is performed based on this shape. If a model includes a starting shape, it is the initial shape for the generation process. If the model does not include the starting shape, the initial shape is defined based on the preserved geometry. In a GD study, only one body of the model can be defined as starting shape. If there is no assigned body as starting shape the algorithm is executed with increased freedom and probably gives more variation in outcomes.

Structural constraints and load cases in a generative study

Constraints are a critical part of the design requirements in a generative study and influence the final shapes of outcomes. At least one constraint must be applied in a GD study. Structural constraints enable to define how the design interacts with the objects that does not include in the model and how it is fixed. Constraints are applied to the model to prevent it from moving in response to applied loads. Structural constraints are applied to the preserved geometry y only.

Loads are a critical part of the design requirements in a generative study and influences the final shapes of outcomes. Enable to simulate pushing, pulling, and twisting forces that the design should withstand. Defining loads, enables specifying expectations towards a design strength. At least one load case must be assigned to a preserve geometry body. A load and constraint cannot be on the same face, edge, or vertex.

5.2 Utilizing Generative Design and Additive Manufacturing in product design process

From the beginning of the 20th century until today, the product design process changed drastically. During the last two decades, a well-established design process generally consists of three phases: a) Learn, b) Design, c) Prototype (see figure 2.2). In this section, we focus on prototyping, which includes:

a) creating prototypes to help designers to evaluate an idea
b) creating prototypes to evaluate their stability
c) creating prototypes of optimized design models, utilizing topology optimization for early design stage decision tools
d) evaluate optimized prototypes with FE analysis and experiment

The potential design solutions of a GD study have to meet the manufacturing constraints of the selected Additive Manufacturing (AM) technique. In many of these techniques additional support structures are needed. The extended use of support structures leads to increased manufacturing cost and energy waste (Jiang et al., 2018). Moreover, the design freedom is limited when complex geometries are involved due to an inability to support the stresses inherent within the manufacturing process. In this work, the Fused Filament Fabrication (FFF) and the Wire Laser Metal Deposition (W-LMD) techniques are selected. A critical parameter in order to reduce the support structure volume is the overhang constraint. For FFF method, the overhang angle should be up to 45 degrees and for W-LMD method it should be up to 25 degrees (Ntintakis et al., 2022; Zapf et al., 2017).

The main point of this chapter is the evaluation of the optimized design using ed printed prototypes. Often, from the results of a Topology Optimization and Generative Design studies, complex 3d models are created, which are difficult or impossible to be produced with traditional manufacturing methods. In most cases, AM is the appropriate method to manufacture these complicated structures. In this section, Inject Binder, which is one of the most common Additive Manufacturing (AM) technique, was used for prototypes production. The initial design model is an ordinary table design. Models with different wall thickness are manufactured and then evaluated in a common compression test device. The experimental results are used to perform Topology Optimization (TO) and Generative Design (GD) studies.

5.3 Methodology

The main research question in this study is how topology optimization and generative design help a designer/engineer to take a design decision for a consumer product, like a table, in the early design stage. To answer in this question the study was executed in five stages. Initially, a CAD model of a common table design with outline dimensions of 550x550x450mm was created. Based on this model three specimens each with different inner wall thicknesses, were fabricated with inject binder 3d printing technique. Afterwards, the printed specimen stability was checked experimentally with a compression test device. From the experimental results, a TO study was executed and the optimized shape was evaluated through a FEA study. Next, an extended generative design study was executed in whole table model with different load conditions and the results were evaluated with FEA. The results were reassessed again, and the weakest areas of the optimized model are redesigned, in order to improve the model strength.

5.4 Design and fabrication of specimens

The outline dimensions of CAD model were 550x550x450mm. The specimens wall thickness was 10, 15 and 20mm respectively and the printing scale was 15%. After the printing process had been completed, the post process stage followed, the models were cleaned up from the excess powder and immersed in hardener (see figure 5.1).

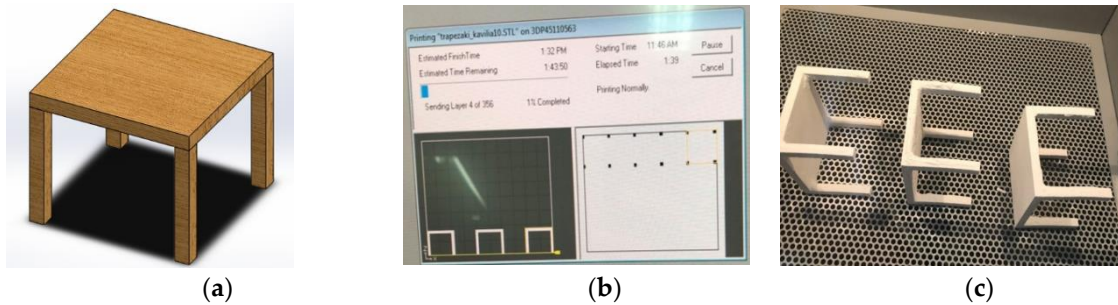(a)   (b)   (c)

Figure 5.1 a) CAD models design b) Printing process and c) post processing stage.

5.5 Compression Tests Results

The fabricated samples were tested in a general compression tester machine. The piston speed was 2mm/min. The samples are forced at the center of crosshead so to be compressed uniformly (see figure 5.2).

Figure 5.2 Compression test processing.

Specimen Type	Force (N)	Duration (s)	Piston Distance (mm)
Table 10	84	38	1,3
Table 15	156	36	1,2
Table 20	244	25	1,5

Table 5.1 Compression test results

The machine piston moved 1.3 mm and the specimen with 10mm wall thickness (table 10) broke on 84 N. The specimen with 15mm wall thickness (see table 5.1) was more durable (156 N) than the first sample. The duration of test was 38sec, by two less than 'table 10' model. This behavior is explained by to the higher durability of this sample. The third specimen with 20 mm wall thickness was the most durable sample (244 N). The machine piston moved for 1.5 mm. The first sample elastic behavior was higher than the others. The above-mentioned experimental results are utilized as boundary conditions for TO and GD studies.

5.6 Topology Optimization study

Afterwards, based on the experimental results, a TO study for the table model is performed on Siemens NX software. The material properties were similar as powder in Z-450 printer [28]. According to the optimization scenario, table legs shape and size remained the same and the upper table surface were optimized. As design space, the total model volume was determined. Only the upper surface of the model is defined as 'keep in', which means that only this body will be optimized topologically. The selected design constrains are a) Void Fill and b) Material Spreading in 35%. The load conditions were based on the results of compression test. A vertical force of 250 N was applied on the upper surface. A fix constraint was added at the bottom of the table legs. An additional design constraint was added to keep the optimized surface in contact with the legs. Figure 5.3 shows the results of TO study.
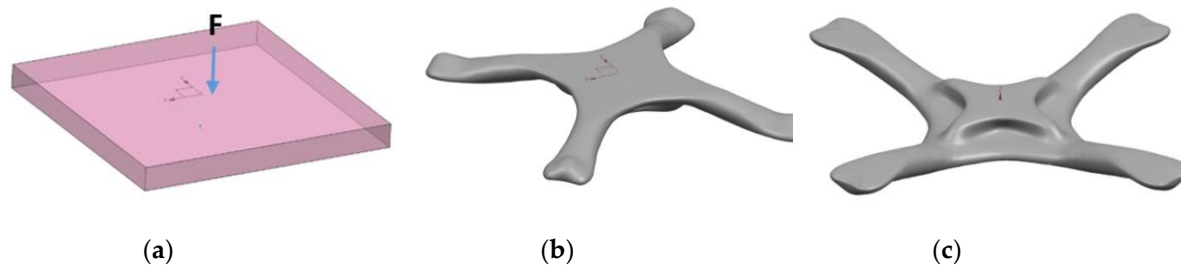
Figure 5.3 a) Initial CAD model of table surface (design space) b), c) the top and bottom view of the optimized table surface.

From the results, it is observed that all design constrains are satisfied. The total volume of the initial design volume was reduced about 86 % and the optimized model is stiffer than before (see figure 5.4) (Ntintakis et al., 2020).
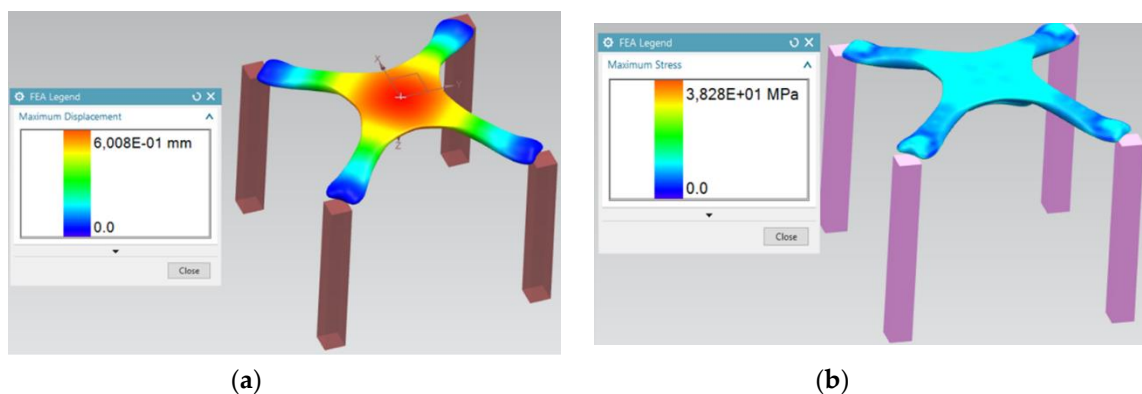

Figure 5.4 a) The maximum displacement color graph and b) the stress graph of the optimized table surface model.

5.7 Generative Design study

From the initial results mentioned above, it is observed that the shape of the optimized structure is not predictable. The optimized model durability has been increased and total mass has been reduced. However, the top surface of the model was not kept flat throughout the length and width of the table design. In the following GD study, new design constrains were added. Initially, the upper surface of the table is defined as flat with a certain thickness and the table legs shape will be optimized too. In addition to the main vertical force of 250N, two horizontal forces of 30 N have been added on the table surface sides. More predictable results will be achieved with additional constraints, such as the space between the table legs, which will be empty of material (see figure 5.5).
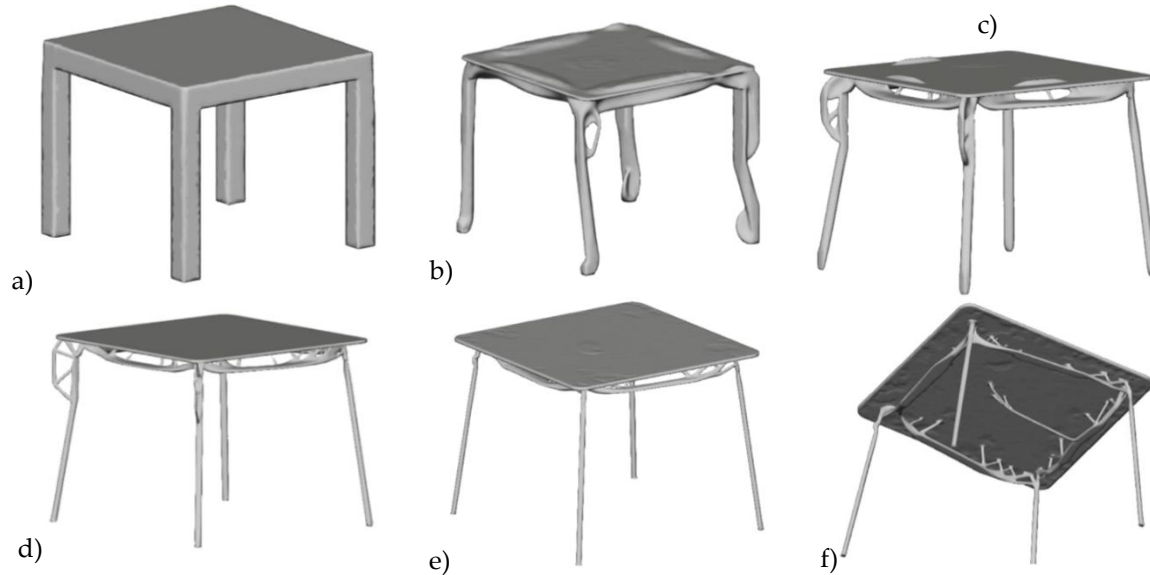
Figure 5.5 Material distribution during generative design process. The algorithm starts from the initial model (a) and after 45 iterations the optimized model created (f), the intermediate model shapes were shown from b to e.

The above GD study was executed in Autodesk Fusion 360, on cloud, in less than an hour. The shape and the structure of the initial model has changed significantly. After judging of all possible design solutions, the design of final iteration was selected. All design constraints were fulfilled, and the shape of the optimized model were accepted. The optimized model is compatible with additive manufacturing techniques.

The material distribution on the upper surface of the table was not as expected; in some case there is an extra amount of material. This amount of material act as ribs and thus affect the material distribution in the rest of the model. Therefore, additional design constraints were defined, so that the table surface is kept flat. Particularly, an 'obstacle geometry' constraint was added, so to keep the table surface empty of material. Adding this constraint, the material distribution throughout the optimized model has changed (see figure 5.6) (Ntintakis et al., 2020).
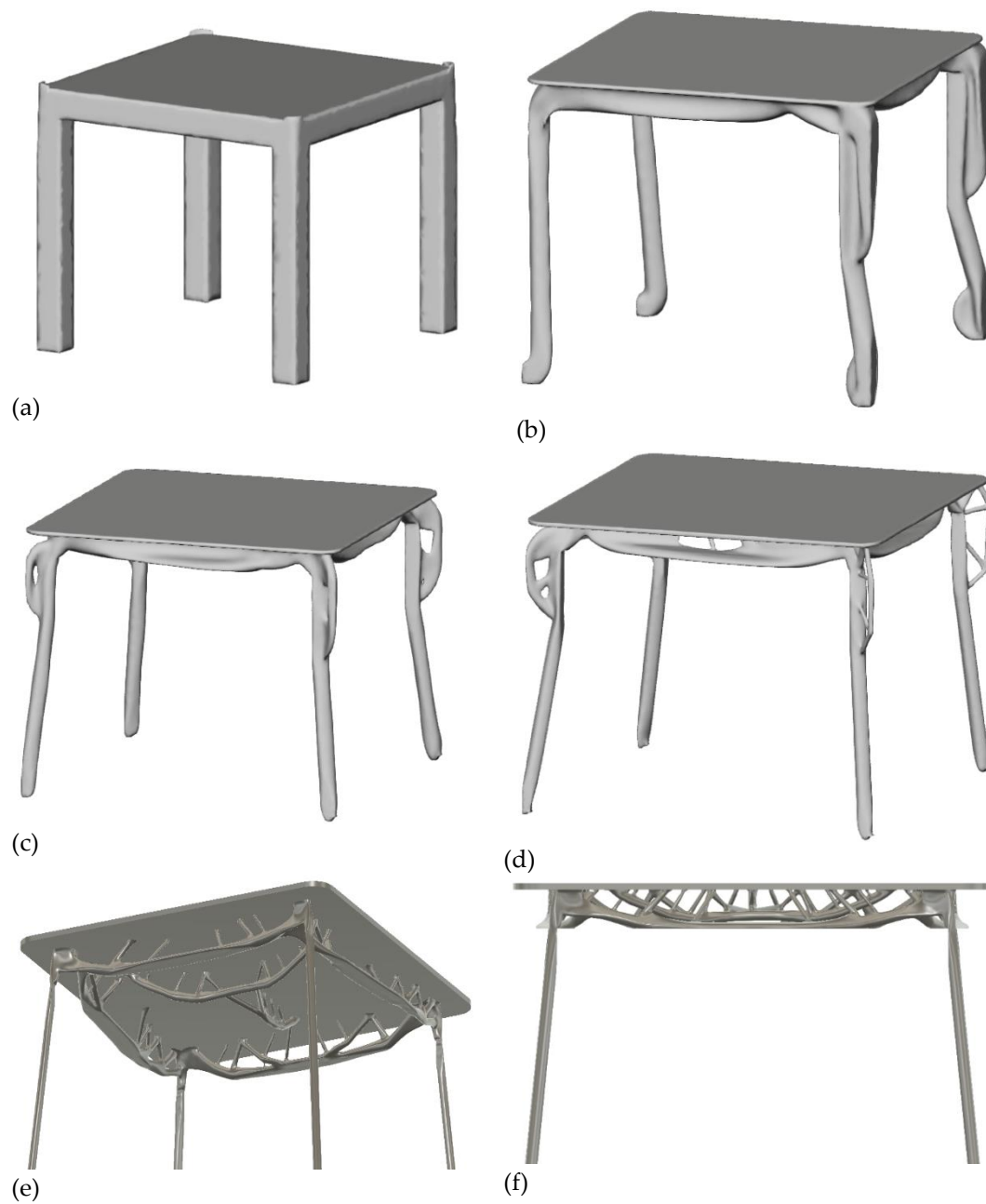
Figure 5.6 Material distribution changed when new design constraints were added. The algorithm starts from the initial model geometry (a) and after 42 iterations a new optimized model is created (f).

5.8 Evaluation of optimized models with Finite Element Analysis (FEA)

The above final model was evaluated with FEA study. The boundary conditions were the same as before (250 N vertical force and two horizontal forces of 30 N). The FE model consists of 108.038 tetrahedral elements with mesh edge length of 1 mm; figure 5.7 shows the results of FE analysis.
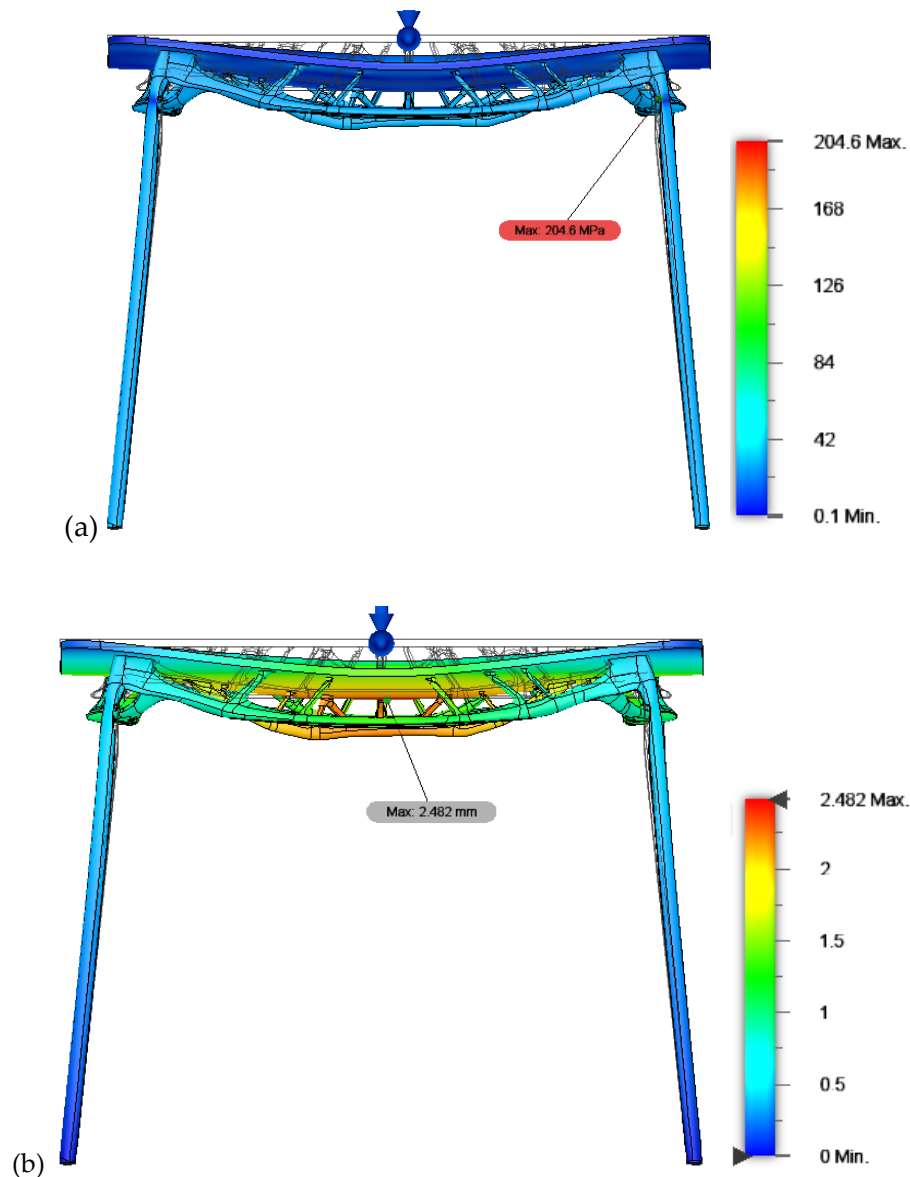

Figure 5.7 FE analysis results, a) Von Misses Stress and b) Total displacement of the optimized model.

The results of FE analysis show that the model was deformed permanently and fractured at the area where legs are connected to the table surface. In the rest model bodies the stress is low (below of 45 MPa). The results of the FE analysis led to re-design the weak area of the legs, in order to improve the whole model strength and to create a more symmetrical structure. Figure 5.8 shows the results of the redesign process around the legs. Then, in order to verify the results of the above analysis, two new FE analysis with lower vertical force of 200 N and 150 N were performed. The other boundary conditions remain the same. Table 2 shows the results of all FEA studies for the initial and the redesign models.
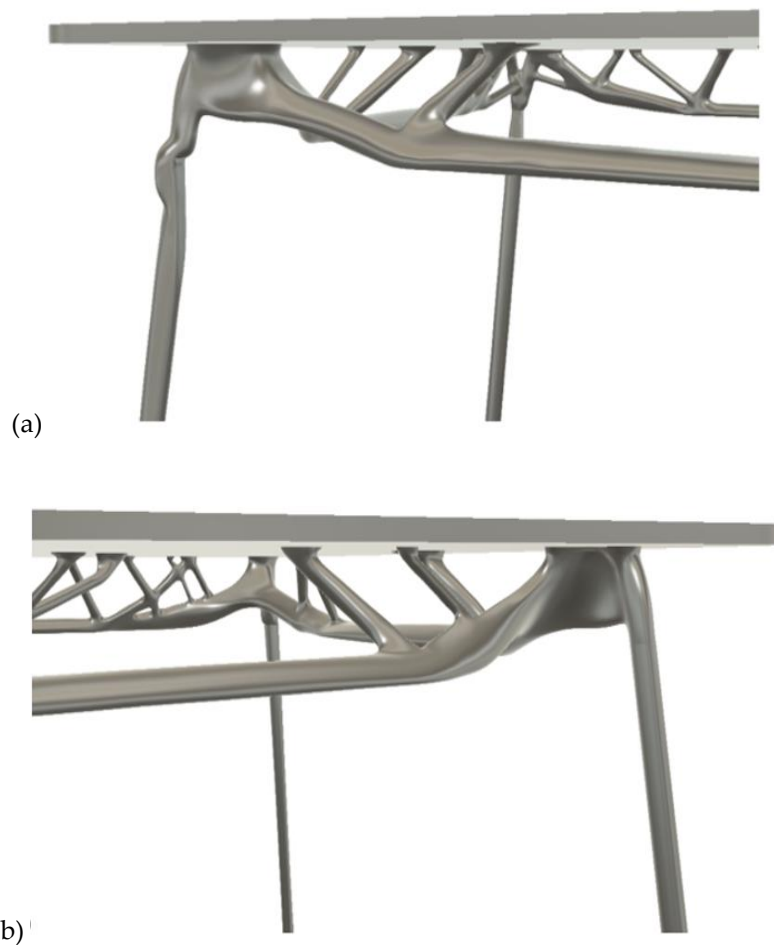

(a)

(b)

Figure 5.8 a) The initial shape of the table legs before the redesign process b) The new leg shape is more durable and uniform.

Figure 5.9 shows the FEA results of the redesigned model; the boundary conditions were kept the same as in the initial study. From the results, it was observed that the total Von Misses stress of the redesigned model was reduced significantly (about 30%). Especially, in the area around the redesign structures, the stress was up to 35MPa. Compared with the pre redesign shape, stress was reduced by about 80%. The total displacement of the model was increased by about 9 %, from 2.48 mm to 2.70 mm.
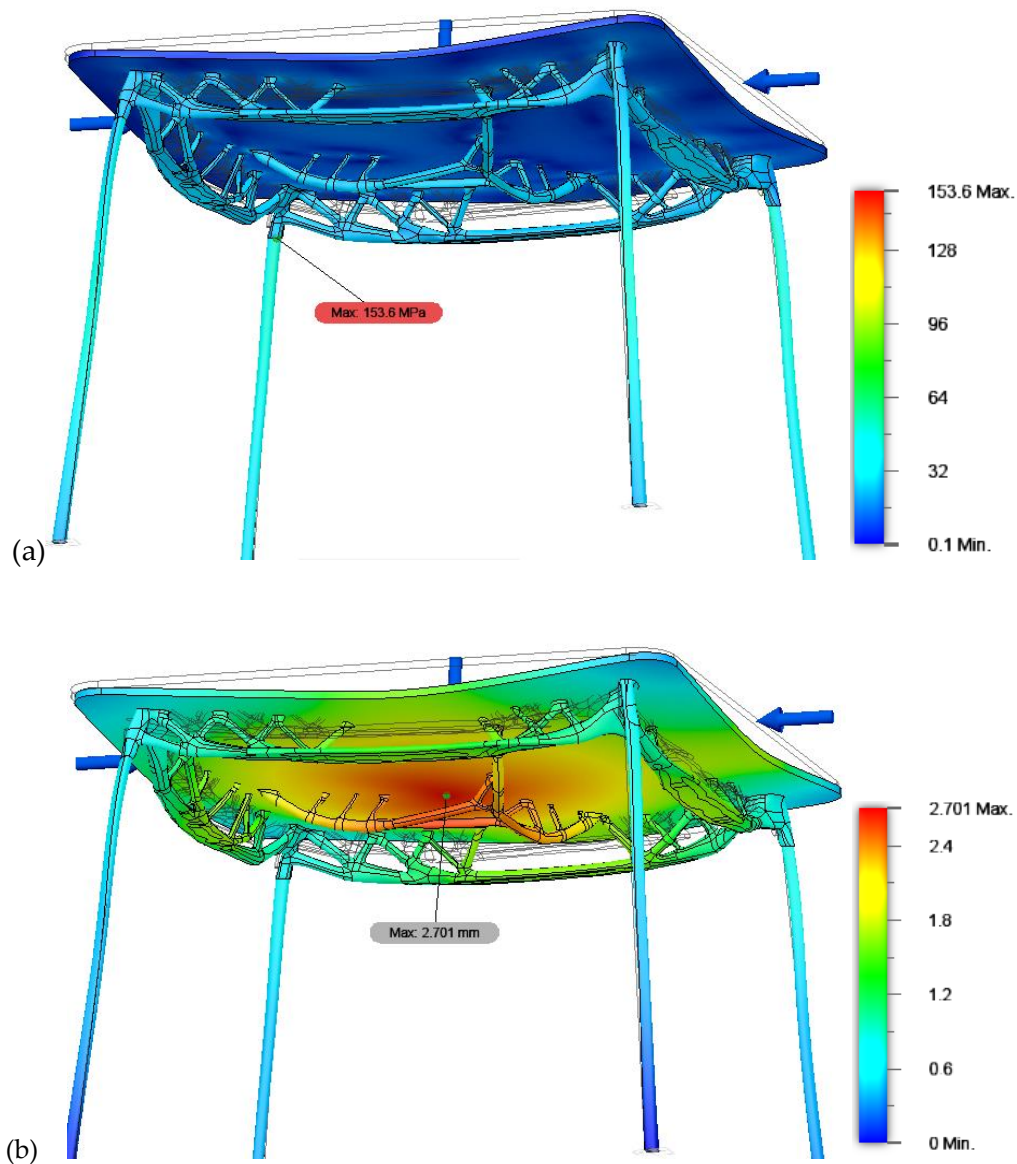

Figure 5.9 a) The behavior of the redesigned model, a) the Von Misses stress, and b) the total displacement.

Table 5.2 shows the results from all FEA studies comparatively. The improvement in model behavior after the redesign process was obvious. The durability of the optimized model improved significantly due to the reduced model stress, especially in the redesigned areas. Possibly, further redesign of the model structure would lead to even better mechanical behavior.

Model	Force (N)	Max Stress Von Misses (MPa)	Total Displacement (mm)
Initial model study_1	250	204	2.48
Redesigned model study_1		153	2.70
Initial model study_2	200	163	1.98
Redesigned model study_2		123	2.16
Initial model study_3	150	123	1.49
Redesigned model study_3		92	1.62

Table 5.2 Results of FEA of the initial and redesigned model.

Product design process has entered a new and extremely interesting period. Engineers have the ability to create new products utilizing computational mechanics and artificial intelligent algorithms. The main research question is how TO and GD can help an engineer to take the right decision for a product design; Taking into account the results of this study the answer is very encouraged. A main conclusion from the aforementioned results is that TO output give only one design solution. On the other hand, GD outputs there are several potential solutions taking into account not only design constraints (like TO), but also other products, cost and production constraints. In both methodologies, the designer must judge carefully the potential design solutions in order to utilize the most appropriate shape. During the early design stage (concept design), generative design is a useful tool for designers to make the right decision about shape, aesthetic, and the durability of the product.

CHAPTER 6

Redesign mechanical components utilizing Generative Design and Additive Manufacturing

6.1 Design of mechanical components

A generative study is a set of data that describes a design problem one wants to solve using generative design. The GD flowchart starts with the input of specific design objectives such as functional, manufacturing, and mechanical requirements. Then the boundary conditions, the definition of material properties, the load cases and the displacement restraints are set. Once the study is set up, a set of designs that meet these requirements will be generated. The purpose of the current study is to redesign the pneumatic cylinder mounts, in order to minimize the weight of the model without significantly affecting the safety factor.

The potential design solutions of a GD study have to meet the manufacturing constraints of the selected Additive Manufacturing (AM) technique. In many of these techniques, additional support structures are needed. The extended use of support structures leads to increased manufacturing cost and energy waste. Moreover, the design freedom is limited when complex geometries are involved, due to an inability to support the stresses inherent within the manufacturing process. In this work, the Fused Filament Fabrication (FFF) and the Wire Laser Metal Deposition (W-LMD) additive manufacturing techniques are selected. A critical parameter to minimize the support structure volume is the overhang constraint. For FFF method, the highest overhang angle is 45 degrees and for W-LMD method 25 degrees.

Pneumatic cylinders are very common mechanical devices which use the power of compressed air to produce a force in a reciprocating linear motion. In the current thesis, a GD study for three pneumatic cylinder mountings is executed. The initial models of standard pneumatic cylinders with detachable mountings are considered conforming to ISO 15552 specification (see figure 6.1) (Ntintakis et al., 2022).
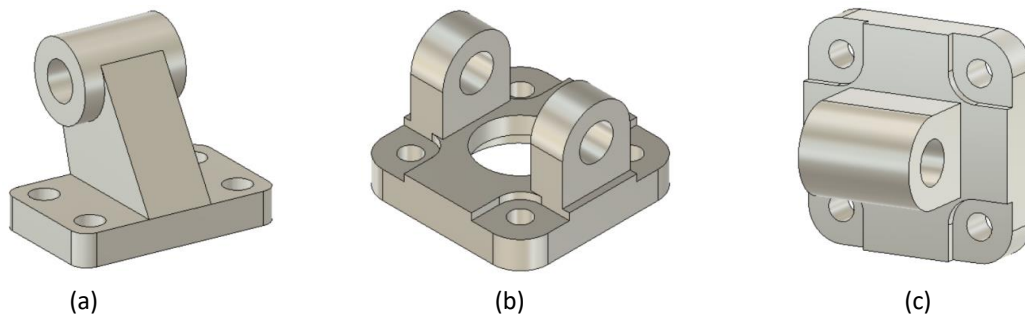
Figure 6.1 The initial models of the three mounting components, a) Pivot bracket with rigid bearing AB7, b) Clevis bracket MP2 and c) Clevis bracket MP4.

6.2 Definition of Objectives

Generative design study allows to specify manufacturing constraints that outcomes should satisfy. In current study the manufacturing constraints are set for FFF and for W-LMD additive manufacturing techniques. Especially, the highest overhang angle should be 45 degrees for FFF and 20 degrees for W-LMD; also, the minimum wall thickness should be no less than 1 mm. Each body of the initial models has to be defined as preserve geometry, starting shape, or obstacle geometry, respectively. Perverse geometry is defined, in this study, as the holes where bolts, bearings and axes are fitted. As starting shapes, the bodies designs are defined, which are in contact with the perverse geometries. Also, the initial shape of the models is defined as space (see figure 6.2). The algorithm starts the redesign process taking into account the initial model shapes. Afterwards, bodies that have to remain empty of material are defined as obstacle geometry. For all models, the aluminum alloy was set as study material (see table 6.1).

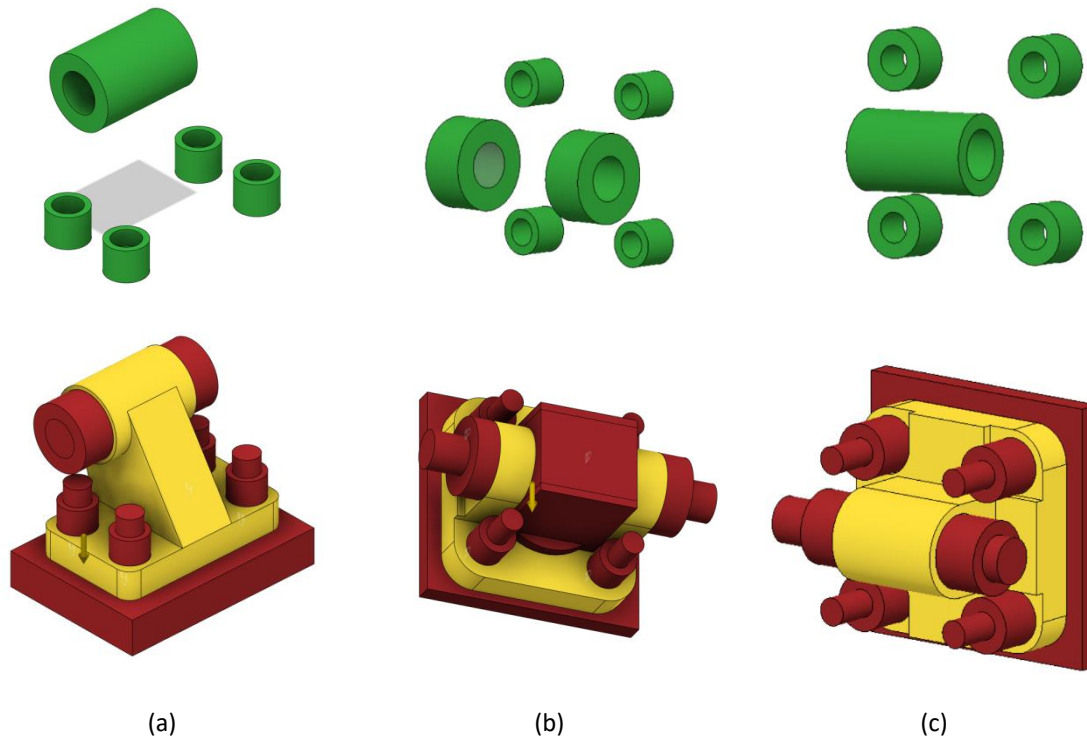(a)   (b)   (c)

Figure 6.2 The assigned perverse geometry displays in green color, the starting geometry displays in yellow color and the obstacle geometry displays in red color.

Young's Modulus (GPa)	Poisson's Ratio	Yield Strength (MPa)	Tensile Strength (MPa)	Density (g/cm^3)
68,900	0,33	275,000	310,000	2,700

Table 6.1 Material properties.

Structural loads and constraints are applied to the preserve geometry only. Because of the cylinder reciprocating linear motion, two different load cases were set. In the outward stroke motion, the force is 804 N and in return stroke is 691 N. At the bolt holes, structural fixed constraints are applied (Ntintakis et al., 2022).

6.3 Generative design results for FFF/FDM additive manufacturing technique

A Generative Design study creates lots of designs in an evolutionary way. According to GD flowchart, the designer judges the outcomes; if the designer does not accept the potential solutions, the source code and the parameters study have to be changed. According to the results, several potential design solutions are created (see figure 6.3). During the judging phase, the most appropriate solutions for further evaluation were selected (see figure 6.4). A number of criteria led to the selection of the optimized

solution. One of these is the weight reduction, in combination with safety factor value. The selected design solutions can be fabricated using FFF technique, without the use of supports. Next, the 3d models of generative designs were created and evaluated using FEA studies. The results were compared with the ones derived from the initial models.
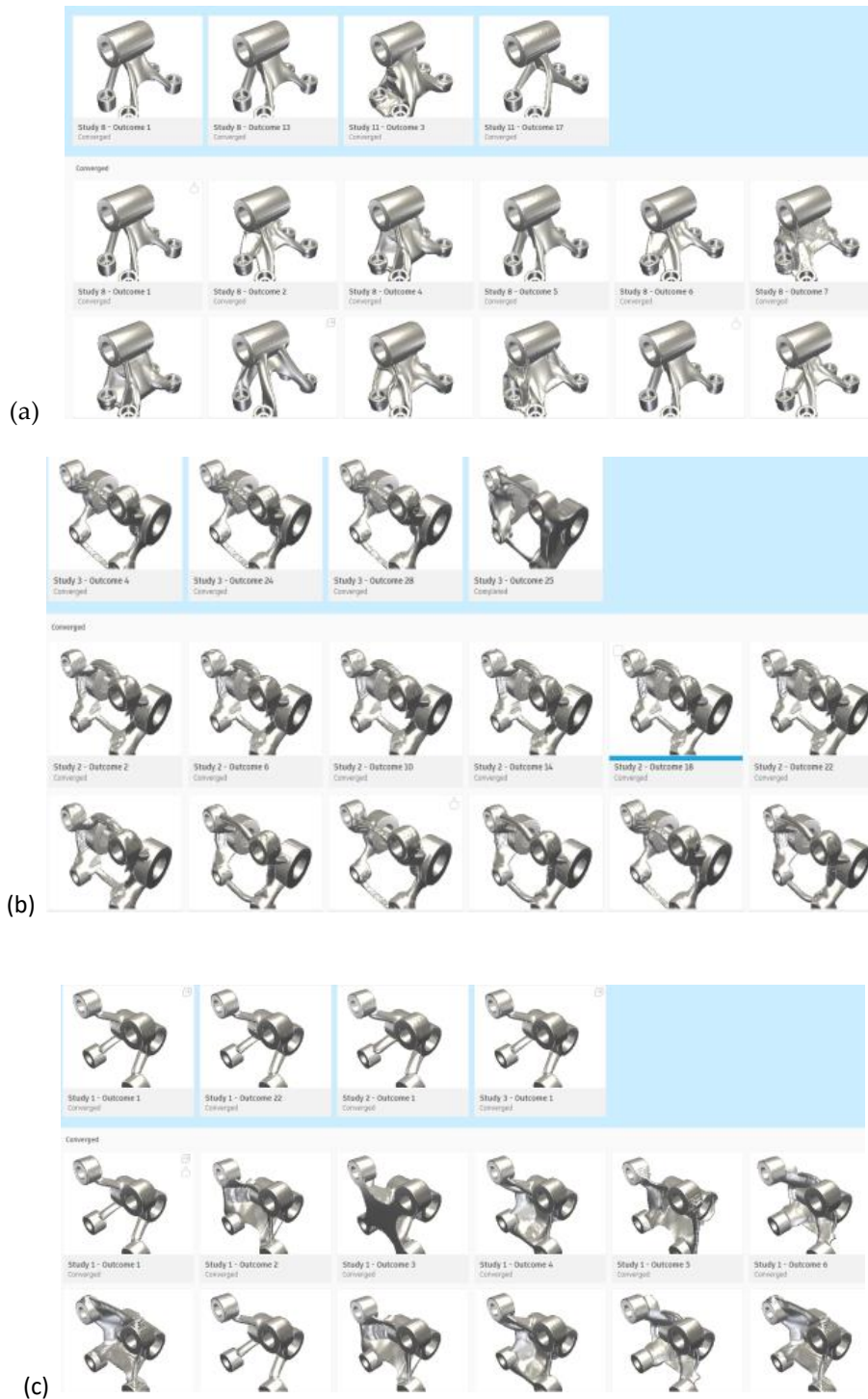

Figure 6.3 Potential design solutions outcomes for the components a) Pivot bracket with rigid bearing AB7, b) Clevis bracket MP2 and c) Clevis bracket MP4.
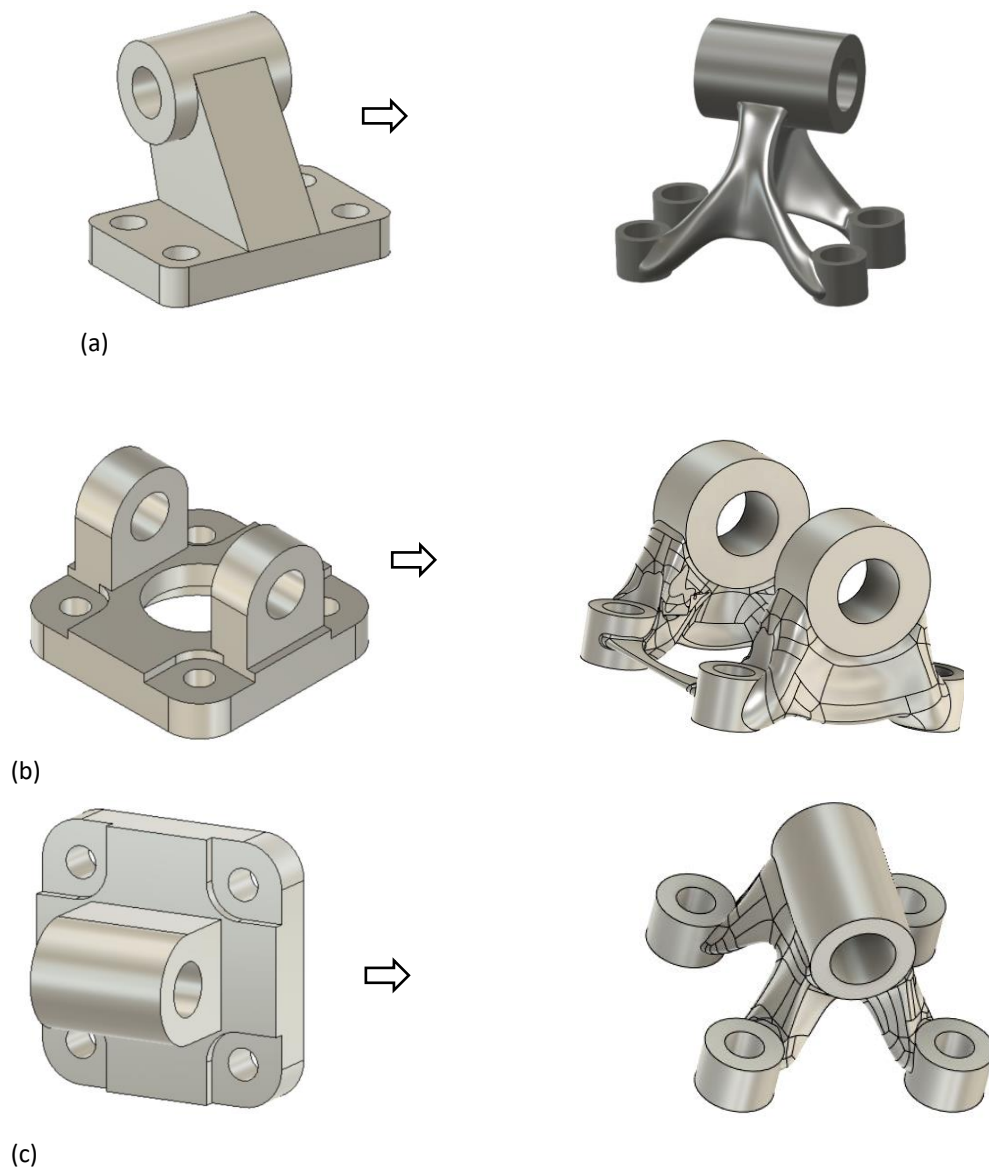
(a)

(b)

(c)

Figure 6.4 The initial and the generated design solution for: a) Pivot bracket with rigid bearing AB7, b) Clevis bracket MP2 and c) Clevis bracket MP4.

6.4 Evaluation of generative models for FFF method

FEA were executed for the initial and generated models. For generative models three meshing models created consisted of 5.696, 32.704 and 6.825 tetrahedral elements of pivot bracket, clevis bracket MP2 and clevis bracket MP4 models respectively (see figure 6.5). Figure 6.6 and figure 6.7 shows the FEA analysis results of total Von Misses stress and total displacement for the generative models in inward and outward stroke linear motion respectively. Table 6.2 shows the compared results of initial and generative models for outward stroke and return stroke linear motion.

In generative model of Pivot Bracket the model mass is reduced about 40%. The Von Misses Stress was 123.7 MPa in outward stork and 153.8 MPa in return stock. Compared with the initial model, the stress is increased significantly. One reason is the assigned fix constraints on the bolts holes, where the maximum stress was observed. On the rest of the body structure, the highest stress is 30 MPa. The total displacement was increased from 0.04 mm to 0.10 mm, as a result of the higher model elasticity.
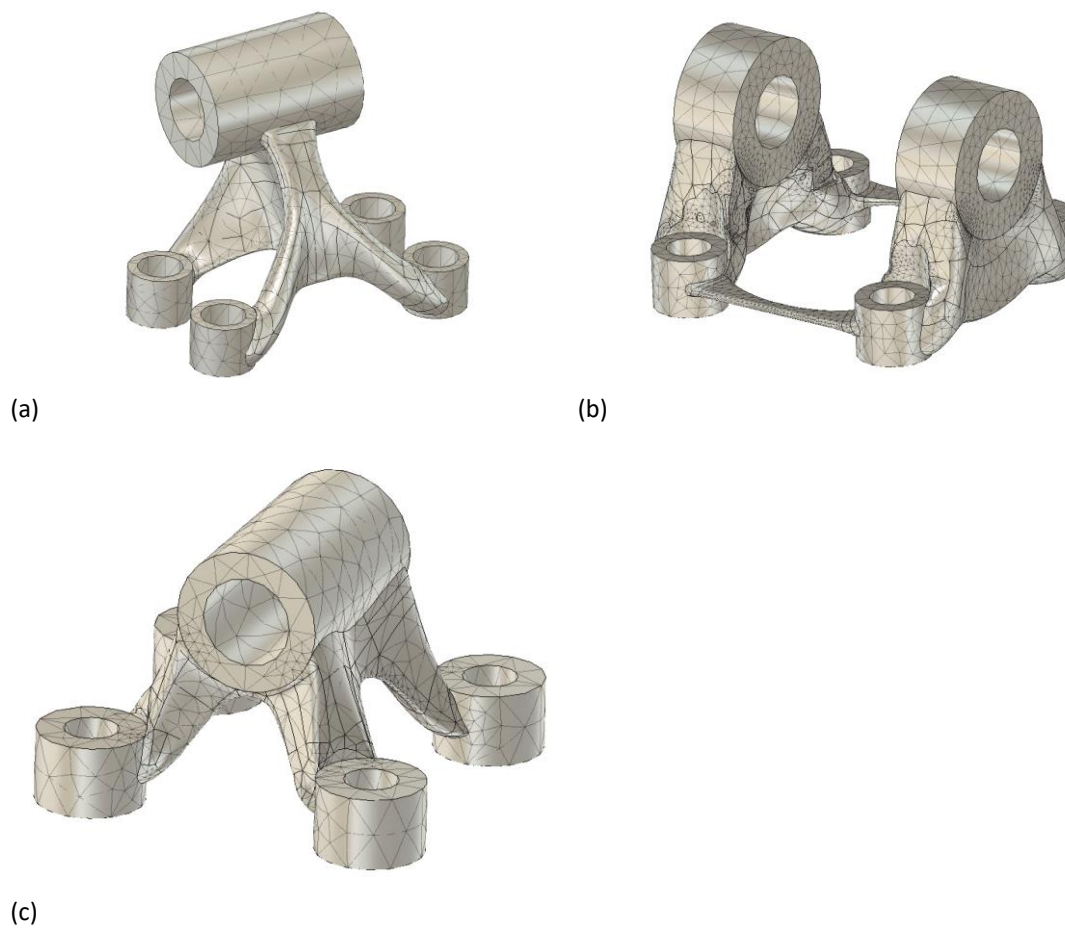

(a)

(b)

(c)

Figure 6.5 Mesh models of: a) Pivot bracket, b) Clevis bracket MP2 and c) Clevis bracket MP4.

(a)

(b)

(c)

Figure 6.6 Results of Von Misses stress (on the left) and the displacement (on the right), for inward linear motion of: a) Pivot bracket, b) Clevis bracket MP2 and c) Clevis bracket MP4.

(a)

(b)

(c)
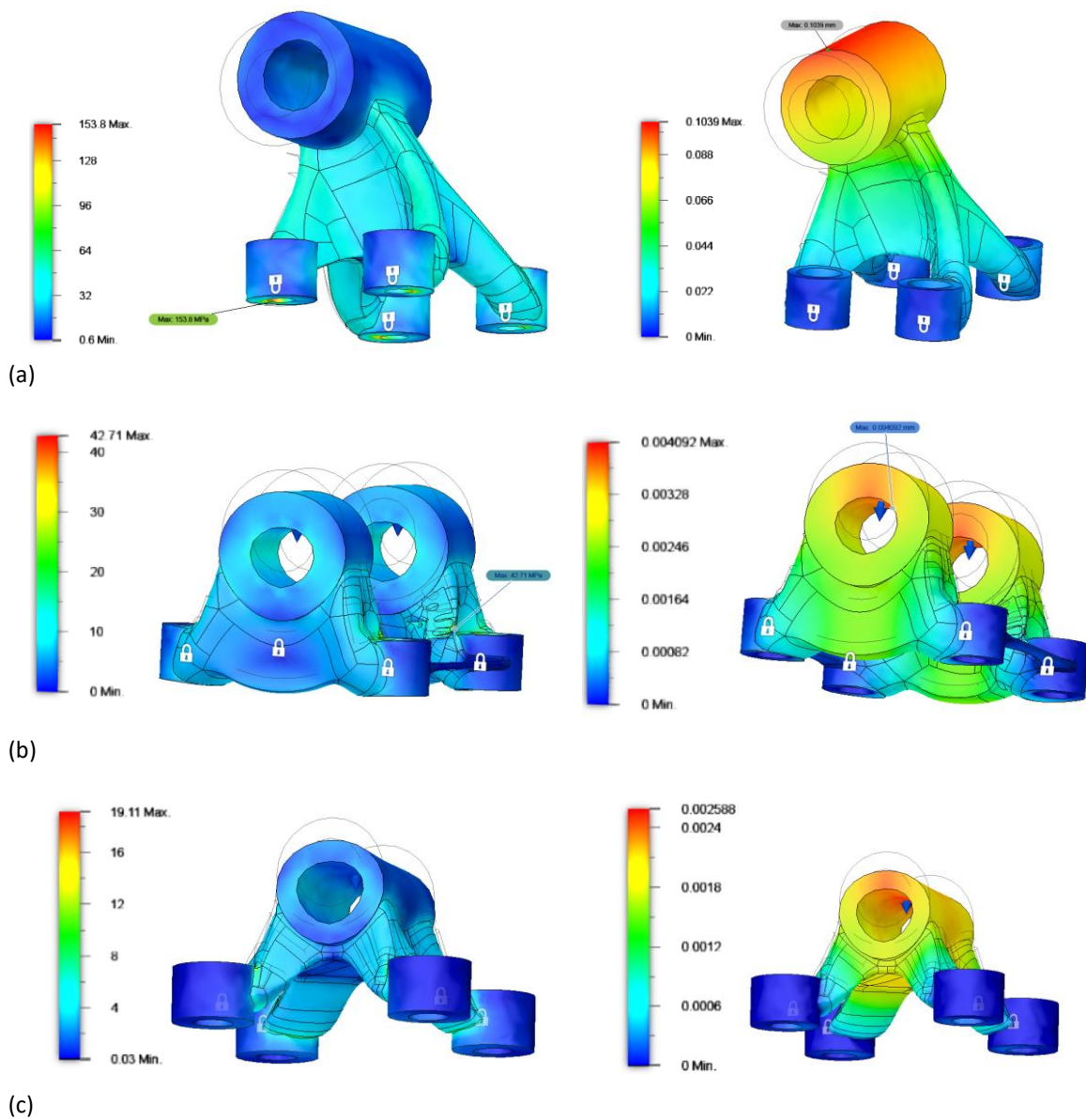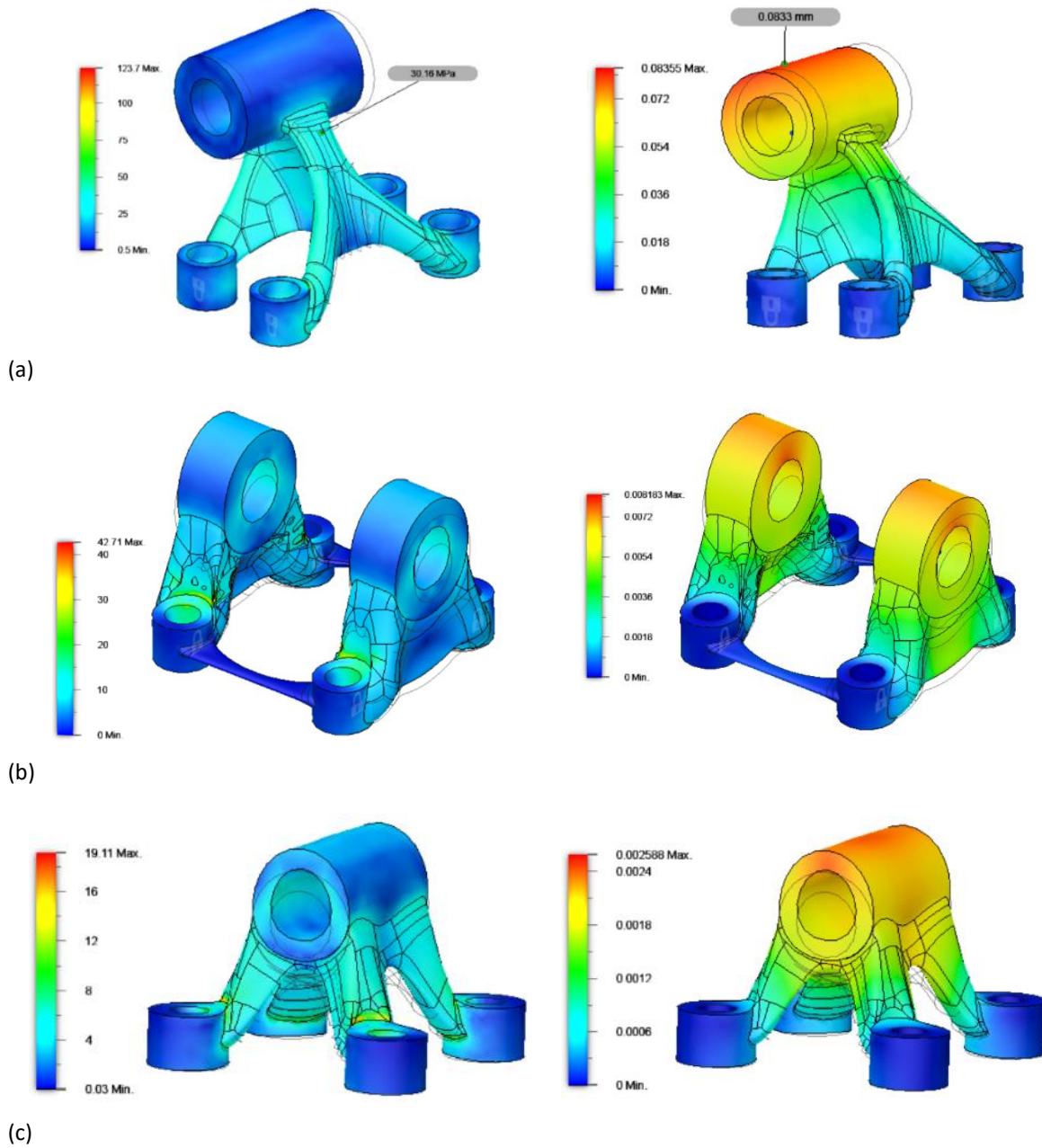
Figure 6.7 Results of Von Misses stress (on the left) and the displacement (on the right) for outward linear motion of: a) Pivot bracket, b) Clevis bracket MP2 and c) Clevis bracket MP4.

On the generative model of Clevis bracket MP2 the Von Misses Stress is about 42 MPa both in outward and in return stock (see table 6.2). The model structure changed significantly and was characterized by an organic shape (see figure 6.4). The total displacement almost doubled from 0.0048 mm to 0.0081 mm in outward stroke linear motion. The model weight was reduced from 52 gr to 31 gr. Although, the stress increased the minimum safety factor being 3.2 on some model edges, while throughout the model is greater than six (see figure 6.7).

Mount Type	Outward Stroke		Return Stroke		
	Max Von Misses Stress (MPa)	Max Displacement (mm)	Max Von Misses Stress (MPa)	Max Displacement (mm)	Weight (gr)
Initial model Pivot bracket	79.6	0.044	79.5	0.044	50
Generative model Pivot bracket	123.7	0.083	153.8	0.1039	29.5
Initial model Clevis bracket MP2	23.3	0.005	22.5	0.0048	52
Generative model Clevis bracket MP2	42.71	0.0081	42.71	0.0041	31
Initial model Clevis bracket MP4	25.86	0.0047	25.2	0.0046	58
Generative model Clevis bracket MP4	19.11	0.0025	19.11	0.0025	33

Table 6.2 FEA results of the generative models.

On the generative Clevis bracket MP4 model, the Von Misses Stress in outward stroke and in return stock is 19.11. Compared to with the initial model, the generated model is stiffer (the stress is reduced from 25.86 MPa to 19.11 MPa), the displacement is also reduced from 0.47 mm to 0.0025 mm (see table 6.2). The model weight is also reduced from 58 gr to 33 gr (Ntintakis et al., 2022).
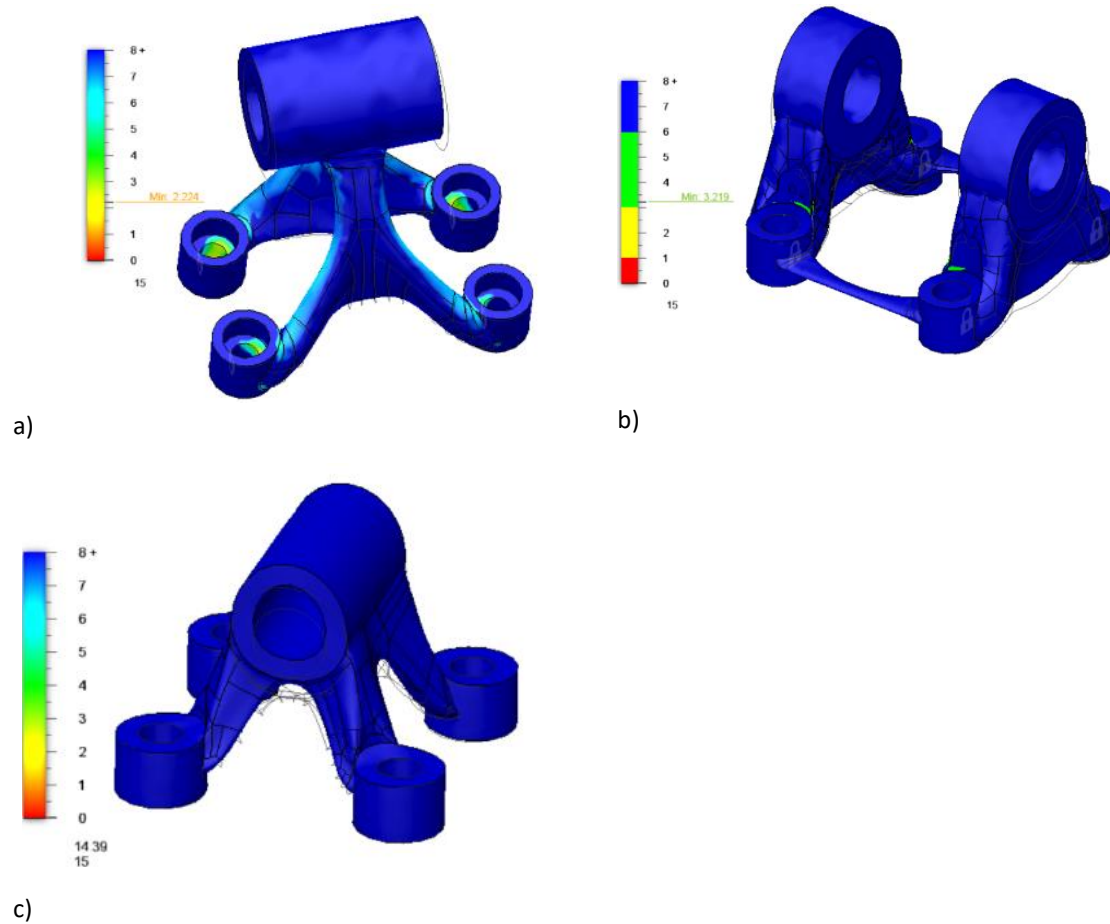

a)

b)

c)

Figure 6.7 The minimum safety factor for each model, a) on pivot bracket model is 2.2, b) on Clevis bracket MP2 is 3.2 and c) on Clevis bracket MP4 is 14.39.

6.5 Generative design results for Wire Laser Metal Deposition (W-LMD) additive manufacturing technique

The results of the above section are referred to generative models for FFF 3d printing technique. In this section new generative design studies are performed with the same initial models and boundary conditions. The only difference is the selection of Wire Laser Metal Deposition technique, as fabrication method. Previously, in order to avoid supports during the printing process, a design constraint of 45 degrees angle was added. According to manufacturing constraints of W-LMD, in order to avoid supports, the overhang angle should be no more than 20-25 degrees. Figure 6.8 shows the intermediate shapes during the GD study. For pivot bracket model the algorithm stops after 20 iterations. Following judgment, the generated model of 18th iteration was accepted as design solution. Compared with the model of 20th iteration, the structure of the 18th iteration model was preferred because it shows similar mechanical behavior, mass properties and structure; also, it is characterized by simplified shape. The W-LMD technique is not preferred for detailed structures and extremely complex structures often fail during the printing process. The generated model of pivot bracket is stiffer than the initial one and the generated model presented a 45 degrees overhang angle. In figure 6.9 the selected 3d model and the stress graph are shown.

(a)   (b)   (c)

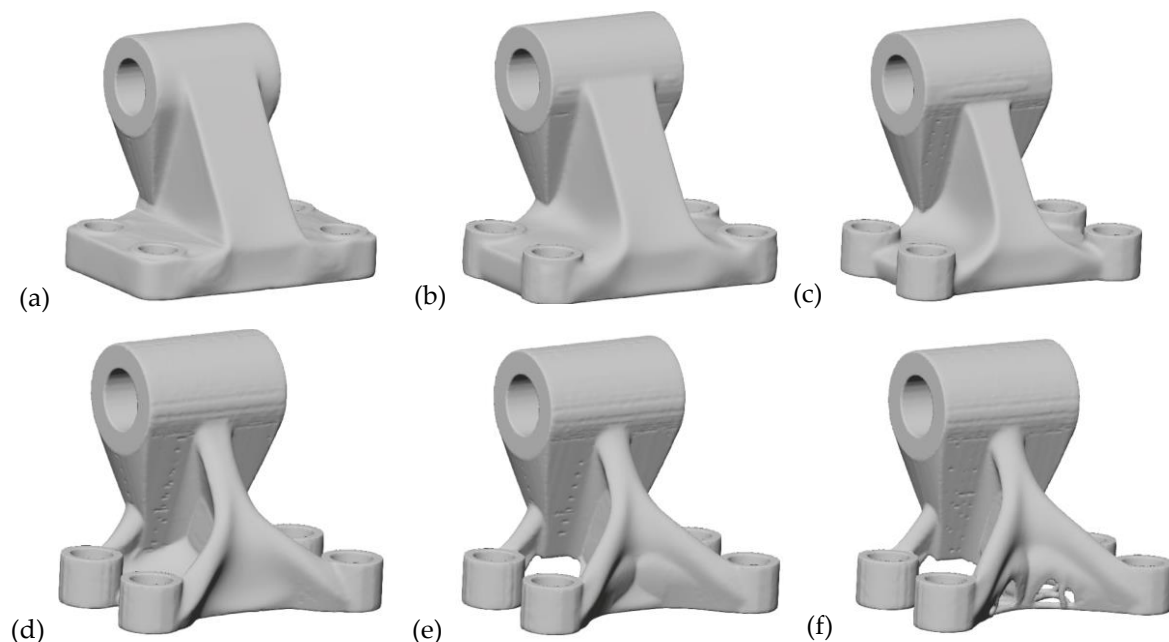(d)   (e)   (f)

Figure 6.8 Material distribution with 20 degrees overhang angle for pivot bracket model, after 20 iterations the process completed a) after 2 iterations b) after 5 iterations, c) after 10 iterations, d) after 15 iterations, e) after 18 iterations and f) after 20 iterations.

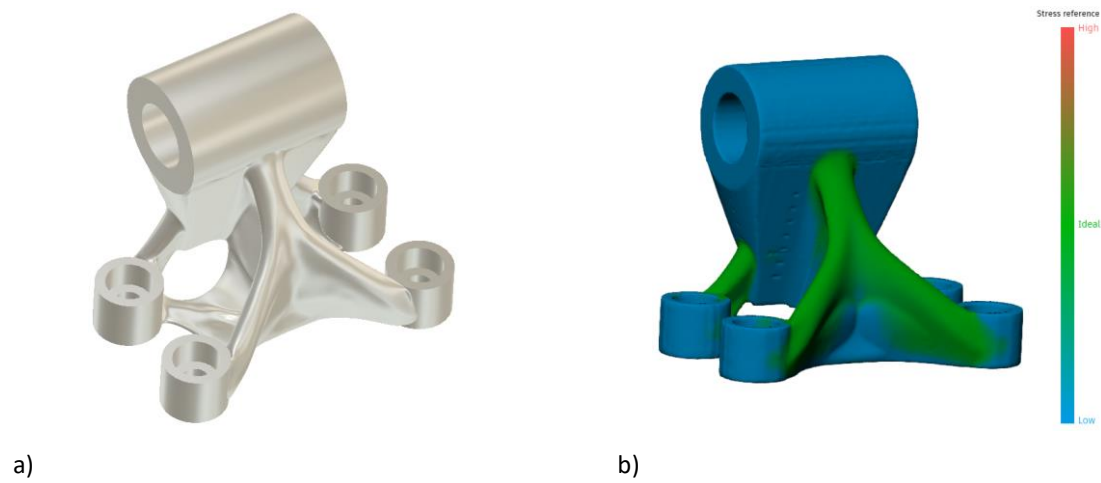a)   b)

Figure 6.9 a) The selected generated model has less detailed structure b) the stress graph of the model.

Figure 6.10 shows the intermediate shapes of clevis bracket MP2 model during GD study. The algorithm stops the process after 13 iterations; after judging the potential solutions, the shapes of 12th iteration were selected. Again, the selected model was characterized by simpler structure than that of the shape of the final suggested model (see figure 6.11). Generative model weight is 30 gr and the maximum Von Misses stress is 100MPa (see table 6.2).

(a)   (b)   (c)

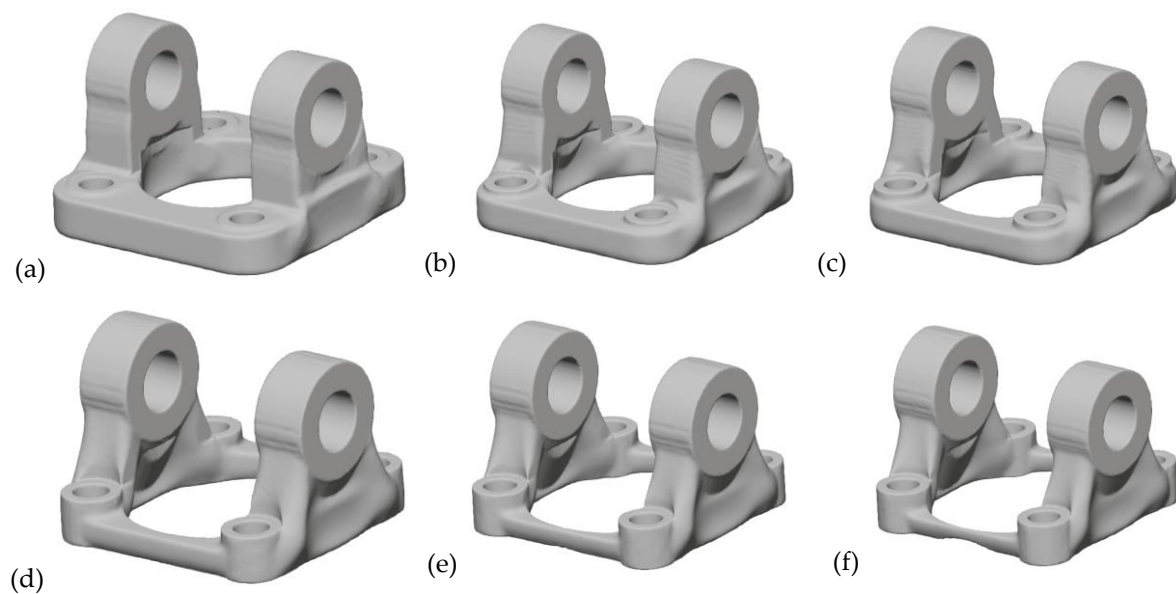(d)   (e)   (f)

Figure 6.10 Material distribution with 20 degrees overhang angle for clevis bracket MP2 model, after 13 iterations the process was completed, the figures show the intermediate shapes after: a) after 2 iterations b) after 5 iterations, c) after 7 iterations, d) after 10 iterations, e) after 12 iterations and f) after 13 iterations.

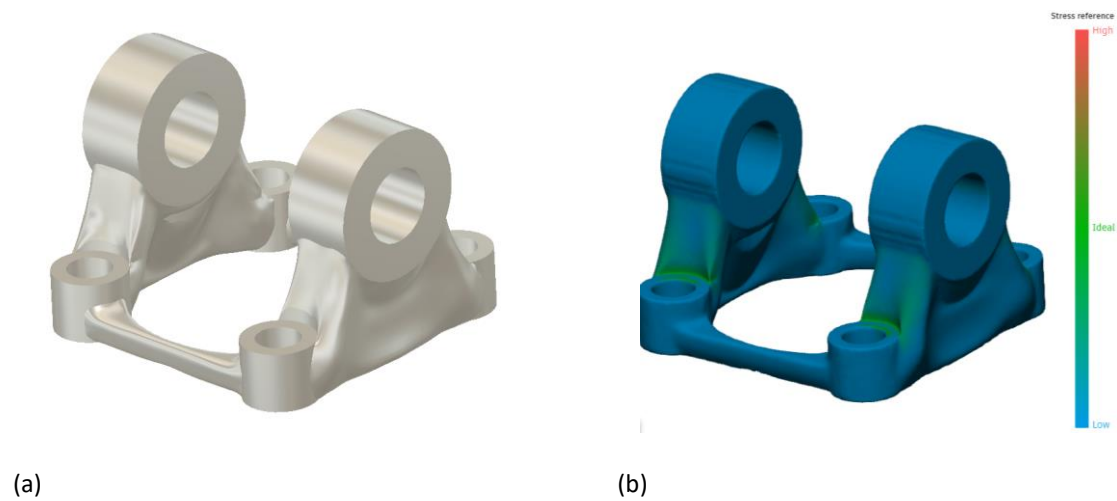(a)   (b)

Figure 6.11 a) The selected generated of clevis bracket MP2 model b) the stress graph of the model.

For clevis bracket MP4 mount, the algorithm was terminated after 29 iterations (see figure 6.12). The suggested model is characterized by a high-stress value (137MPa) and a low safety factor (2). Because of the high complexity, the proposed structure is inappropriate for a W-LMD printer. Continuing the judgment process, the solution of the 15th iteration was selected (see figure 6.13). Compared with the 29th iteration model, the structure complexity and the safety factor are significantly lower (see table 6.3).

(a)   (b)   (c)

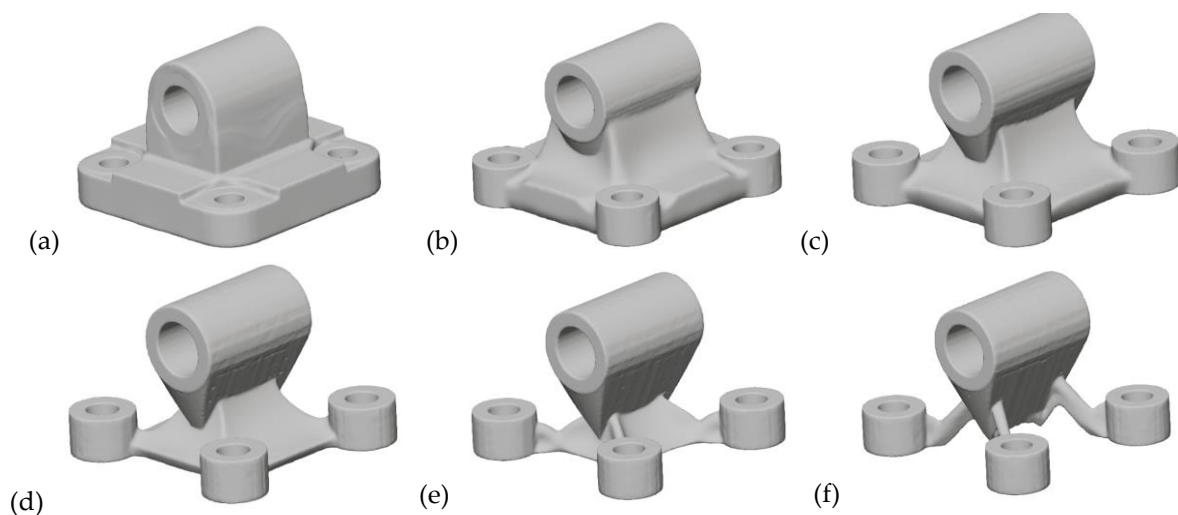(d)   (e)   (f)

Figure 6.12 Material distribution with 20 degrees overhang angle for Clevis bracket MP4 model, after 29 iterations the process was completed, the figures show the intermediate shapes after: a) after 2 iterations b) after 10 iterations, c) after 15 iterations, d) after 20 iterations, e) after 25 iterations and f) after 29 iterations.
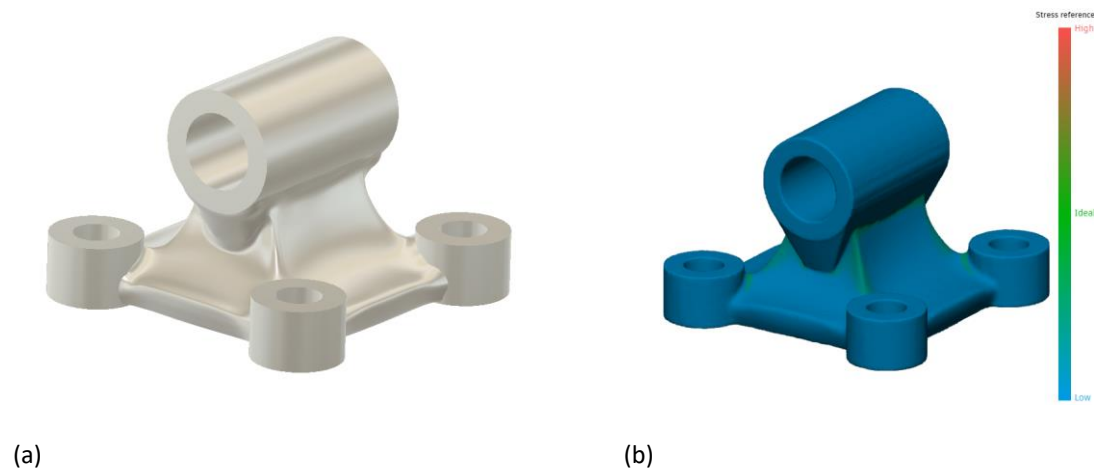
(a)   (b)

Figure 6.13 a) The selected generated of Clevis bracket MP4 model after 15 iterations b) the stress graph of the model.

Type of Mount	Max Von Misses Stress (MPa)	Max Displacement (mm)	Mass (gr)	Min Factor of Safety
Pivot bracket	91	0.10	31	3.0
Clevis bracket MP2	98	0.01	30	2.8
Clevis bracket MP4	53	0.009	39	5.1

Table 6.3 Characteristics of generative models for W-LMD 3d printer.

From the results above-mentioned studies, it is observed that the outcome solutions are different, due to the changes of manufacturing constraints for FFF and W- LMD Additive Manufacturing techniques. A critical parameter to minimize the support structure volume, is the overhang angle constraint. For FFF models, the overhang angle is set to 45 degrees and for W-LMD is set to 20 degrees. Comparing the generative models of FFF and W-LMD, significant changes on the structures are observed, due only to the different overhang angle. For all generative models, the mass was reduced without affecting the safety factor significantly.

CHAPTER *7*

Topological optimized microstructures infills for additive manufacturing

7.1 Design outline

In this chapter, a hybrid approach of topology optimization and homogenization is being used to evaluate the behavior of two topological optimized microstructures. The evaluated lattices are going to be utilized as infill structure for additive manufacturing. In order to characterize the new lattices, the elastic moduli and the Zener ratio have been calculated. Using material extrusion, specimens lattice microstructure was fabricated and then put to compressive and tensile strength tests. Due to the fact that the methodology is straightforward, it could be adapted in conceptual design of other lattices.

The selected TO method (SIMP) and other general algorithms predicted in an accurate manner the optimal material distribution within a given design domain. However, the isotropy of the optimized microstructure is not considered based on the classical Topology Optimization algorithms. In the current work, the homogenization of the topology optimized structures is selected, as an appropriate additional postprocessing step after TO. The homogenized microstructures behavior was evaluated with finite element analysis on a coarser mesh with the calculated homogenized properties.

The proposed methodology is illustrated in figure 7.1. Initially, two TO studies are carried out with different penalty factors and design constraints. Next, a homogenization study is executed. The behavior of the homogenized structure in a predefined design domain was studied. Afterwards, the anisotropy of the structures is checked by calculating the Zener ratio (Ntintakis and Stavroulakis, 2022). Utilizing FFF technique, specimens of

Acrylonitrile Butadiene Styrene (ABS) samples were fabricated and evaluated using compression and tensile strength tests.
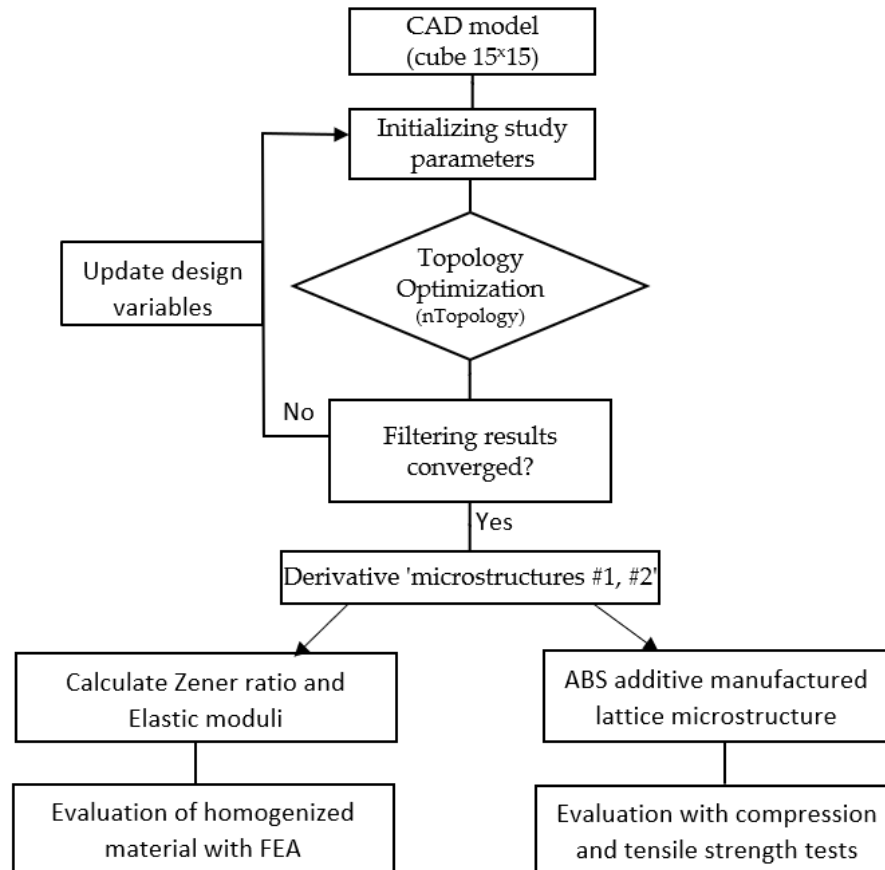

Figure 7.1 Adopted methodology flowchart.

7.2 Topology optimization study

The design process began from a cubic volume design domain of 15 × 15 × 15 mm. The topology optimization block of nTopology was used to carry out the TO studies. The boundary conditions involve a constraint restraint applied to the bottom face of the cube, and all degrees of freedom are excluded. The initial cube has been assigned with an isotropic elastic material (see table 7.1). During the meshing process, a solid mesh model consisting of 25,781 tetrahedral elements with an average edge length of 1 mm is created. The fulfillment of the objective function is achieved with the minimization of the material within the specified design domain. The fulfillment of the volume fraction restraint plays a decisive role in the configuration of the optimized model. The value, which is required for the volume fraction restraint, may range from 0 to 1, while the optimized volume will have a volume fraction equal to or less than the required value. The creation of different structures results from the different load

constraints. In the first study, a force of 300N applied in plane to all model vertices. On the contrary, in the second study, a same force applied in plane but only on the vertices of the top cube surface (Ntintakis and Stavroulakis, 2022).

Young's Modulus (MPa)	Density (kg/mm³)	Poisson's Ratio
187,000	0.0079	0.33

Table 7.1 Linear isotropic material properties.

From the actualization of TO studies, two topologically optimized structures have been created, 'structure #1' and 'structure #2'. The first structure is performed after twenty-three iterations. The intermediate shapes appear in figure 7.2. Respectively, figure 7.3 shows the progressing shape of the second structure in different iterations, the algorithm terminated after thirty-three iterations. In both studies, the volume fraction decreased sharply in the first 10 steps until asymptotically approaching the minimum (see figures 7.4a and 7.5a).

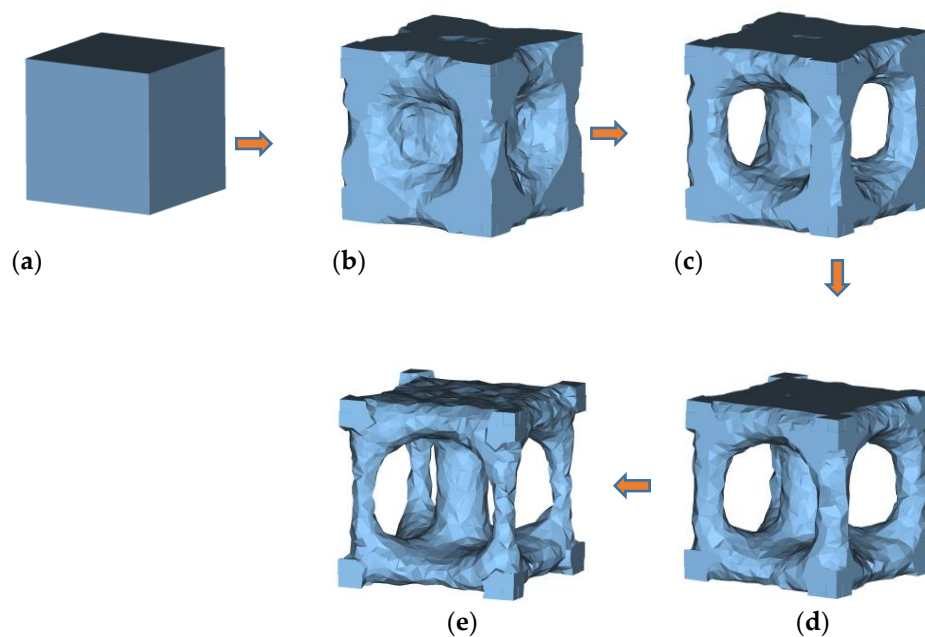(a)   (b)   (c)

(e)   (d)

Figure 7.2 Intermediate shapes, different iteration stages (b–e) from the initial design area (a) of Topology Optimized 'structure #1': (a) design domain, (b) step 5, (c) step 10, (d) step 18 and (e) step 23.
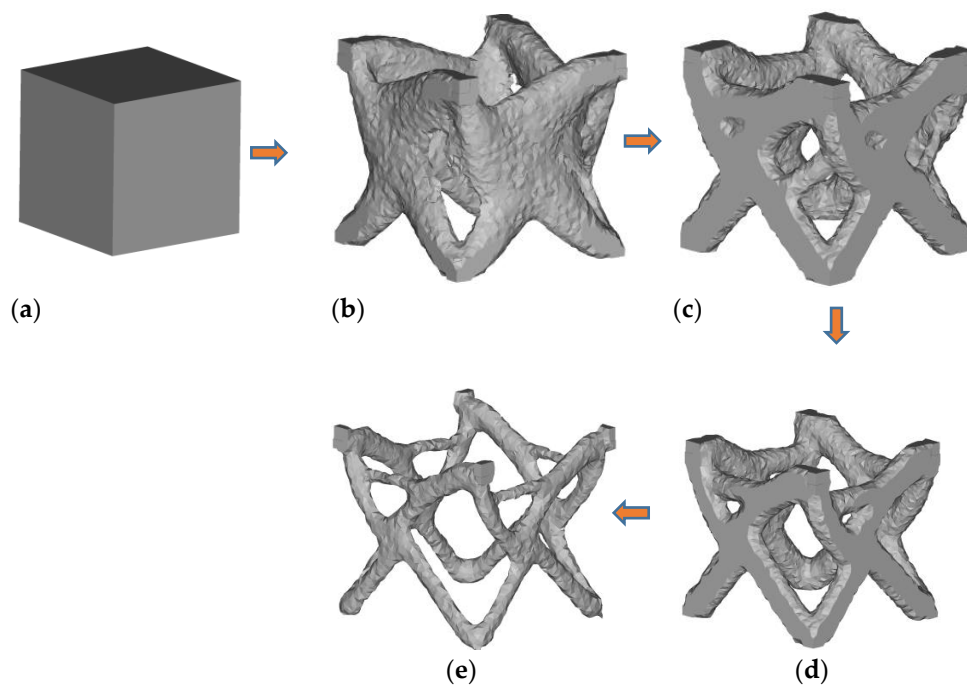
Figure 7.3 Iterations steps (a–e) of the Topology Optimization study for 'structure 2': (a) design area, (b) step 10, (c) step 20, (d) step 25 and (e) step 33.

Resulting from evaluation, the target of the volume fraction constraint value for 'structure #1' was 0.4 and for 'structure #2', was 0.1 (see figures 7.4b and 7.5b). Topology Optimization is correlated with the material distribution in a specific domain, in order to design constraints that need to be followed. In essence, a more rigid and stiff structure combined with material minimization is sought. Therefore, the problem-goal is to minimize its compliance, in order to increase the stiffness of the optimal structures. From the TO outcome results, the volume mass of the initial cubic domain is reduced significantly for both microstructures.
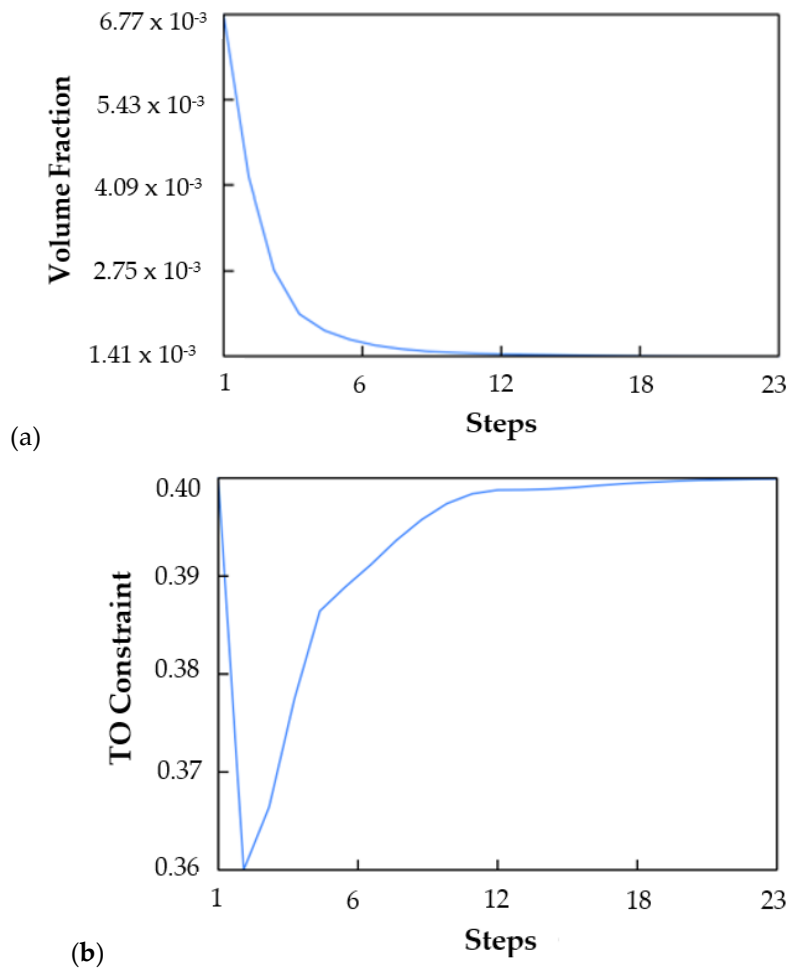
(a)

(b)

Figure 7.4 Volume fraction per step (b), and the value of the volume fraction constraints on each iteration step of 'structure #1'.
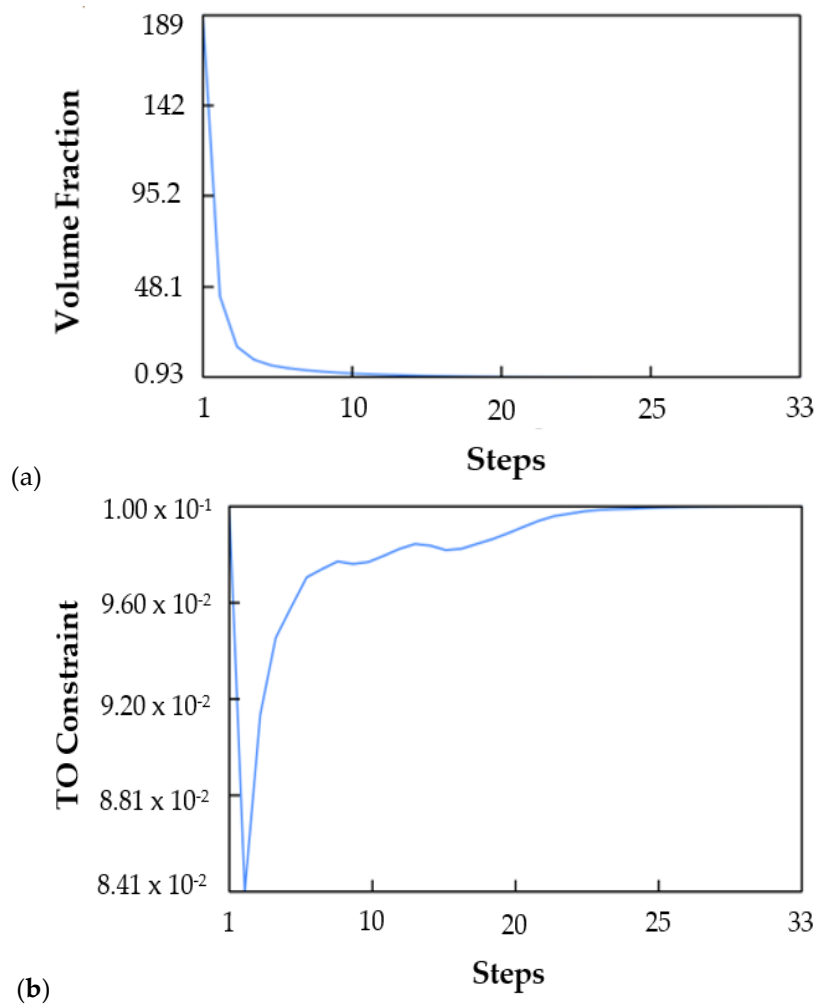
Figure 7.5 (a) Volume fraction per step, and (b) volume fraction constraints on each iteration step of 'structure #2'.

The optimized structures are refined and reconstructed in a specific design volume. After this process, two new custom unit cell lattices are created (see figure 7.6a). From these cells, new lattice structures are designed (see figure 7.6b).
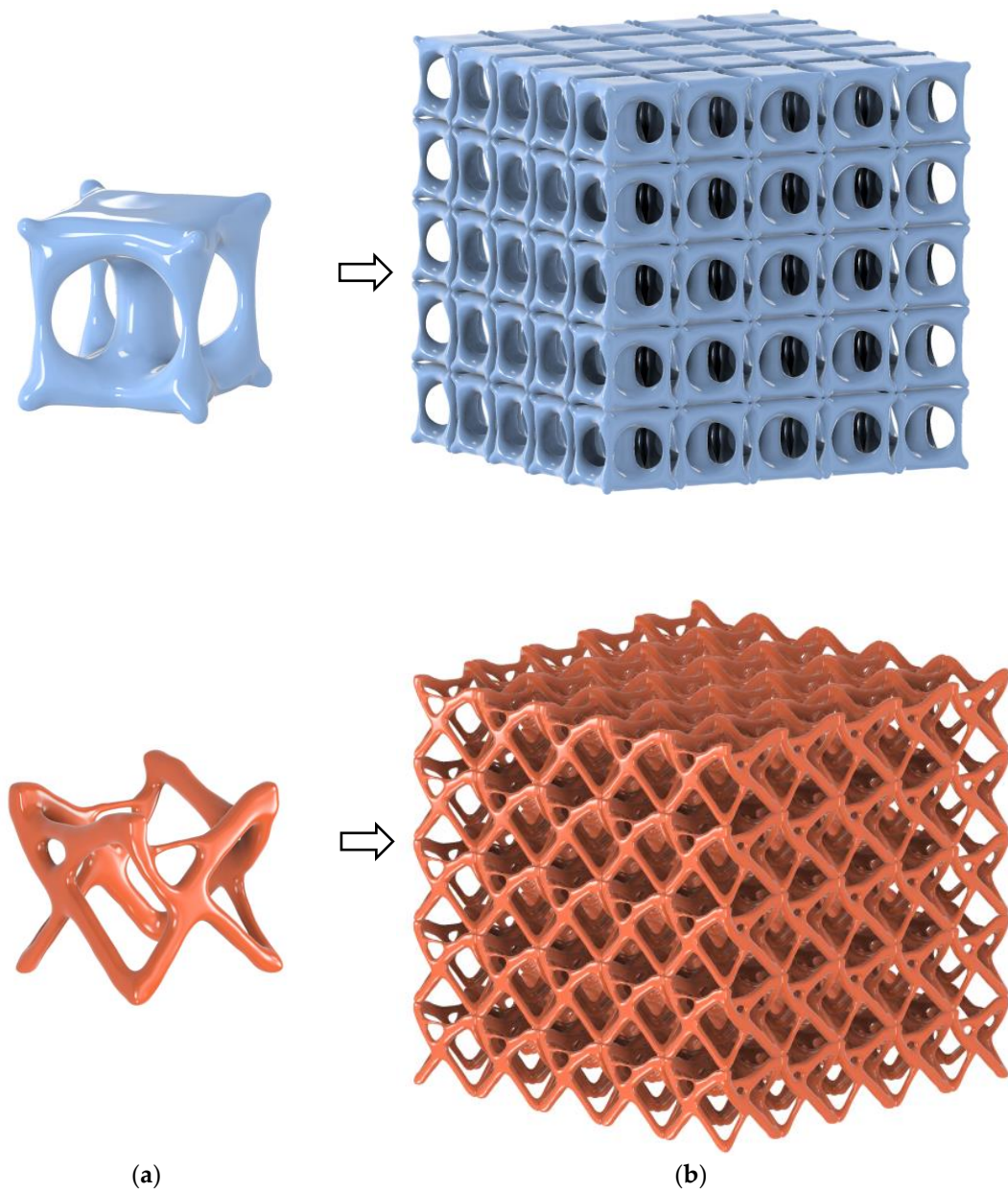

(a)   (b)

Figure 7.6 Refined unit cell structures and (b) Mapping of the 5 × 5 × 5 lattice structures.

7.3 Utilizing homogenization for lattices evaluation

After evaluating the Topology Optimization results, the definition of lattice cell follows. The homogenized cells were created in a design volume with dimensions being 15×15×15 mm. In order to execute the homogenization study, two solid mesh models were created, with an edge length of 0.7 mm and 75,489, as well as 62,595 tetrahedral elements, respectively. As a result of using the homogenization unit cell block of nTopology software, new homogenized structures are emerging and can now be utilized as materials that will be evaluated by performing a structural static analysis.

The SIMP method predicts an optimal material distribution within a given design space. Other structure characteristics such as anisotropy, are not easily integrated into a general topology optimization algorithm. Respectively, the avoidance of fatigue or buckling effects in microstructures produced with topology optimization, cannot be guaranteed. Therefore, the homogenization of the topology optimized structures is an appropriate step. Auxetic microstructures is an exception, where topology optimization is used to design compliant microstructures, so that the desired flexibility leads macroscopically to auxetic behavior (Kaminakis et al., 2015).

A key parameter to understand lattice behavior is the relative density ($\bar{\rho}$). Provided that relative density is defined as the density ratio of the lattice material to the solid material ($\bar{\rho} = \rho^* / \rho_s$), if a lattice has high porosity, the value of the relative density will be low; otherwise, a high value of the latter indicates a low porosity (Somnic and Jo, 2022b). The relative density increases for the higher volume fraction. In figure 7.7, the relative density of the proposed lattices against the volume fraction is presented. The homogenized domain of structure #2 showed similar trends as structure #1; however, the slope is lower. The lower the slope is, the larger the amount of material that can be added for a given relative density. In Figure 7.8 the Maximum Young's modulus for different relative density values is presented. Structure #2 seems to perform better, in comparison to structure #1 with the use of a lower amount of material.

In the current study, a general homogenization method is utilized to evaluate and characterize the results of the above proposed structures. Specifically, the anisotropy of the proposed structures through the measure of the maximum Young's modulus (Emax) and local minimum Young's modulus (Emin) is checked (see figure 7.8). According to Tancogne Dejean, a measure of the anisotropy of the lattice structure is derived from Emax/Emin (Ntintakis and Stavroulakis, 2022; Tancogne-Dejean et al., 2018).
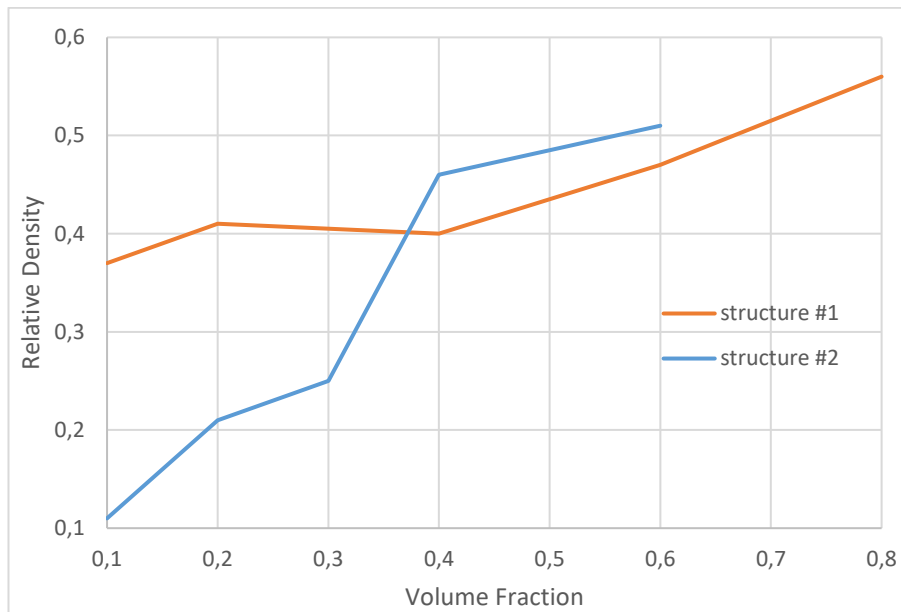
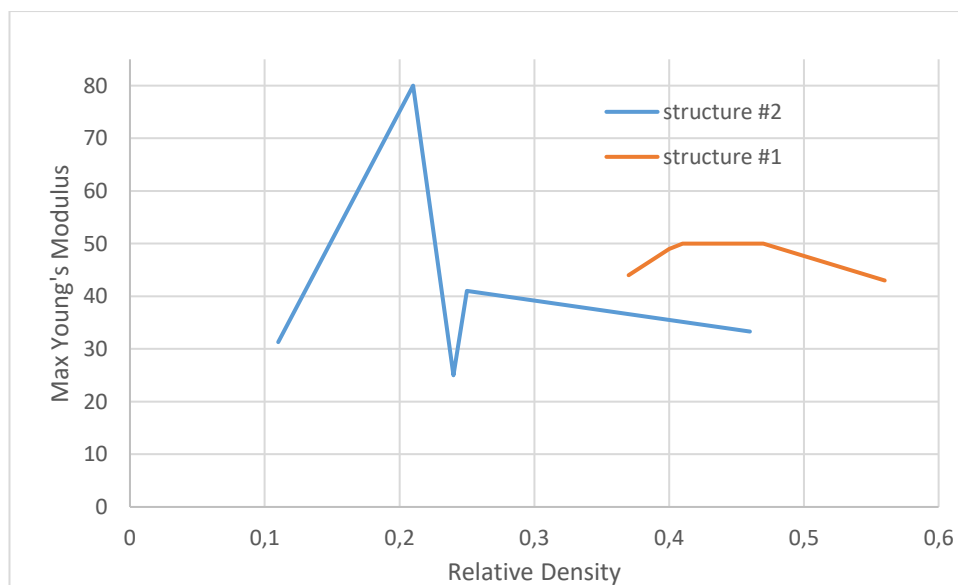Figure 7.7 Relative density against the volume fraction of homogenized lattices.

Figure 7.8 Maximum Young's modulus vs. the relative density for both lattice structures.

7.4 Zener ratio calculation

The proposed lattices are characterized by cubic symmetry; the Zener (A) ratio is calculated for each structure. In figures 7.9-7.10 the results of the Zener ratio for different relative density values are presented. When Z= 1 represents an isotropic material, a deviation less than or greater than unity, signifies the degree of anisotropy.

Both lattices seem to have anisotropic behavior. In structure #1, the Zener ratio is lower than unit (up to 0.51 for a relative density of 0.48), and vice versa in structure #2, where the Zener ratio is greater than unit (from 0.99 to 1.56). As shown in Figure 14, microstructure #1 has worse isotropy than microstructure #2. Young's modulus surface is spread in three dimensions, instead of structure #2, which has a box-like surface.
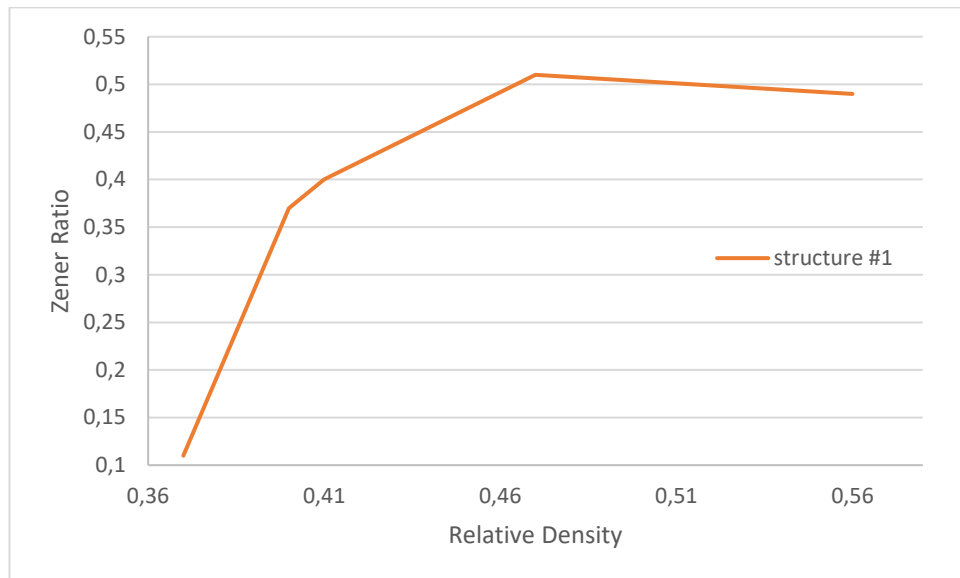

Figure 7.9 Zener ratio values for different relative densities of structure #1.
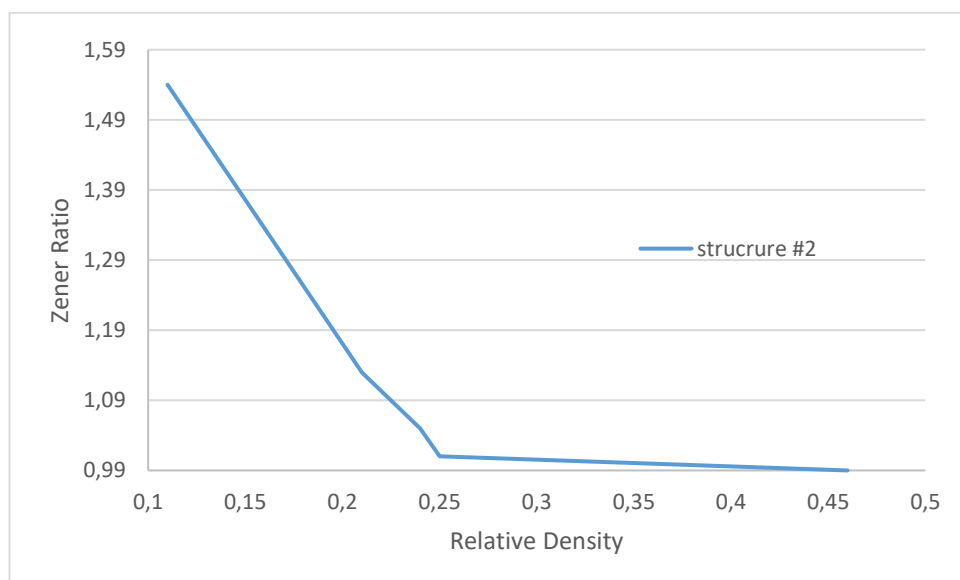

Figure 7.10 Zener ratio values of different relative densities structure #2.

Both lattice structures show a significant level of anisotropy in the uniaxial modulus. Structure #2 exhibits lower uniaxial modulus anisotropy. Therefore, for

higher relative density values, the anisotropy did not significantly change the uniaxial modulus; especially; for $\bar{\rho}$ = 0.25, the Zener ratio is equal to 1 (see figure 7.11).
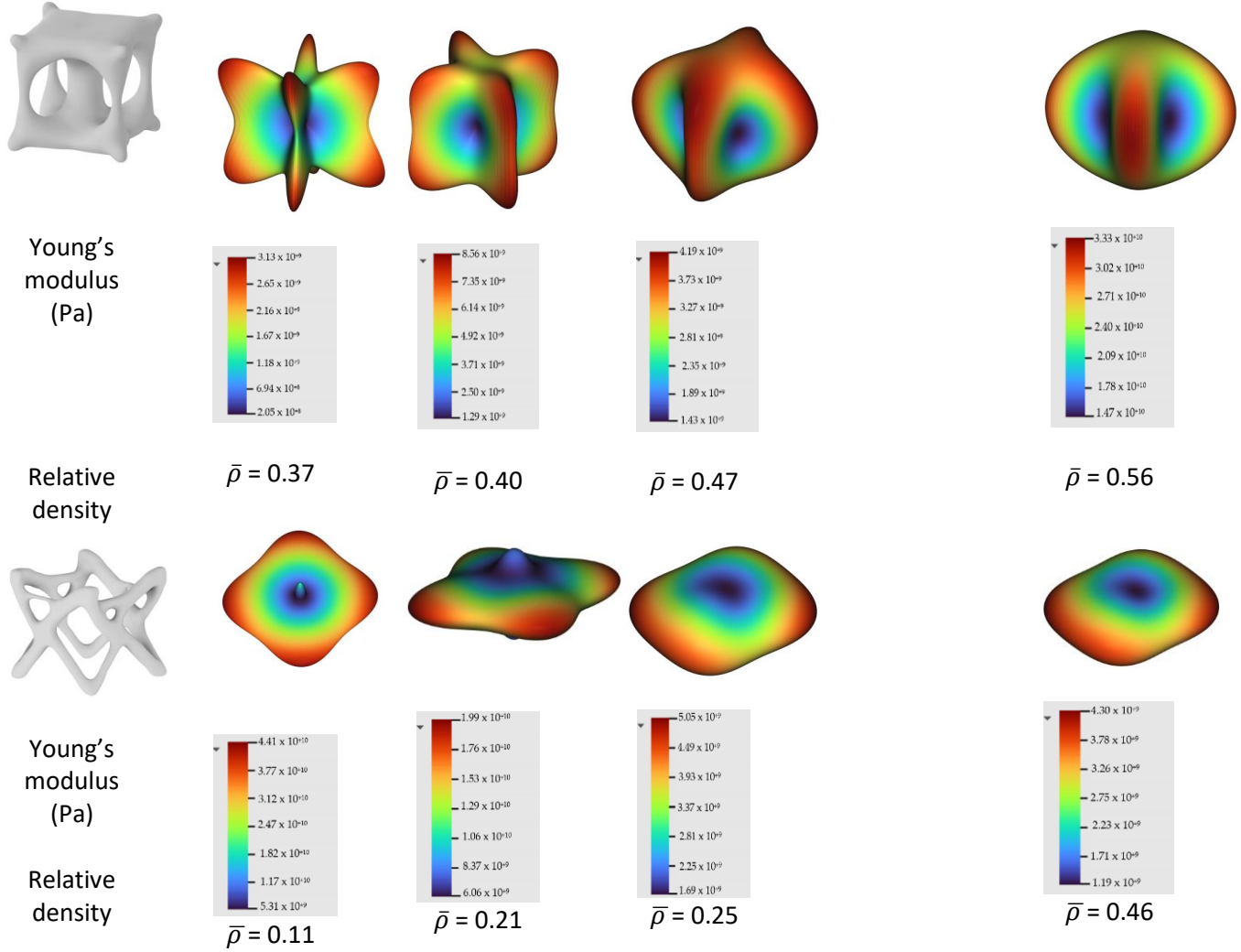

Figure 7.11 The elastic moduli of both homogenized lattices in different relative densities ($\bar{\varrho}$)

According to the results mentioned above, we can observe that both microstructures have Zener ratios lower or greater than unit. The second microstructure was characterized by better and smoother isotropy; for = 0.25, the Zener ratio was equal to unit, since this Zener ratio did not change significantly (Ntintakis and Stavroulakis, 2022).

7.5 Validation of homogenized material with FEA

In order to evaluate the homogenized microstructures as an Additive Manufacturing infill, two Finite Element Analysis are executed by the use of a cantilever model, , the dimension being 50 × 10 × 10 mm. A FE mesh of 64.424 tetrahedral elements of the cantilever model is created. According to the boundary conditions, the back face is

fixed, and at the upfront edge of the model, a vertical force was applied. Afterwards, a FE analysis for each microstructure was executed.

As in the cantilever with microstructure #1, the infill increased, so the deflection at the end of the beam was higher. As the relative density increased, the Von mises stress decreased (about 10%). In contrary, the deflection and Von mises stress in microstructure #2 decreased, as the relative density increased (see figure 7.12). Based on the results, it was observed that microstructure #2 was stiffer for the same relative density value. Also, isotropy is better and more efficient, because the stress was lower in the same or lesser amount of material (Ntintakis and Stavroulakis, 2022).
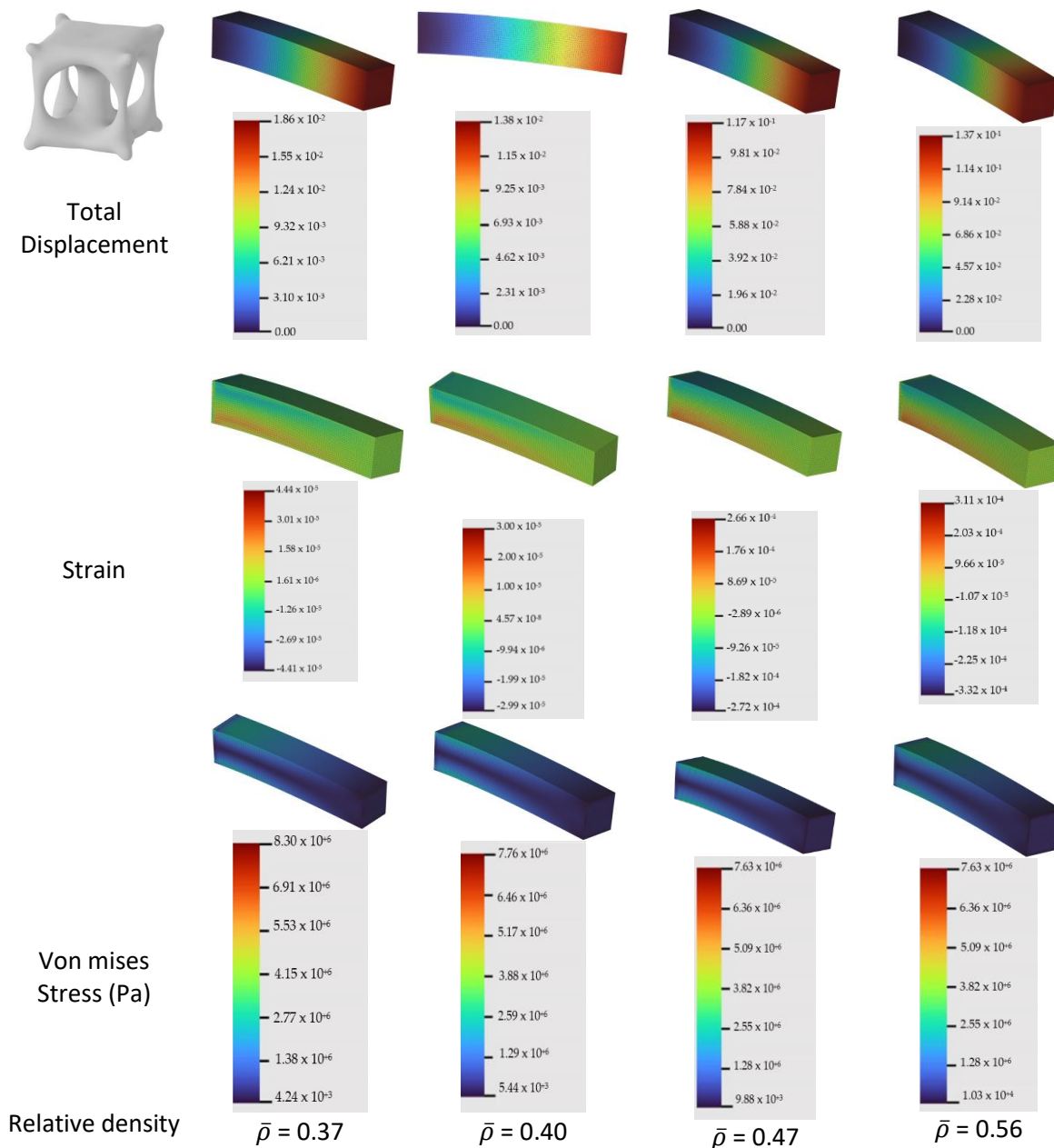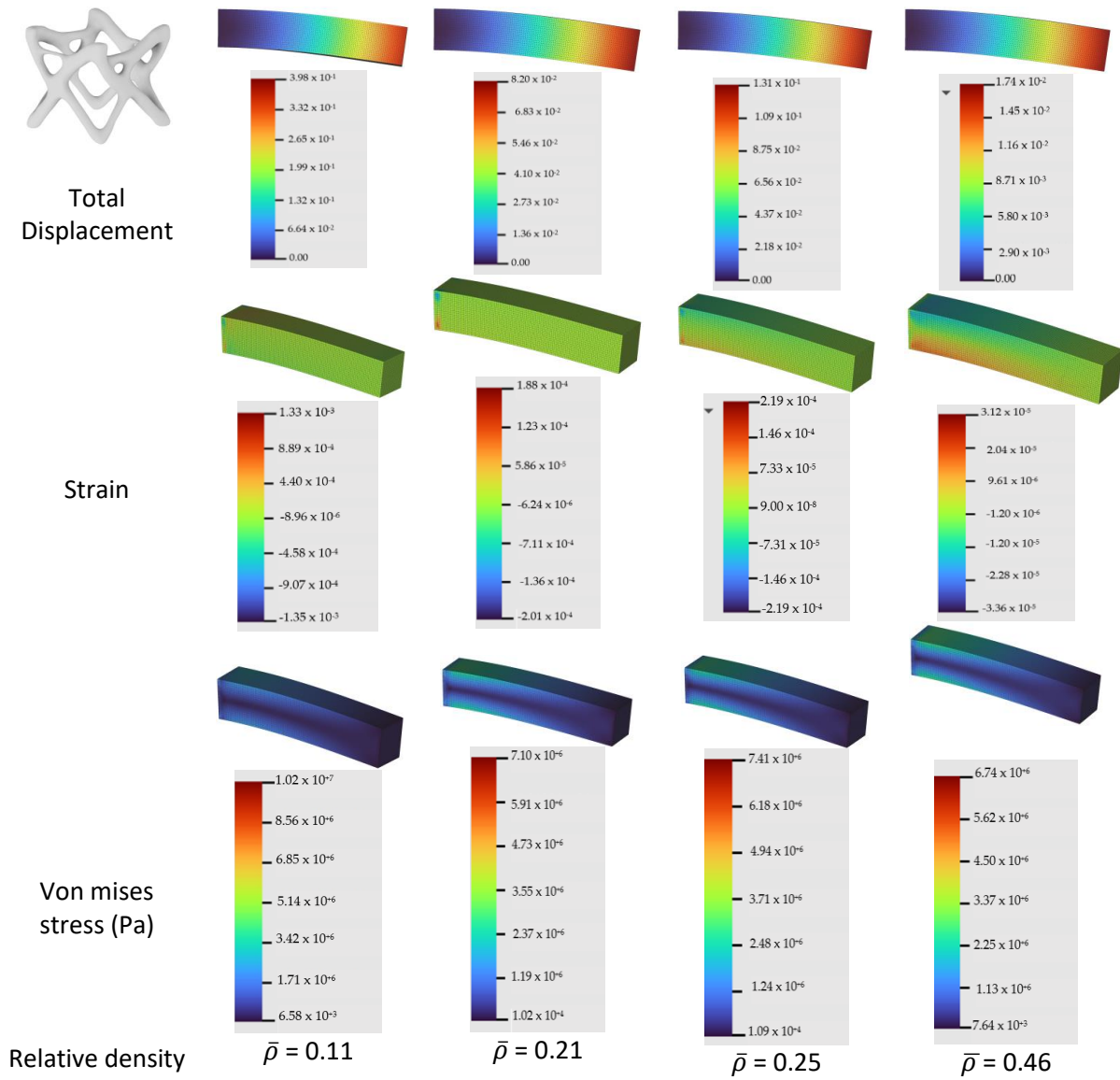
Figure 7.12 Displacement, strain and Von mises stress of homogenized structures #1 and #2 for different values of relative density.

7.6 Utilizing Application Programming Interface (API) in topology optimization process

The optimized shape of the above microstructures depends on design or manufacturing constrains. The above process executed by hand utilizing SIMP algorithm and homogenization in nTopology platform. In order to automate the proposed hybrid approach, an Application Programming Interface (API) utilized. The following workflow starts with the creation of the appropriate input and output JavaScript Object Notation (JSON) files (see figure 7.13). The penalty factor was selected as input variable. As output, the relative density value was set out.

```json
{
    "description": "",
    "inputs": [
        {
            "description": "",
            "name": "Boundary penalty",
            "type": "real",
            "value": 0.11
        }
    ],
    "title": "New Notebook"
}
```

(**a**)

```json
[
    {
        "components": [],
        "name": "relative_density",
        "type": "real",
        "value": {
            "isFinite": true,
            "units": {},
            "val": 0.4860237911504641
        }
    }
]
```

(**b**)

Figure 7.13 a) The input and b) the output JSON files

The JSON files were utilized in order the SIMP and homogenization method to be executed in a Python script in an automatic way. The boundary penalty factor ranges from zero to unity. For each boundary penalty value, the relative density

differs. In figure 7.14 are presented the different relative density values while the boundary penalty increment-step is 0.01.

```
1, {'Boundary penalty': 0.0, 'Relative Density': 0.4103373897412391})
2, {'Boundary penalty': 0.01, 'Relative Density': 0.41576638106597347})
3, {'Boundary penalty': 0.02, 'Relative Density': 0.4208151120842099})
4, {'Boundary penalty': 0.03, 'Relative Density': 0.4254464561507694})
5, {'Boundary penalty': 0.04, 'Relative Density': 0.42986163934236865})
6, {'Boundary penalty': 0.05, 'Relative Density': 0.43407944529159564})
7, {'Boundary penalty': 0.06, 'Relative Density': 0.4381391359940165})
8, {'Boundary penalty': 0.07, 'Relative Density': 0.44206902629882944})
9, {'Boundary penalty': 0.08, 'Relative Density': 0.4457795162511755})
10, {'Boundary penalty': 0.09, 'Relative Density': 0.4494205818601768})
11:{'Boundary penalty': 0.1, 'Relative Density': 0.45296418022308643}
12:{'Boundary penalty': 0.11, 'Relative Density': 0.45634263625453814}
13:{'Boundary penalty': 0.12, 'Relative Density': 0.4597434754475302}
14:{'Boundary penalty': 0.13, 'Relative Density': 0.4628683626069661}
15:{'Boundary penalty': 0.14, 'Relative Density': 0.4659152202523944}
16:{'Boundary penalty': 0.15, 'Relative Density': 0.46880919564502893}
17:{'Boundary penalty': 0.16, 'Relative Density': 0.4716064264682573}
18:{'Boundary penalty': 0.17, 'Relative Density': 0.4742305196029464}
19:{'Boundary penalty': 0.18, 'Relative Density': 0.4767413543206658}
20:{'Boundary penalty': 0.19, 'Relative Density': 0.4790468341240872}
21:{'Boundary penalty': 0.2, 'Relative Density': 0.48115005876457223}
22:{'Boundary penalty': 0.21, 'Relative Density': 0.4829571424211946}
23:{'Boundary penalty': 0.22, 'Relative Density': 0.4844018654186943}
24:{'Boundary penalty': 0.23, 'Relative Density': 0.48551453013802637}
25:{'Boundary penalty': 0.24, 'Relative Density': 0.4862811732521755}
26:{'Boundary penalty': 0.25, 'Relative Density': 0.4867178420230033}
27:{'Boundary penalty': 0.26, 'Relative Density': 0.4869076269395123}
28:{'Boundary penalty': 0.27, 'Relative Density': 0.48692181025250514}
29:{'Boundary penalty': 0.28, 'Relative Density': 0.486775621873737}
30:{'Boundary penalty': 0.29, 'Relative Density': 0.48646669689700234}
31:{'Boundary penalty': 0.3, 'Relative Density': 0.4860237911504641}
32:{'Boundary penalty': 0.31, 'Relative Density': 0.4856224192699286}
33:{'Boundary penalty': 0.32, 'Relative Density': 0.4850543029939483}
34:{'Boundary penalty': 0.33, 'Relative Density': 0.4844018005581985}
35:{'Boundary penalty': 0.34, 'Relative Density': 0.48361453132978066}
36:{'Boundary penalty': 0.35, 'Relative Density': 0.4827849374749697}
37:{'Boundary penalty': 0.36, 'Relative Density': 0.4818716194035769}
38:{'Boundary penalty': 0.37, 'Relative Density': 0.48095122682503844}
39:{'Boundary penalty': 0.38, 'Relative Density': 0.48006633005691185}
40:{'Boundary penalty': 0.39, 'Relative Density': 0.47916198144309935}
41:{'Boundary penalty': 0.4, 'Relative Density': 0.47831256222563673}
42:{'Boundary penalty': 0.41, 'Relative Density': 0.4775066421380561}
43:{'Boundary penalty': 0.42, 'Relative Density': 0.47660685371220773}
44:{'Boundary penalty': 0.43, 'Relative Density': 0.47573554227345777}
45:{'Boundary penalty': 0.44, 'Relative Density': 0.4748853653161484}
46:{'Boundary penalty': 0.45, 'Relative Density': 0.4739832727353106}
47:{'Boundary penalty': 0.46, 'Relative Density': 0.47300583567886123}
48:{'Boundary penalty': 0.47, 'Relative Density': 0.4719923946240276}
49:{'Boundary penalty': 0.48, 'Relative Density': 0.4709006613503774}
50:{'Boundary penalty': 0.49, 'Relative Density': 0.46978441337320415}
51:{'Boundary penalty': 0.5, 'Relative Density': 0.468611515900545}
52:{'Boundary penalty': 0.51, 'Relative Density': 0.46737720680981804}
53:{'Boundary penalty': 0.52, 'Relative Density': 0.4661381046369586}
54:{'Boundary penalty': 0.53, 'Relative Density': 0.4648299029856985}
55:{'Boundary penalty': 0.54, 'Relative Density': 0.4635100686411464}
```

```
56:{'Boundary penalty': 0.55, 'Relative Density': 0.4621414583594307}
57:{'Boundary penalty': 0.56, 'Relative Density': 0.460799751298994}
58:{'Boundary penalty': 0.57, 'Relative Density': 0.45950227696060303}
59:{'Boundary penalty': 0.58, 'Relative Density': 0.4581988849955615}
60:{'Boundary penalty': 0.59, 'Relative Density': 0.4570604302468275}
61:{'Boundary penalty': 0.6, 'Relative Density': 0.4557220871689326}
62:{'Boundary penalty': 0.61, 'Relative Density': 0.45449890116104164}
63:{'Boundary penalty': 0.62, 'Relative Density': 0.4533284969692565}
64:{'Boundary penalty': 0.63, 'Relative Density': 0.45223757189153185}
65:{'Boundary penalty': 0.64, 'Relative Density': 0.4511274856169053}
66:{'Boundary penalty': 0.65, 'Relative Density': 0.45009087996123603}
67:{'Boundary penalty': 0.66, 'Relative Density': 0.44913744816857526}
68:{'Boundary penalty': 0.67, 'Relative Density': 0.4482159681535008}
69:{'Boundary penalty': 0.68, 'Relative Density': 0.44731403837589856}
70:{'Boundary penalty': 0.69, 'Relative Density': 0.4464334716132561}
71:{'Boundary penalty': 0.7, 'Relative Density': 0.4455625967406407}
72:{'Boundary penalty': 0.71, 'Relative Density': 0.4447402012998447}
73:{'Boundary penalty': 0.72, 'Relative Density': 0.44391292688861844}
74:{'Boundary penalty': 0.73, 'Relative Density': 0.4431298134566977}
75:{'Boundary penalty': 0.74, 'Relative Density': 0.44239906376477567}
76:{'Boundary penalty': 0.75, 'Relative Density': 0.4416982823832731}
77:{'Boundary penalty': 0.76, 'Relative Density': 0.4410120975713665}
78:{'Boundary penalty': 0.77, 'Relative Density': 0.440355199070493}
79:{'Boundary penalty': 0.78, 'Relative Density': 0.4396950925079301}
80:{'Boundary penalty': 0.79, 'Relative Density': 0.4391055939464805}
81:{'Boundary penalty': 0.8, 'Relative Density': 0.43853134483066286}
82:{'Boundary penalty': 0.81, 'Relative Density': 0.43842150985937495}
83:{'Boundary penalty': 0.82, 'Relative Density': 0.4373961695418561}
84:{'Boundary penalty': 0.83, 'Relative Density': 0.43685285672722957}
85:{'Boundary penalty': 0.84, 'Relative Density': 0.436342320315715}
86:{'Boundary penalty': 0.85, 'Relative Density': 0.4358290065145329}
87:{'Boundary penalty': 0.86, 'Relative Density': 0.43532844987650887}
88:{'Boundary penalty': 0.87, 'Relative Density': 0.4348694066807379}
89:{'Boundary penalty': 0.88, 'Relative Density': 0.4343870791862667}
90:{'Boundary penalty': 0.89, 'Relative Density': 0.43396088067257516}
91:{'Boundary penalty': 0.9, 'Relative Density': 0.4335216504689363}
92:{'Boundary penalty': 0.91, 'Relative Density': 0.4331084957890897}
93:{'Boundary penalty': 0.92, 'Relative Density': 0.4326900778878773}
94:{'Boundary penalty': 0.93, 'Relative Density': 0.4323002404876159}
95:{'Boundary penalty': 0.94, 'Relative Density': 0.43190748420325215}
96:{'Boundary penalty': 0.95, 'Relative Density': 0.43154558127864245}
97:{'Boundary penalty': 0.96, 'Relative Density': 0.43159607382633547}
98:{'Boundary penalty': 0.97, 'Relative Density': 0.43086690203735195}
99:{'Boundary penalty': 0.98, 'Relative Density': 0.4305819473734296}
100:{'Boundary penalty': 0.99, 'Relative Density': 0.43025521787269844}
101:{'Boundary penalty': 1.0, 'Relative Density': 0.4299350483291212}
```

Figure 7.14 Relative density values for each boundary penalty

The outline shape of the optimized microstructures change according to different boundary penalty values (see figure 7.15).
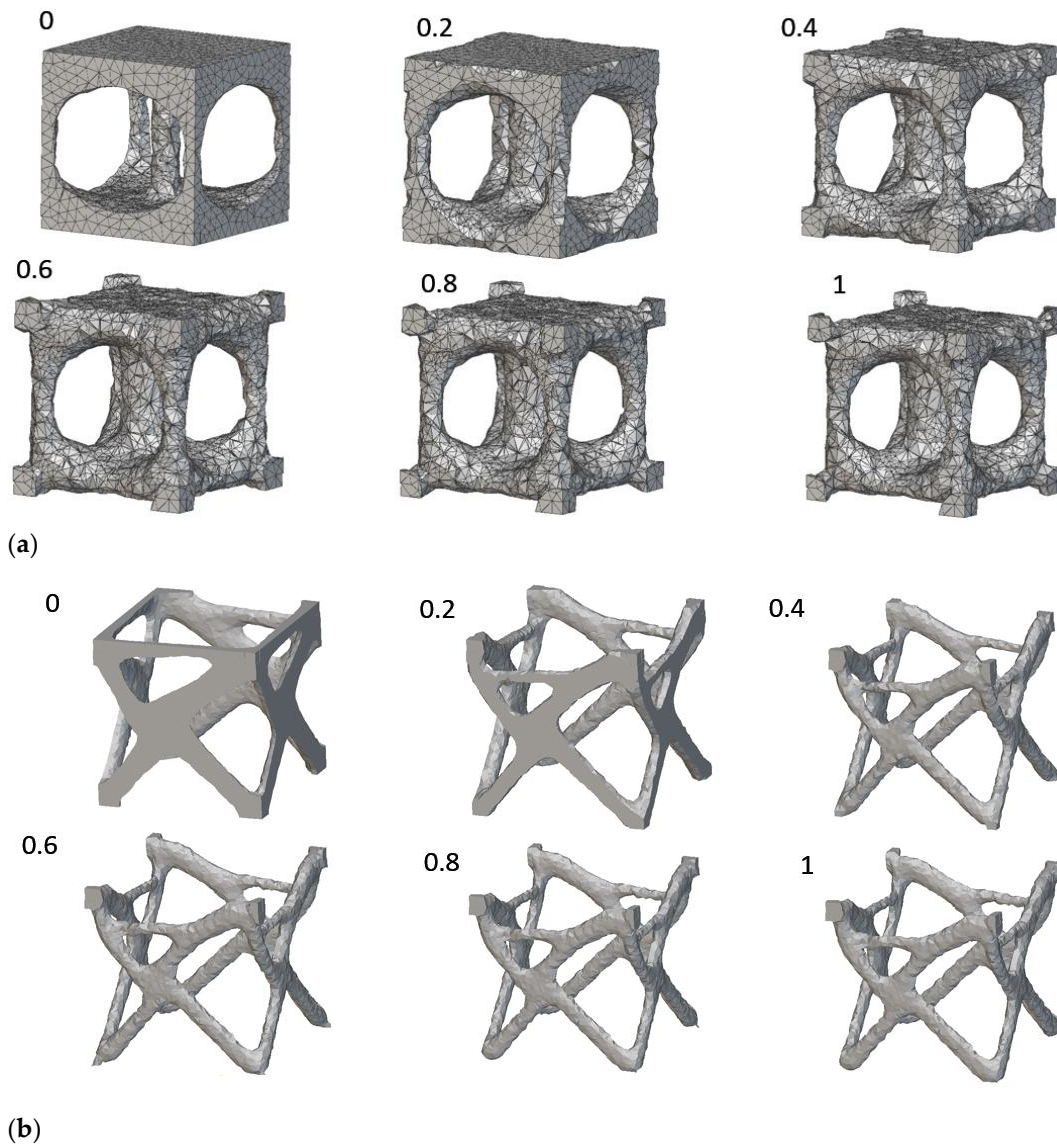
(**a**)

(**b**)

Figure 7.15 Microstructures shapes for different boundary penalty values

Executing topology optimization and homogenization method in an automated way can lead to create a generator of solutions. The proposed process allows the execution of the hybrid approach in combination with the production constrains of additive manufacturing.

# 7.7 Design of Lattices Specimens for Additive Manufacturing

For both lattice structures, specimens without supports have been fabricated. The specimens of the proposed lattice structures were manufactured by the FFF printing process, using a Zortrax m200 dual fusion 3D printer. The proposed lattice structures have been evaluated experimentally through compression and tensile strength tests.

7.7.1 Specimens for compression test

For compression tests, lattice structures consisting of a specimen of 15×15 ×15 mm, of 3×3 mapping, in a rectangular shape of 45 mm height, 45 mm width and 15 mm thickness, 15 mm have been designed and manufactured. The computer aided design (CAD) models of both lattice structures, illustrated in figure 7.16, were employed to investigate the compressive behavior of the lattice structures. Figure 7.17 shows photographs from the fabricated lattice structures. The relative density of both structures is 0.4 and 0.1, respectively. In order to ensure the truth of the compression test results, five specimens for each lattice structure were fabricated and tested (see figure 6.14) (Ntintakis and Stavroulakis, 2022).
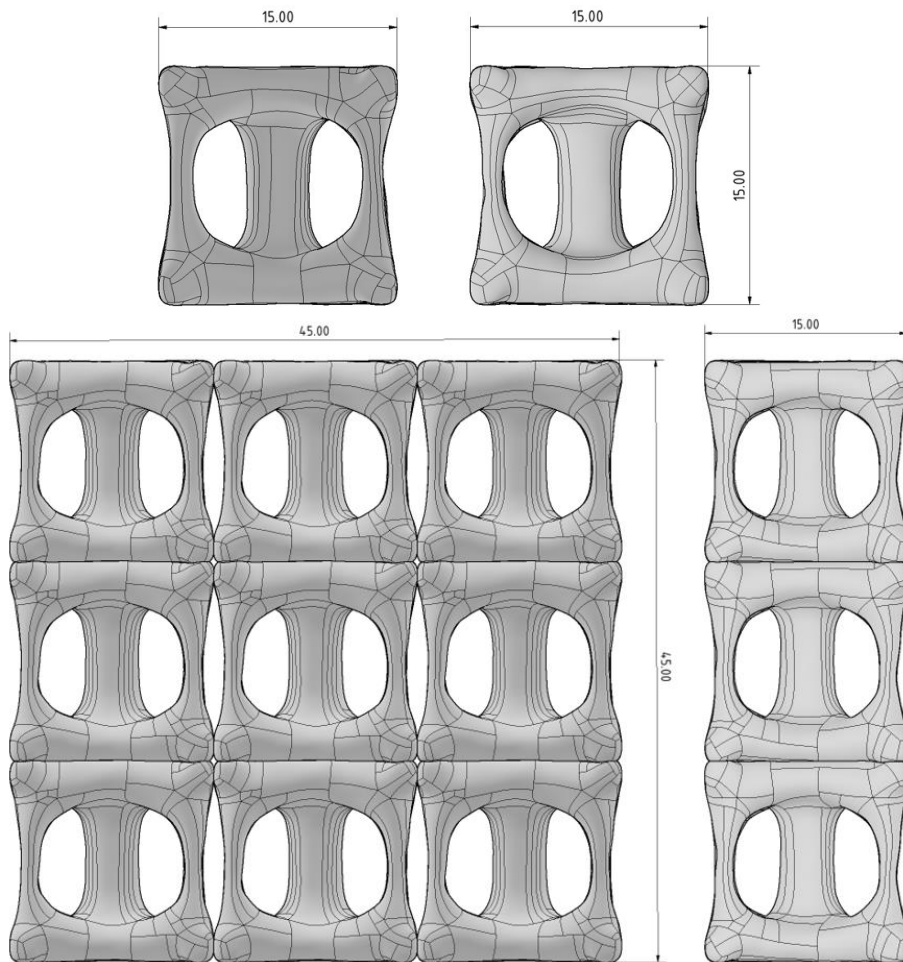
(a)
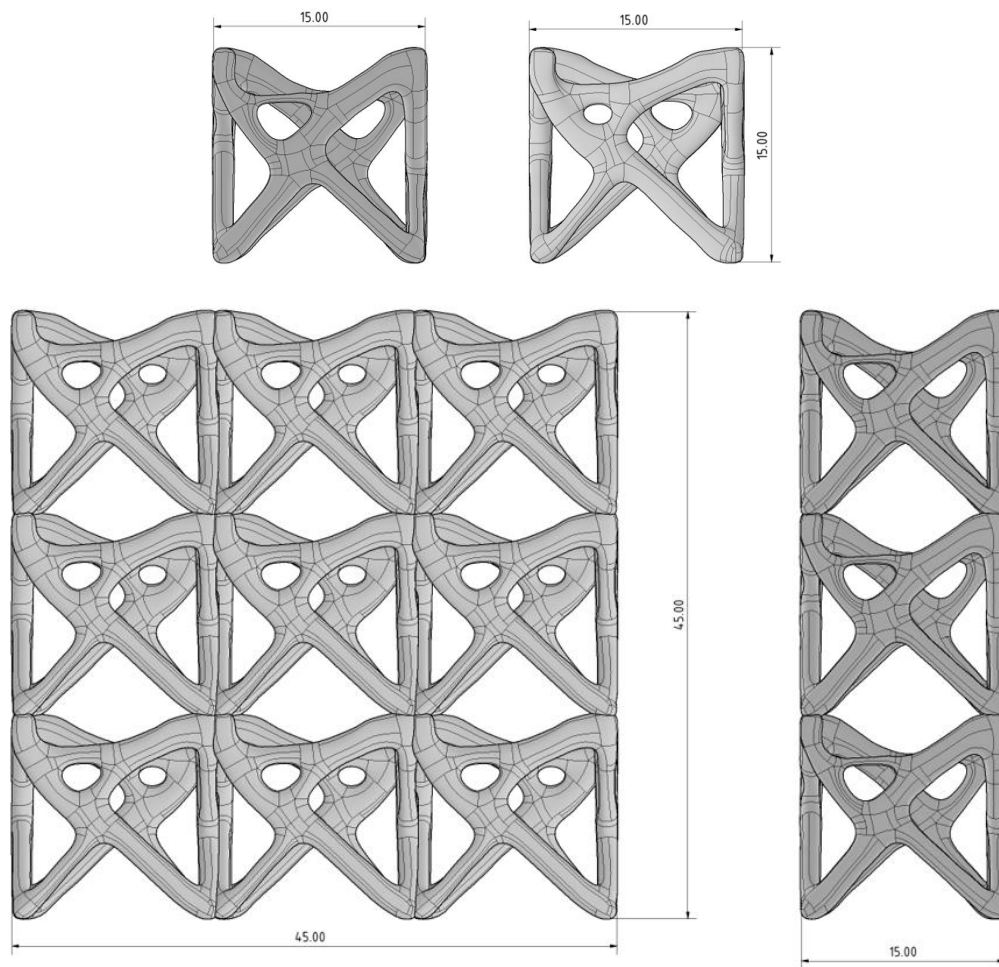
(b)

Figure 7.16 Outline dimensions of unit cells and lattice models for the compression test of (a) structure #1 with a volume fraction constraint = 0.4 and (b) structure #2 with a volume fraction constraint = 0.1.
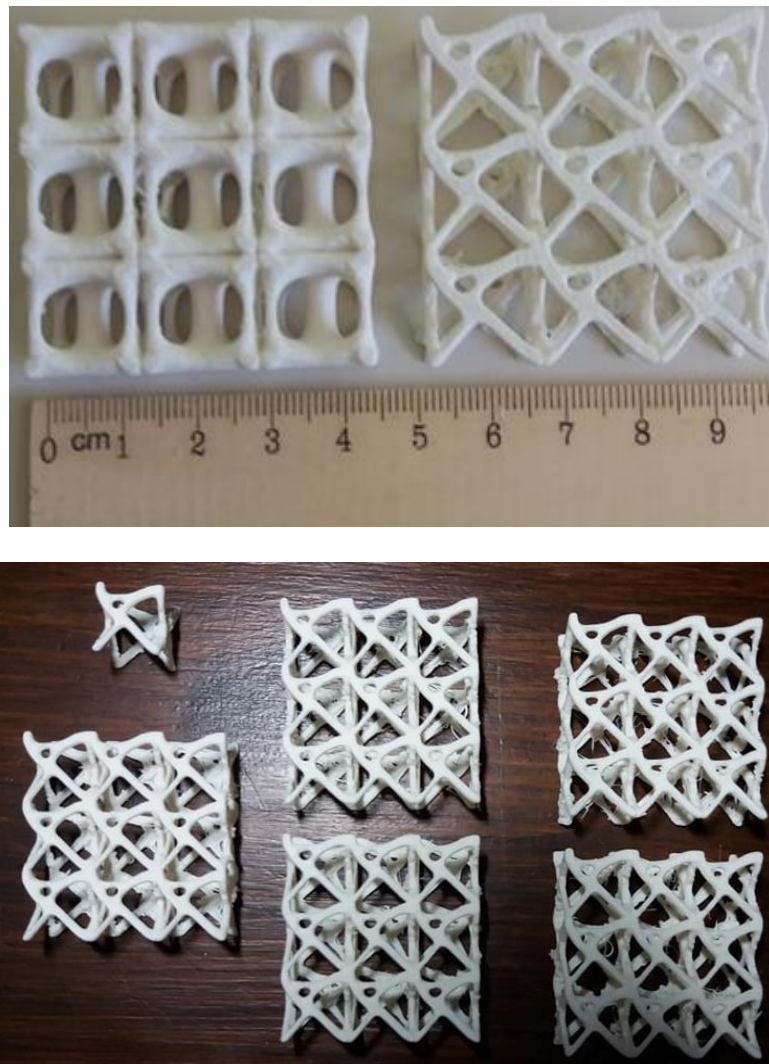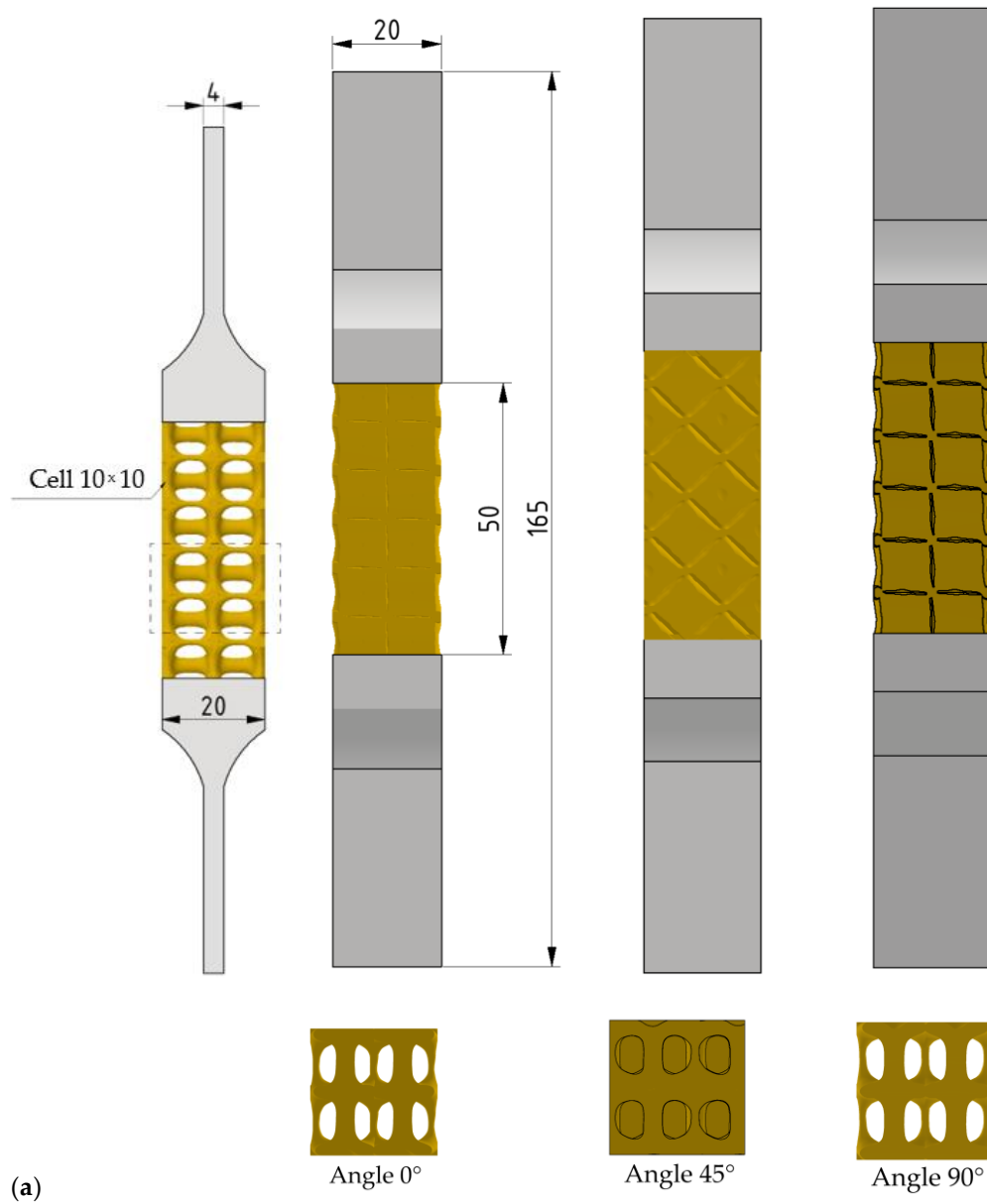
Figure 7.17 ABS specimens was fabricated without supports for both structures for the tensile strength test with a relative density of 0.4 for structure #1 and 0.1 for structure #2.

7.7.2 Specimens for tensile test

To indicate further the mechanical properties of the proposed lattices, tensile tests were performed. Figure 7.18 shows the CAD models with the outline dimensions. In order to check the mechanical behavior of the proposed lattices, three specimens for each structure, with different cell orientation angles (0°, 45° and 90°), were designed and fabricated. Photographs from the fabricated specimens with different lattice structure mapping angles are presented in figure 7.19.

Cell 10×10

20

4

20

165

50

Angle 0°   Angle 45°   Angle 90°

(**a**)

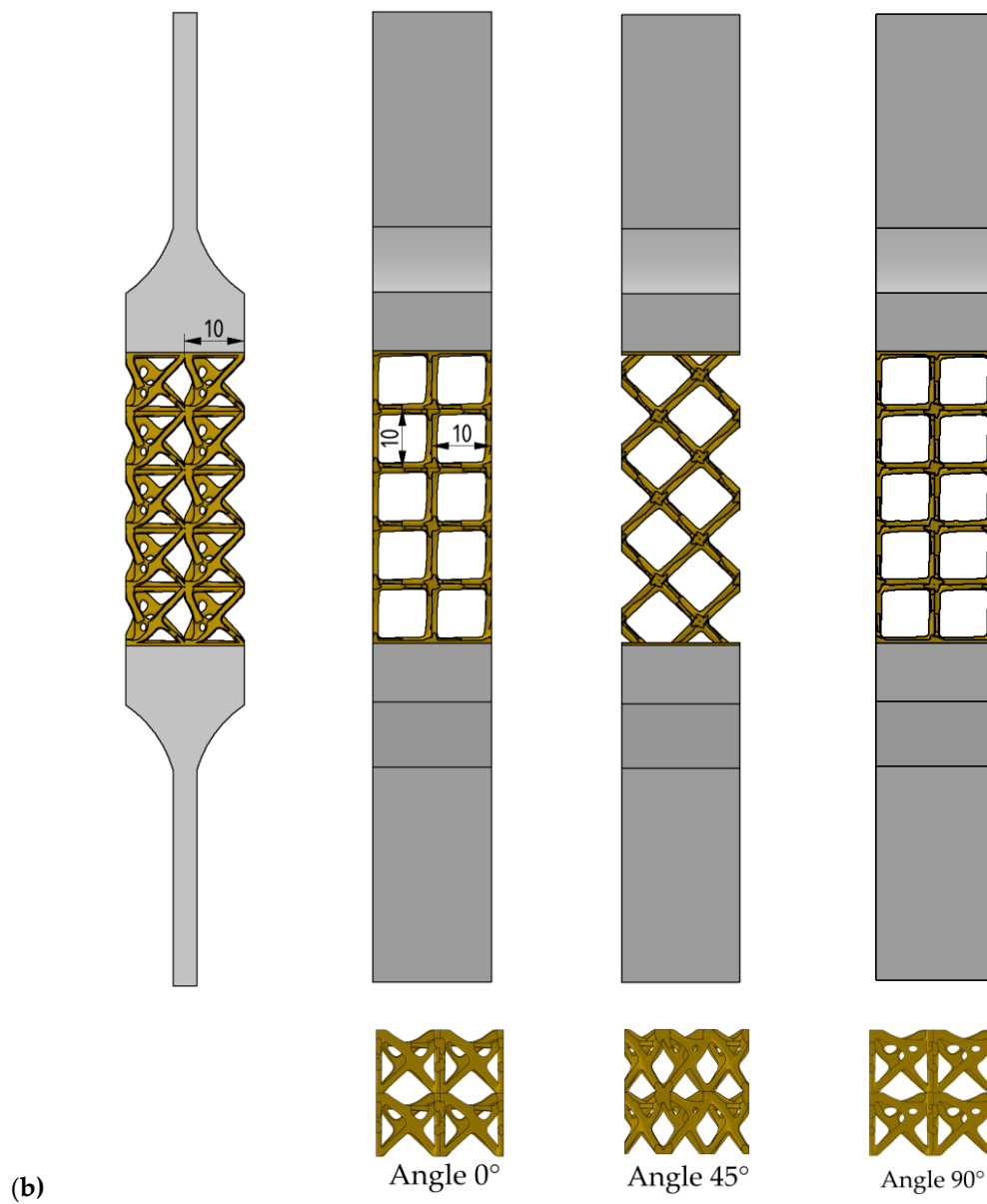(**b**)   Angle 0°   Angle 45°   Angle 90°

Figure 7.18 Outline dimensions of the tensile strength specimens (a,b), each lattice structure was fabricated with 0°, 45° and 90° angles of single unit cell mapping.
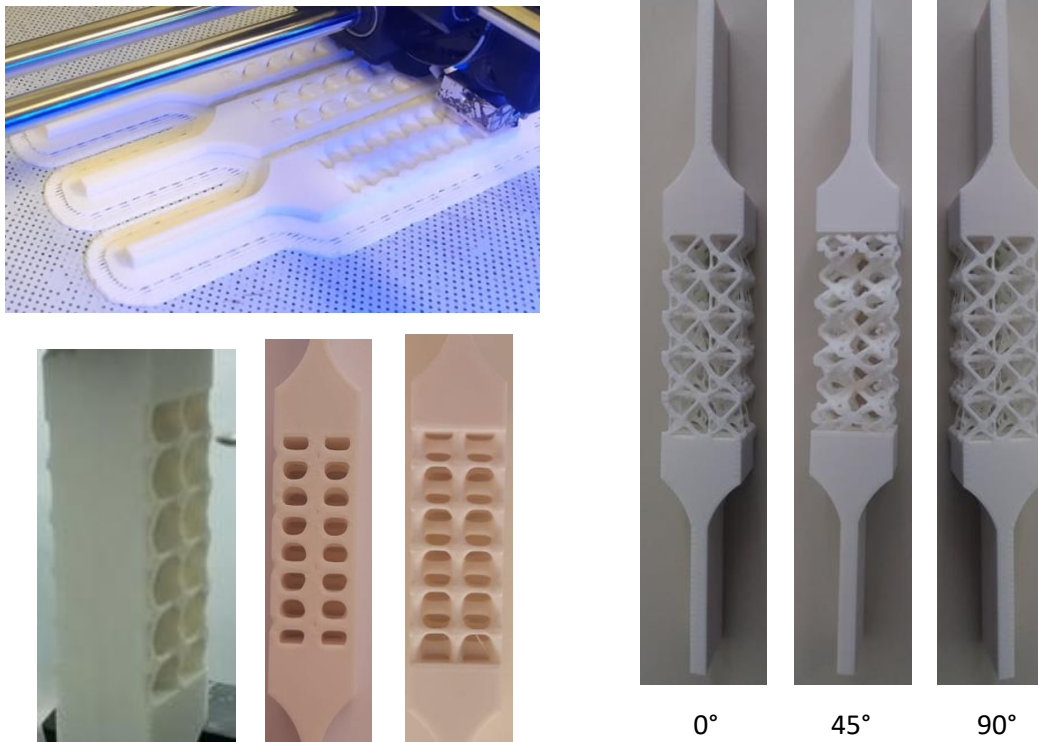
Figure 7.19 Preparation and printing of the tensile strength samples in different angles of 0°, 45° and 90°.

7.8 Experimental results

7.8.1 Compression test results

 As mentioned above, five specimens of each lattice structures were manufactured and tested in compression test. The speed of the moving platform was 6 m/min. From the compression test results of each set of five samples, the mean values of the maximum applied force were 3.613 N for lattice structure#1, and 361 N for lattice structure #2 (see figure 7.20). The behavior for each lattice is different, as the result of their different relative density amounts. The structure#1 relative density is four times larger ($\bar{\rho}$ = 0.4) than structure#2 ($\bar{\rho}$ = 0.1). As a result of this, structure#1 is much stiffer than structure#2.
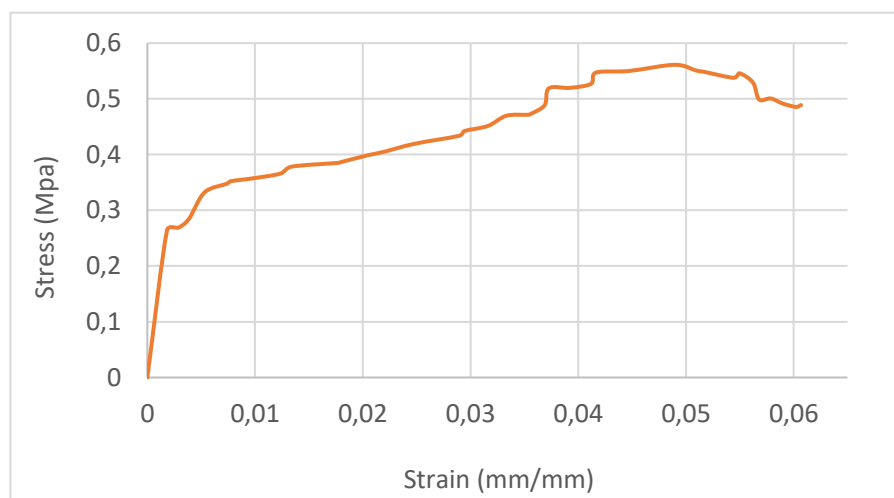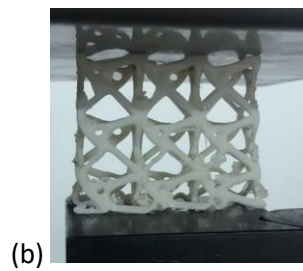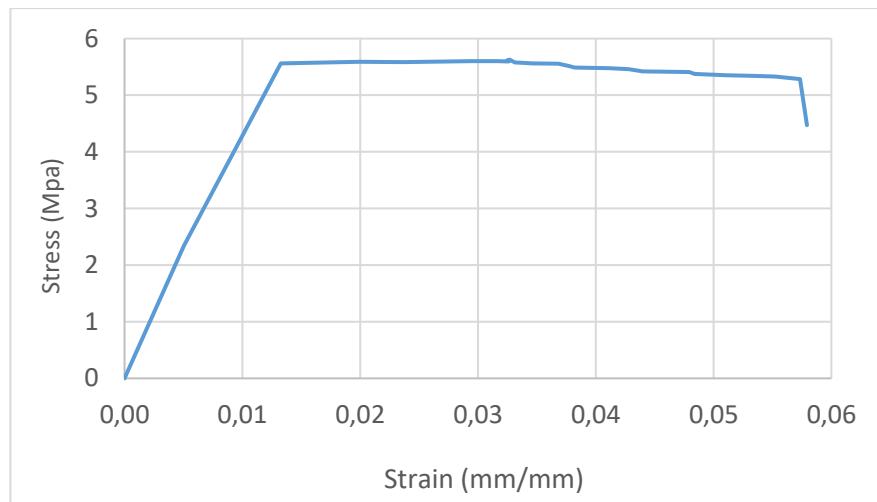
(a)

(b)
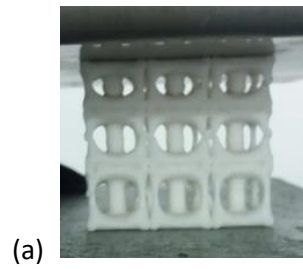
Figure 7.20 Specimens' behavior in compression test: (a) lattice structure #1 and (b) lattice structure #2.

7.8.2 Tensile strength test results

According to CAD models (see figure 7.18), the specimens are printed and tested with tensile strength test, using universal testing machines. Figures 7.21–7.22 show the results of the tensile strength tests for microstructure_1. The lattice structure #1 tensile strength force was at least 4500 N for all three specimens. The maximum tensile force for lattice #2 was 301 N, 75 N and 251 N for 0°, 45° and 90° cell mapping, respectively.

Figure 7.21 Samples behavior on the tensile strength test, and stress/strain curve of lattice structure #1 for 0°, 45° and 90° angles.

Figure 7.22 Strain at sB, Modulus of Elasticity, sB value and toughness of lattice structure #1 for different cell mapping angles.

According to the above results, it was observed that lattice #1 strength is higher than specimen's material yield point. In order to check the strength of lattice microstrure#1, smaller specimens are designed, fabricated and tested (see figures 7.23-7.24). The outer dimensions of the new specimens are presented in figure 7.23.
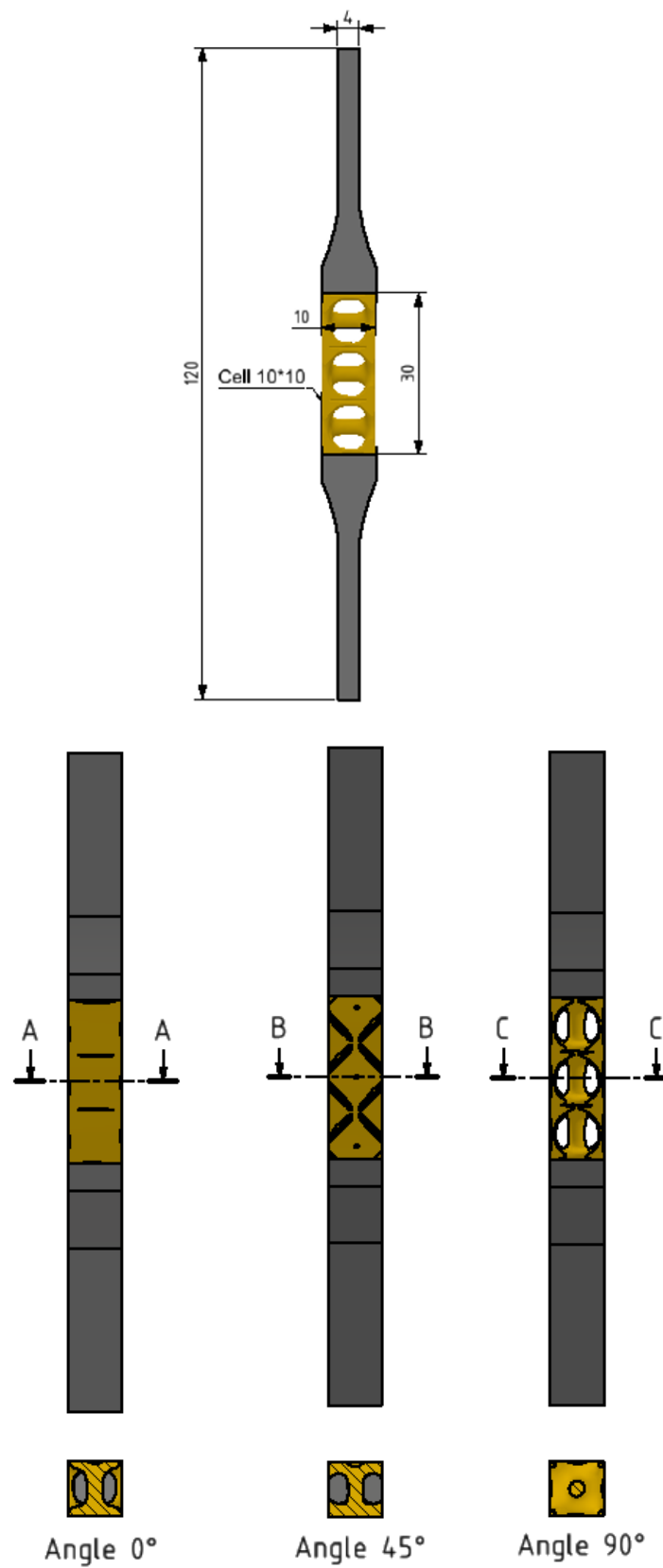
Figure 7.23 CAD models of the smaller tensile strength specimens of structure #1.

0°   45°   90°
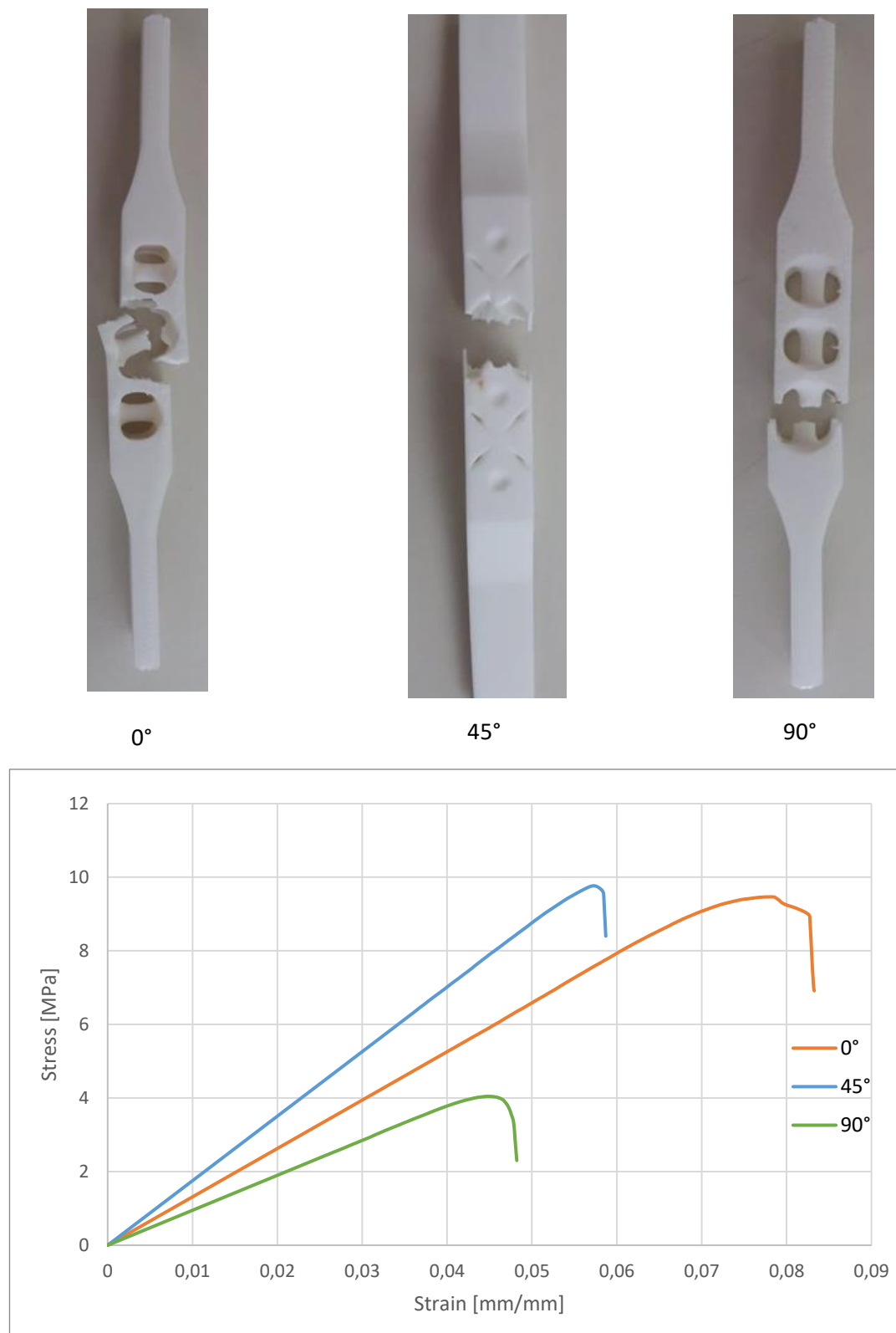
Figure 7.24 Specimens behavior on the tensile strength test, and stress/strain curve of the smaller lattice structure #1 of 0°, 45° and 90° angles.
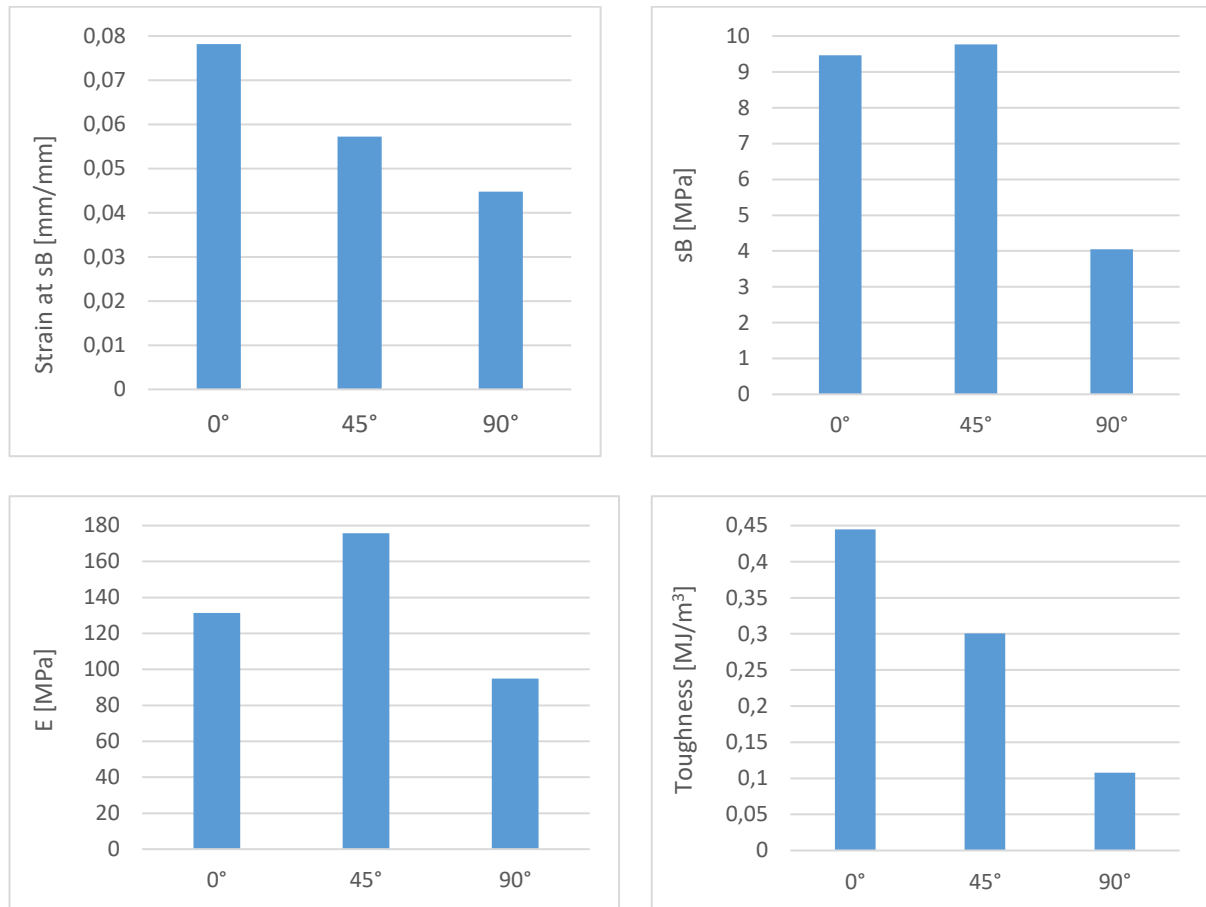
Figure 7.25 Strain at sB, Modulus of Elasticity, sB value and toughness of new smaller lattice structure #1 for 0°, 45° and 90° cell mapping angles.

From the aforementioned results (see figures 7.24-7.25), it was observed that, even though the lattice dimensions were limited, the strength is higher than the initial lattice structure. The strength values differ in each direction, so the results of homogenization study were approved. The results of tensile tests of microstructure_2 are presented bellow (see figures 7.26-7.27)
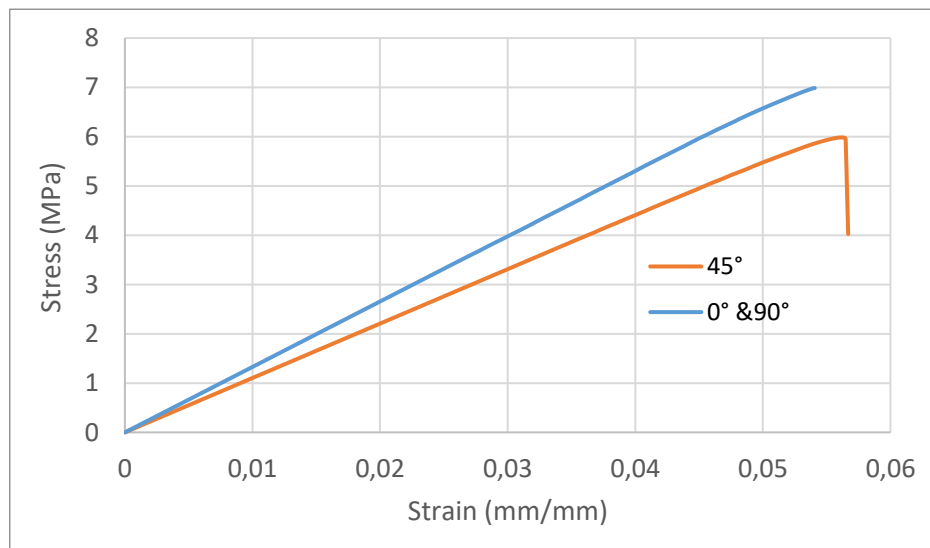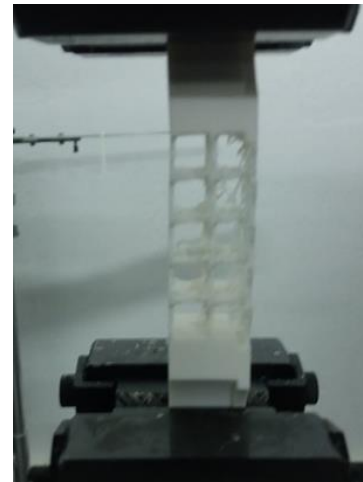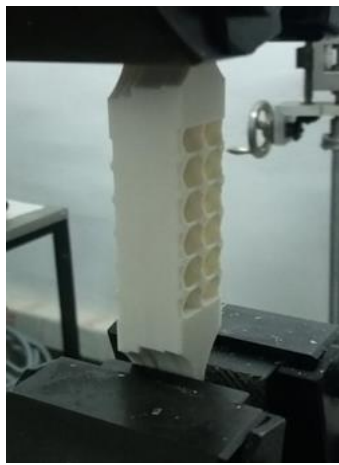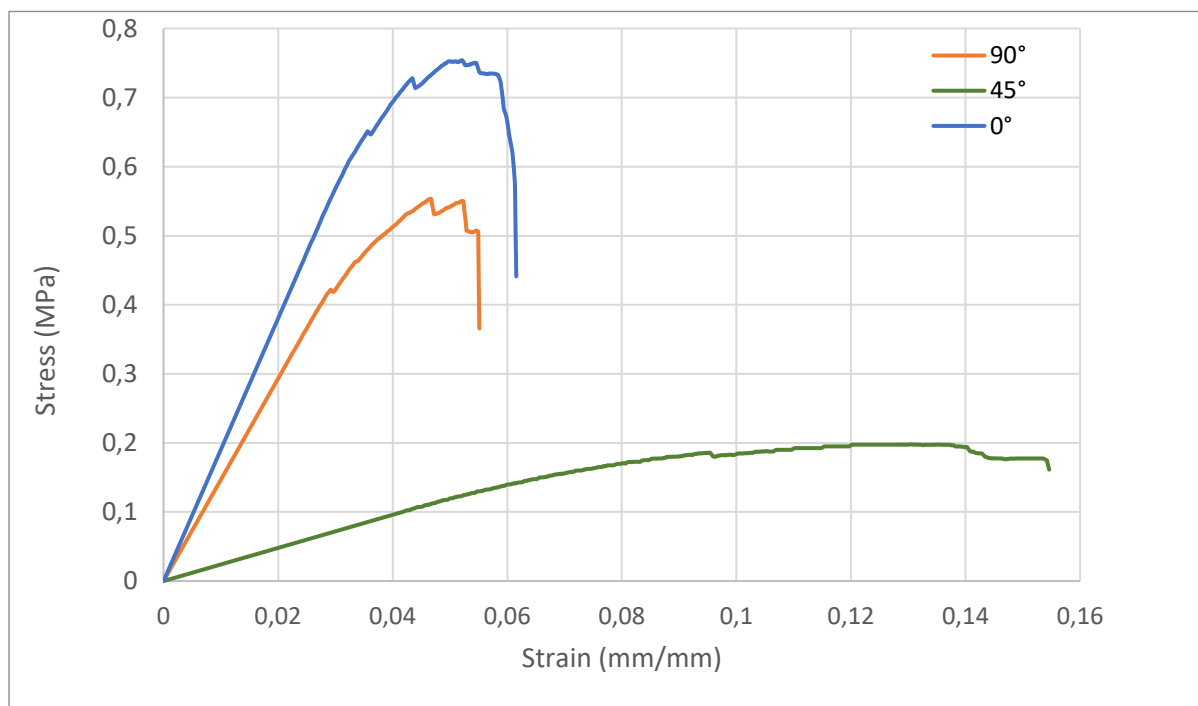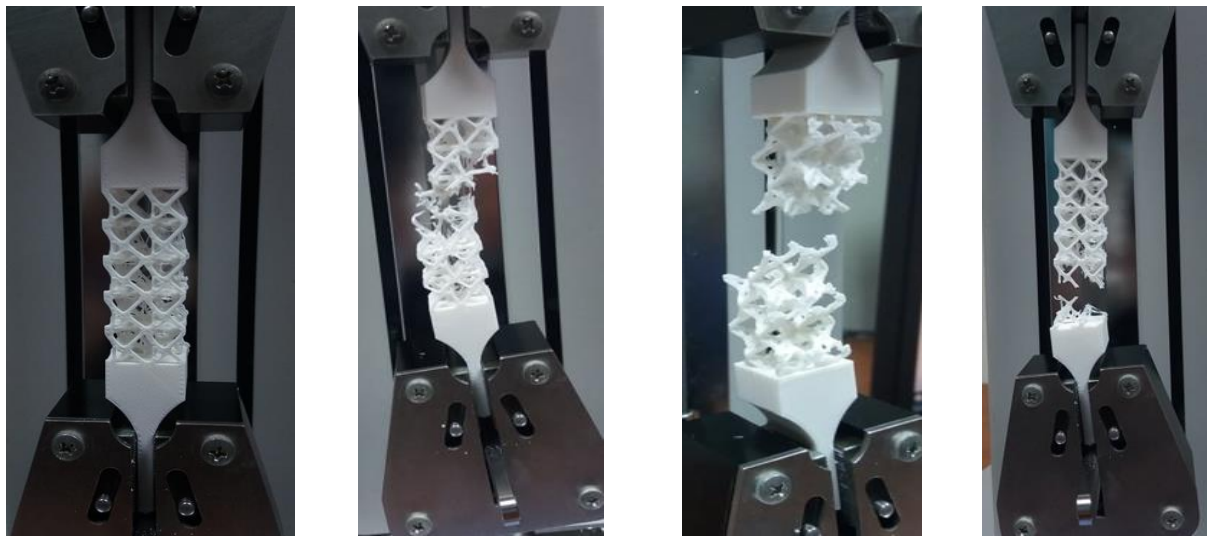
Figure 7.26 Samples behavior on the tensile strength test, and stress/strain curve of lattice structure #2 for 0°, 45° and 90° angles.
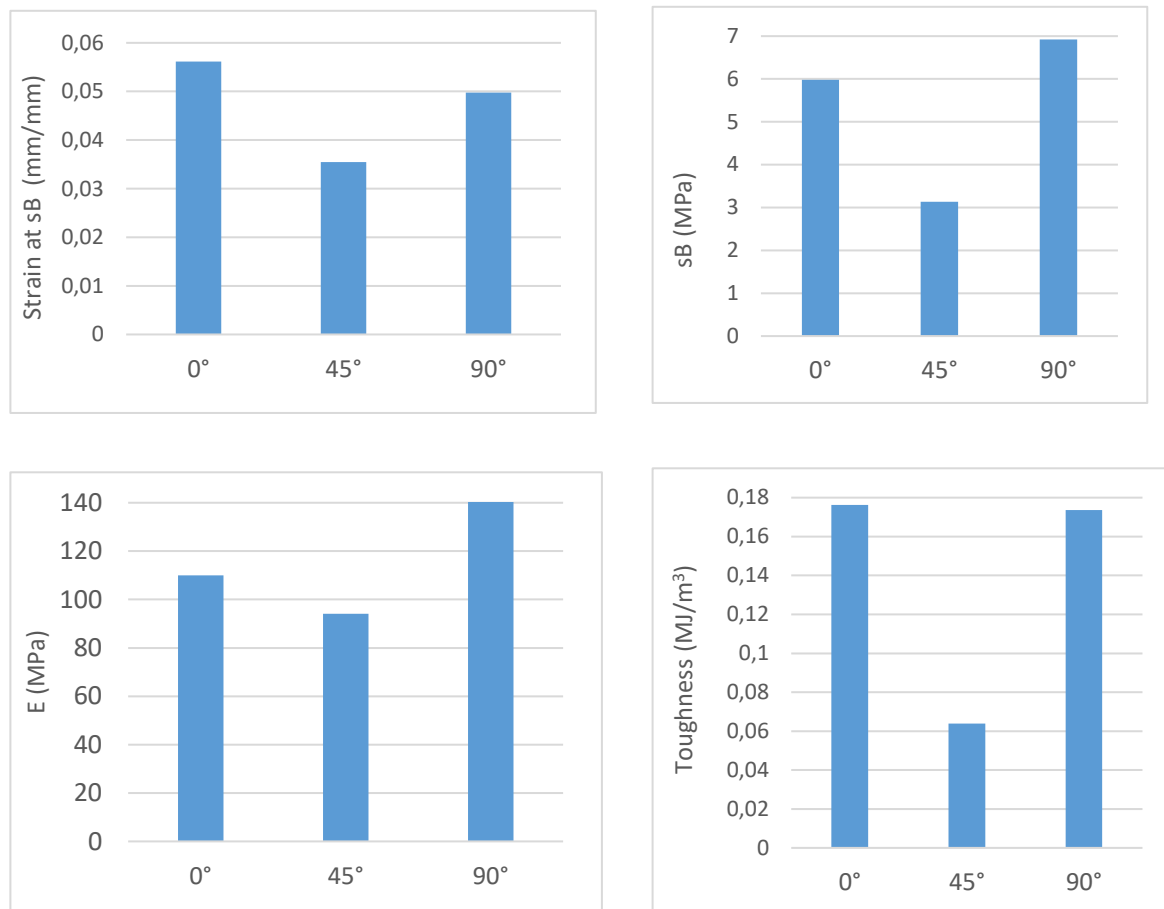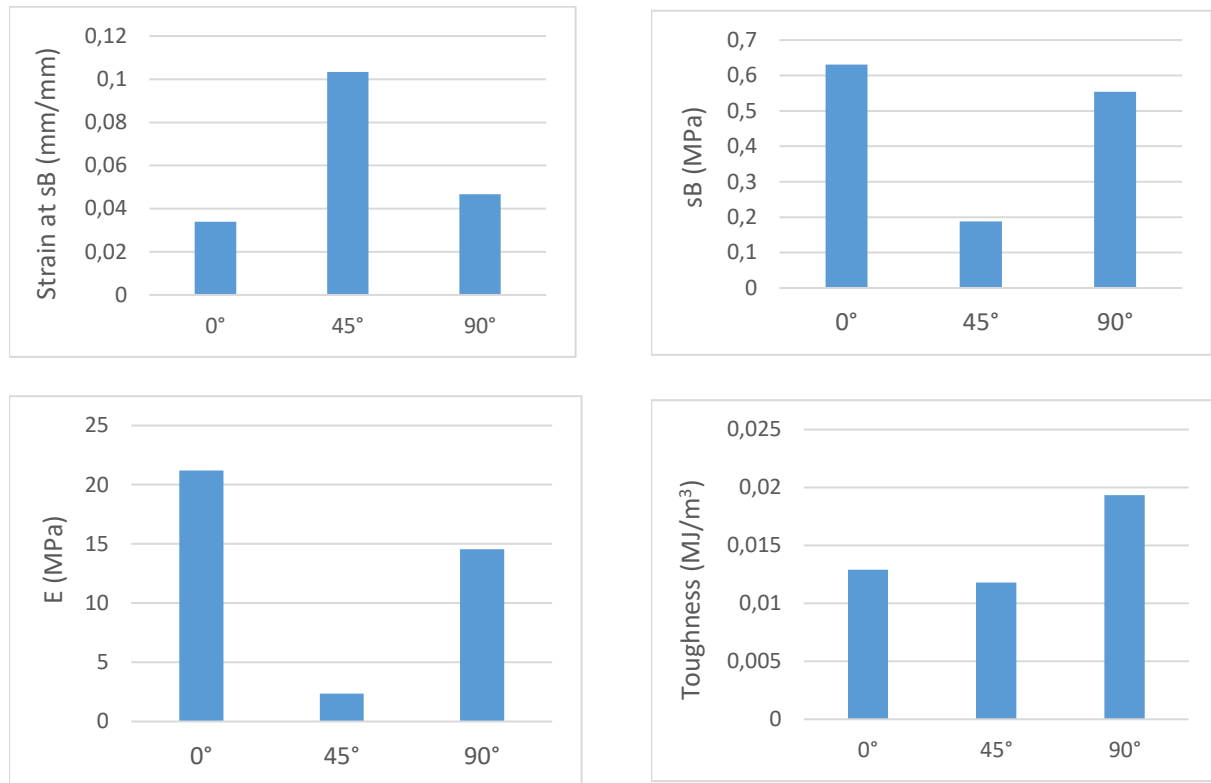
Figure 7.27 Strain at sB, Modulus of Elasticity, sB value and toughness of lattice structure #2 for different cell mapping angles.

From the compression test experimental results, the significant difference in the stress–strain curve was observed, and especially the appearance of elastic–plastic plateau and apparent strain behavior. Structure #1 has a significantly increased elastic strain behavior and better elastic stability up to the fracture point. The stress–strain plateau of structure #2 shows that the lattice inner bonds absorb the energy in a nonuniform way, as lattice #1 does.

In structure #1, the fracture starts from the top layer of the lattice, closer to the moving platform and then fails at the middle layer of lattices. The bottom layer of the structures seems to be unaffected during the test. On the other hand, the structure #2 failure point starts from the bottom row of the lattice, followed by a failure start of the middle row, the top row of the lattice being affected the last. This behavior was explained by the different shapes of the structures, which led to vertical stresses in structure #1 and to shearing stresses in structure #2.

Tensile strength tests help to evaluate and characterize the proposed lattice structures further. The structure #1 lattice is very stiff, and the yield strength is higher than the printing material durability. Therefore, it can be used as the infill in structures where a high durability is demanded; at the same time, the relative density of the proposed structure is 60% lighter than the solid infill. Lattice structure #2, being lighter

(relative density 0.1), is an appropriate infill for a lower stress demand structure with very efficient stress–strain behavior. The experimental results show that the mechanical behavior of the lattice structure changes significantly when the cell mapping angle differs (Ntintakis and Stavroulakis, 2022).

CHAPTER 8

Conclusion and Future work

8.1 Conclusions

Topology optimization and generative design are promising and well-developed tools for the design of consumer products or mechanical components. Additive Manufacturing is the appropriate fabrication method than can be coupled with TO & GD with excellent positive benefits for product design designers/engineers. The role of infill structure is critical for the utilization of AM in industrial production. The presented results indicate that the hybrid approach of topology optimization and homogenization leads to the design of advanced infill microstructures. In addition to the benefits of lightweight and strength structures, the presented iterative approach allows us to modify the resulting microstructure by introducing additional requirements, such as that which specifies that the microstructures will be isotropic.

Two new infill microstructures have been created by utilizing the SIMP method within the selected cubic volume. Using different boundary conditions, two new microstructures were created, as infill for additive manufacturing methods. The TO study has been executed in this thesis by taking into account two selected in-plane loadings.

The proposed microstructures were evaluated by taking into account the isotropy with the help of Zener's ratio and the modulus of elasticity. The strength of the homogenized microstructures has been evaluated as infill material in a cantilever model. For the homogenization study, a representative volume element has been checked for each microstructure. The comparative results from the homogenization study showed that both microstructures exhibit anisotropic behavior and an accepted response in the stress test similar to the one of the homogenized materials. The theoretical results of the homogenization study are compared with the experimental results. Also, the experimental results show that the mechanical behavior of the lattice structure changes significantly when the cell mapping angle differs.

8.2 Achievements of the Thesis

The proposed hybrid method can provide an applicable solution for the design of microstructures. Due to the nature of topology optimization algorithms, not all requirements can be introduced for the definition of the optimal structure. The proposed approach overcomes this defect by controlling for other characteristics of the optimized structures such as isotropy. The new proposed method compares well with experiments and can be used as a conceptual design tool.

8.3 Future Work

The present work can be extended in order to cover further loading cases, if needed, for every point of a loaded structure, enabling functionally graded lattice microstructures to be produced. This is possible within a multiscale analysis framework, provided that the technological restrictions of AM support it. In order to improve the computational results of the hybrid method, they can be enforced by utilizing Application Programming Interface (API) supported by Python script. The hybrid method can be extended to other topology optimization methods or other multi-objective optimization problems.

8.4 Publications

During the current study the following journals articles and conference papers were published:

Journals papers:

Ntintakis, I., Stavroulakis, G.E., 2022. Infill Microstructures for Additive Manufacturing. Appl. Sci. 12, 7386. https://doi.org/10.3390/app12157386

- Tairidis, G., Ntintakis, I., Drosopoulos, G., Koutsianitis, P., & Stavroulakis, G. (2022). Auxetic metamaterials subjected to dynamic loadings. Theoretical and Applied Mechanics.

- Ntintakis, I., Stavroulakis, G.E., Sfakianakis, G., Fiotodimitrakis, N. (2022). Utilizing Generative Design for Additive Manufacturing. In: Dave, H.K., Dixit, U.S., Nedelcu, D. (eds) Recent Advances in Manufacturing Processes and Systems. Lecture Notes in Mechanical Engineering. Springer, Singapore. https://doi.org/10.1007/978-981-16-7787-8_78

- Ntintakis, I., Stavroulakis, G. E., & Plakia, N. (2020). Topology optimization by the use of 3D printing technology in the product design process. HighTech and Innovation Journal, 1(4), 161-171.

Conference paper:

- Ntintakis, I., & Stavroulakis, G. E. (2020). Progress and recent trends in generative design. In MATEC web of conferences (Vol. 318, p. 01006). EDP Sciences.

- Ntintakis, I.; Stavroulakis, G.E.; Plakia, N. The perspective of topology optimization on 3d printed furniture prototypes. A: Sim-AM 2019. "Sim-AM 2019 : II International Conference on Simulation for Additive Manufacturing". CIMNE, 2019, p. 225-236. ISBN 978-84-949194-8-0.

Bibliography

Alexander, C., 1971. The state of the art in design methods. DMG Newsl. 5, 3–7.

Alomarah, A., Xu, S., Masood, S.H., Ruan, D., 2020. Dynamic performance of auxetic structures: experiments and simulation. Smart Mater. Struct. 29, 055031.

Babalis, A., Ntintakis, I., Chaidas, D., Makris, A., 2013. Design and Development of Innovative Packaging for Agricultural Products. Procedia Technol. 8, 575–579. https://doi.org/10.1016/j.protcy.2013.11.082

Bean, P., Lopez-Anido, R.A., Vel, S., 2022. Numerical Modeling and Experimental Investigation of Effective Elastic Properties of the 3D Printed Gyroid Infill. Appl. Sci. 12, 2180. https://doi.org/10.3390/app12042180

Bendsøe, M.P., 1989. Optimal shape design as a material distribution problem. Struct. Optim. 1, 193–202. https://doi.org/10.1007/BF01650949

Bendsøe, M.P., Sigmund, O., 2004. Topology optimization by distribution of isotropic material, in: Topology Optimization. Springer Berlin Heidelberg, Berlin, Heidelberg, pp. 1–69. https://doi.org/10.1007/978-3-662-05086-6_1

Bikas, H., Stavropoulos, P., Chryssolouris, G., 2016. Additive manufacturing methods and modelling approaches: a critical review. Int. J. Adv. Manuf. Technol. 83, 389–405.

Bohnacker, H., Gross, B., Laub, J., Lazzeroni, C., 2012. Generative design: visualize, program, and create with processing. Princeton Architectural Press.

Bose, S., Bandyopadhyay, A., 2019. Additive Manufacturing, in: Bandyopadhyay, A., Bose, S. (Eds.), Additive Manufacturing. CRC Press, pp. 451–461. https://doi.org/10.1201/9780429466236-15

Buonamici, F., Carfagni, M., Furferi, R., Volpe, Y., Governi, L., 2020. Generative design: an explorative study. Comput.-Aided Des. Appl. 18, 144–155.

Caldas, L., Duarte, J., 2004. Implementational issues in generative design systems, in: First International Conference on Design Computing and Cognition.

Chase, S.C., 2005. Generative design tools for novice designers: Issues for selection. Autom. Constr. 14, 689–698.

Chatzigeorgiou, G., Meraghni, F., Charalambakis, N. (Eds.), 2022. About the authors, in: Multiscale Modeling Approaches for Composites. Elsevier, p. xi. https://doi.org/10.1016/B978-0-12-823143-2.00005-9

Checkland, P., 1981. Systems thinking, systems practice John Wiley & Sons. N. Y.

Clausen, A., Wang, F., Jensen, J.S., Sigmund, O., Lewis, J.A., 2015. Topology optimized architectures with programmable Poisson's ratio over large deformations. Adv Mater 27, 5523–5527.

Dae SeungKang, S.C., n.d. Two nature-mimicking auxetic materials with potential for high energy absorption.

Drosopoulos, G.A., Stavroulakis, G.E., 2022. Nonlinear mechanics for composite heterogeneous structures. Routledge, Abingdon, Oxon ; New York, NY.

Eiben, A.E., Hinterding, R., Michalewicz, Z., 1999. Parameter control in evolutionary algorithms. IEEE Trans. Evol. Comput. 3, 124–141. https://doi.org/10.1109/4235.771166

Eschenauer, H.A., Olhoff, N., 2001. Topology optimization of continuum structures: A review*. Appl. Mech. Rev. 54, 331–390. https://doi.org/10.1115/1.1388075

Evans, K. E., 1991. The design of doubly curved sandwich panels with honeycomb cores. Compos. Struct. 17, 95–111. https://doi.org/10.1016/0263-8223(91)90064-6

Evans, Ken E, 1991. Auxetic polymers: a new range of materials. Endeavour 15, 170–174. https://doi.org/10.1016/0160-9327(91)90123-S

Evans, K.E., 1990. Tailoring the negative Poisson's ratio. Chem. Ind. 20, 654.

Feng, J., Jianzhong, F., Lin, Z., Shang, C., Niu, X., 2018. Layered infill area generation from triply periodic minimal surfaces for additive manufacturing. Comput.-Aided Des. 107. https://doi.org/10.1016/j.cad.2018.09.005

Gabriele Imbalzano, S.L., Tuan Duc Ngo, Peter Vee Sin Lee, Phuong Tran, n.d. Blast resistance of auxetic and honeycomb sandwich panels: Comparisons and parametric designs.

Ganesh Rajkumar, N., Adam Khan, M., Rajesh, S., Faris, W.F., 2021. Design optimization of office chair star base leg using product LCM and anisotropic material properties from injection moulding simulation. Mater. Today Proc. 45, 1087–1093. https://doi.org/10.1016/j.matpr.2020.03.187

Gebisa, A.W., Lemu, H.G., 2017. A case study on topology optimized design for additive manufacturing. IOP Conf. Ser. Mater. Sci. Eng. 276, 012026. https://doi.org/10.1088/1757-899X/276/1/012026

Ghazlan, A., Nguyen, T., Ngo, T., Linforth, S., Le, V.T., 2020. Performance of a 3D printed cellular structure inspired by bone. Thin-Walled Struct. 151, 106713. https://doi.org/10.1016/j.tws.2020.106713

Gibson, L.J., Ashby, M.F., 1997. Cellular Solids: Structure and Properties, 2nd ed. Cambridge University Press. https://doi.org/10.1017/CBO9781139878326

Gong, C., Bai, Z., Lv, J., Zhang, L., 2020. Crashworthiness analysis of bionic thin-walled tubes inspired by the evolution laws of plant stems. Thin-Walled Struct. 157, 107081. https://doi.org/10.1016/j.tws.2020.107081

Gutman, R. (Ed.), 2017. People and Buildings, First edition. ed. Taylor and Francis, London.

Hajare, D.M., Gajbhiye, T.S., 2022. Additive manufacturing (3D printing): Recent progress on advancement of materials and challenges. Mater. Today Proc.

Haslinger, J., Mäkinen, R.A.E., 2003. Introduction to shape optimization: theory, approximation, and computation, Advances in design and control. SIAM, Society for Industrial and Applied Mathematics, Philadelphia.

Hillier, B., Leaman, A., 1974. How is design possible? J. Archit. Res. 4–11.

Hitesh D Vora and Young Chang, C.Y., n.d. Behavior of auxetic structures under compression and impact forces.

Hoang, V.-N., Tran, P., Nguyen, N.-L., Hackl, K., Nguyen-Xuan, H., 2020. Adaptive Concurrent Topology Optimization of Coated Structures with Nonperiodic Infill for Additive Manufacturing. Comput.-Aided Des. 129, 102918. https://doi.org/10.1016/j.cad.2020.102918

Imbalzano, G., Tran, P., Ngo, T.D., Lee, P.V., 2017. Three-dimensional modelling of auxetic sandwich panels for localised impact resistance. J. Sandw. Struct. Mater. 19, 291–316.

Imbalzano, G., Tran, P., Ngo, T.D., Lee, P.V., 2016. A numerical study of auxetic composite panels under blast loadings. Compos. Struct. 135, 339–352.

Jauhar, S., Asthankar, K.M., Kuthe, A.M., 2012. Cost benefit analysis of rapid manufacturing in automotive industries. Adv. Mech. Eng. Its Appl. AMEA 2, 181–188.

Jiang, J., Ma, Y., 2020. Path Planning Strategies to Optimize Accuracy, Quality, Build Time and Material Use in Additive Manufacturing: A Review. Micromachines 11, 633. https://doi.org/10.3390/mi11070633

Jiang, J., Xu, X., Stringer, J., 2018. Support Structures for Additive Manufacturing: A Review. J. Manuf. Mater. Process. 2, 64. https://doi.org/10.3390/jmmp2040064

Kaminakis, N.T., Drosopoulos, G.A., Stavroulakis, G.E., 2015. Design and verification of auxetic microstructures using topology optimization and homogenization. Arch. Appl. Mech. 85, 1289–1306. https://doi.org/10.1007/s00419-014-0970-7

Kaminakis, N.T., Stavroulakis, G.E., 2012. Topology optimization for compliant mechanisms, using evolutionary-hybrid algorithms and application to the design of auxetic materials. Compos. Part B Eng. 43, 2655–2668. https://doi.org/10.1016/j.compositesb.2012.03.018

Kazi, R.H., Grossman, T., Cheong, H., Hashemi, A., Fitzmaurice, G.W., 2017. DreamSketch: Early Stage 3D Design Explorations with Sketching and Generative Design., in: UIST. pp. 401–414.

Kechagias, J., Stavropoulos, P., Koutsomichalis, A., Ntintakis, I., Vaxevanidis, N., 2014. Dimensional accuracy optimization of prototypes produced by PolyJet direct 3D printing technology. Adv Eng Mech Mater 61–65.

Khan, S., Awan, M.J., 2018. A generative design technique for exploring shape variations. Adv. Eng. Inform. 38, 712–724. https://doi.org/10.1016/j.aei.2018.10.005

Krish, S., 2011. A practical generative design method. Comput.-Aided Des. 43, 88–100.

Lakes, R., 1987. Foam structures with a negative Poisson's ratio. Science 235, 1038–1040.

Lee, J., Kwon, C., Yoo, J., Min, S., Nomura, T., Dede, E.M., 2021. Design of spatially-varying orthotropic infill structures using multiscale topology optimization and explicit de-homogenization. Addit. Manuf. 40, 101920. https://doi.org/10.1016/j.addma.2021.101920

Li, X., Ashraf, M., Li, H., Zheng, X., Wang, H., Al-Deen, S., Hazell, P.J., 2019. An experimental investigation on Parallel Bamboo Strand Lumber specimens under quasi static and impact loading. Constr. Build. Mater. 228, 116724. https://doi.org/10.1016/j.conbuildmat.2019.116724

Liu, J., Gaynor, A., Chen, S., Kang, Z., Suresh, K., Takezawa, A., Li, L., Kato, J., Tang, J., Wang, C., Cheng, L., Liang, X., To, A., 2018. Current and future trends in topology optimization for additive manufacturing. Struct. Multidiscip. Optim. 57. https://doi.org/10.1007/s00158-018-1994-3

Madke, R.R., Chowdhury, R., 2020. Anti-impact behavior of auxetic sandwich structure with braided face sheets and 3D re-entrant cores. Compos. Struct. 236, 111838.

McKnight, M., 2017. Generative Design: What it is? How is it being used? Why it's a game changer. KnE Eng. 2, 176. https://doi.org/10.18502/keg.v2i2.612

Ntintakis, I., Stavroulakis, G.E., 2022. Infill Microstructures for Additive Manufacturing. Appl. Sci. 12, 7386. https://doi.org/10.3390/app12157386

Ntintakis, I., Stavroulakis, G.E., 2020. Progress and recent trends in generative design. MATEC Web Conf. 318, 01006. https://doi.org/10.1051/matecconf/202031801006

Ntintakis, I., Stavroulakis, G.E., Plakia, N., 2020. Topology Optimization by the use of 3D Printing Technology in the Product Design Process. HighTech Innov. J. 1, 161–171. https://doi.org/10.28991/HIJ-2020-01-04-03

Ntintakis, I., Stavroulakis, G.E., Sfakianakis, G., Fiotodimitrakis, N., 2022. Utilizing Generative Design for Additive Manufacturing, in: Dave, H.K., Dixit, U.S., Nedelcu, D. (Eds.), Recent Advances in Manufacturing Processes and Systems, Lecture Notes in Mechanical Engineering. Springer, Singapore, pp. 977–989. https://doi.org/10.1007/978-981-16-7787-8_78

Oh, S., Jung, Y., Kim, S., Lee, I., Kang, N., 2019. Deep Generative Design: Integration of Topology Optimization and Generative Models. J. Mech. Des. 141, 111405. https://doi.org/10.1115/1.4044229

Osher, S., Sethian, J.A., 1988. Fronts propagating with curvature-dependent speed: Algorithms based on Hamilton-Jacobi formulations. J. Comput. Phys. 79, 12–49. https://doi.org/10.1016/0021-9991(88)90002-2

Perez, R.E., Behdinan, K., 2007. Particle swarm approach for structural design optimization. Comput. Struct. 85, 1579–1588. https://doi.org/10.1016/j.compstruc.2006.10.013

Plocher, J., Panesar, A., 2019. Review on design and structural optimisation in additive manufacturing: Towards next-generation lightweight structures. Mater. Des. 183, 108164. https://doi.org/10.1016/j.matdes.2019.108164

Podroužek, J., Marcon, M., Ninčević, K., Wan-Wendner, R., 2019. Bio-Inspired 3D Infill Patterns for Additive Manufacturing and Structural Applications. Materials 12, 499. https://doi.org/10.3390/ma12030499

Querin, O.M., 2017. Topology design methods for structural optimization. Academic Press, London, United Kingdom.

Rao, S.S., 1996. Engineering optimization: theory and practice. Wiley, New York.

Rehme, O., Emmelmann, C., 2006. Rapid manufacturing of lattice structures with selective laser melting, in: Bachmann, F.G., Hoving, W., Lu, Y., Washio, K. (Eds.), . Presented at the Lasers and Applications in Science and Engineering, San Jose, CA, p. 61070K. https://doi.org/10.1117/12.645848

Rozvany, G.I.N., 2009. A critical review of established methods of structural topology optimization. Struct. Multidiscip. Optim. 37, 217–237. https://doi.org/10.1007/s00158-007-0217-0

Rozvany, G.I.N., Bendsoe, M.P., Kirsch, U., 1995. Layout Optimization of Structures. Appl. Mech. Rev. 48, 41–119. https://doi.org/10.1115/1.3005097

Sauerwein, M., Doubrovski, E., Balkenende, R., Bakker, C., 2019. Exploring the potential of additive manufacturing for product design in a circular economy. J. Clean. Prod. 226, 1138–1149. https://doi.org/10.1016/j.jclepro.2019.04.108

Seharing, A., Azman, A.H., Abdullah, S., 2020. A review on integration of lightweight gradient lattice structures in additive manufacturing parts. Adv. Mech. Eng. 12, 1687814020916951. https://doi.org/10.1177/1687814020916951

Shea, K., Aish, R., Gourtovaia, M., 2005. Towards integrated performance-driven generative design tools. Autom. Constr. 14, 253–264. https://doi.org/10.1016/j.autcon.2004.07.002

Sigmund, O., Maute, K., 2013. Topology optimization approaches. Struct. Multidiscip. Optim. 48, 1031–1055. https://doi.org/10.1007/s00158-013-0978-6

Sokół, T., Rozvany, G.I.N., 2013. Exact truss topology optimization for external loads and friction forces. Struct. Multidiscip. Optim. 48, 853–857. https://doi.org/10.1007/s00158-013-0984-8

Somnic, J., Jo, B.W., 2022a. Status and Challenges in Homogenization Methods for Lattice Materials. Materials 15, 605. https://doi.org/10.3390/ma15020605

Somnic, J., Jo, B.W., 2022b. Status and Challenges in Homogenization Methods for Lattice Materials. Materials 15, 605. https://doi.org/10.3390/ma15020605

Stava, O., Vanek, J., Benes, B., Carr, N., Měch, R., 2012. Stress relief: improving structural strength of 3D printable objects. ACM Trans. Graph. 31, 1–11. https://doi.org/10.1145/2185520.2185544

Stavroulakis, G.E., 2005. Auxetic behaviour: appearance and engineering applications. Phys. Status Solidi B 242, 710–720. https://doi.org/10.1002/pssb.200460388

Stavroulakis, G.E., Kaminakis, N., Marinakis, Y., Marinaki, M., 2009. Multiobjective global topology optimization for structures and mechanisms, in: SEECCM, 2nd South-East European Conference on Computational Mechanics, M. Papadrakakis, M. Kojic, V. Papadopoulos (Eds.), Rhodes, Greece. pp. 22–24.

Stavroulakis, G.E., Kaminakis, N., Marinakis, Y., Marinaki, M., Skaros, N., 2008. Optimal structural and mechanism design using topology optimization, in: Proc. of the Int. Conference on Modelling and Simulation (MS 08 Jordan), Petra. pp. 101–105.

Suárez, A., Veiga, F., Bhujangrao, T., Aldalur, E., 2022. Study of the Mechanical Behavior of Topologically Optimized Arc Wire Direct Energy Deposition

Aerospace Fixtures. J. Mater. Eng. Perform. https://doi.org/10.1007/s11665-022-06702-x

Suwanprateeb, J., Sanngam, R., Panyathanmaporn, T., 2010. Influence of raw powder preparation routes on properties of hydroxyapatite fabricated by 3D printing technique. Mater. Sci. Eng. C 30, 610–617.

Tairidis, G., Ntintakis, I., Drosopoulos, G., Koutsianitis, P., Stavroulakis, G., 2022. Auxetic metamaterials subjected to dynamic loadings. Theor. Appl. Mech. 49, 1–14. https://doi.org/10.2298/TAM211103002T

Tancogne-Dejean, T., Diamantopoulou, M., Gorji, M.B., Bonatti, C., Mohr, D., 2018. 3D Plate-Lattices: An Emerging Class of Low-Density Metamaterial Exhibiting Optimal Isotropic Stiffness. Adv. Mater. 30, 1803334. https://doi.org/10.1002/adma.201803334

Tang, Y., Kurtz, A., Zhao, Y.F., 2015. Bidirectional Evolutionary Structural Optimization (BESO) based design method for lattice structure to be fabricated by additive manufacturing. Comput.-Aided Des. 69, 91–101. https://doi.org/10.1016/j.cad.2015.06.001

Theocaris, P.S., Stavroulakis, G.E., Panagiotopoulos, P.D., 1997. Negative Poisson's ratios in composites with star-shaped inclusions: a numerical homogenization approach. Arch. Appl. Mech. 67, 274–286. https://doi.org/10.1007/s004190050117

Tomlin, M., Meyer, J., 2011. Topology optimization of an additive layer manufactured (ALM) aerospace part, in: Proceeding of the 7th Altair CAE Technology Conference. pp. 1–9.

Tsavdaridis, K.D., Kingman, J.J., Toropov, V.V., 2015. Application of structural topology optimisation to perforated steel beams. Comput. Struct. 158, 108–123.

Tucker, B.M., Meikle, J.L., 1982. Twentieth Century Limited: Industrial Design in America, 1925-1939. Technol. Cult. 23, 680. https://doi.org/10.2307/3104838

Umetani, N., Igarashi, T., Mitra, N.J., 2012. Guided exploration of physically valid shapes for furniture design. ACM Trans. Graph. 31, 1–11. https://doi.org/10.1145/2185520.2185582

Vaneker, T., Bernard, A., Moroni, G., Gibson, I., Zhang, Y., 2020. Design for additive manufacturing: Framework and methodology. CIRP Ann. 69, 578–599.

Varotsis, A.B., 2018. Introduction to binder jetting 3D printing. Hämtad Från Httpswww 3dhubs Comknowledge-Baseintroduction-Bind.-Jet.-3d-Print. Hämtad 2019-05-16.

Veiga, F., Suárez, A., Aldalur, E., Goenaga, I., Amondarain, J., 2021. Wire Arc Additive Manufacturing Process for Topologically Optimized Aeronautical Fixtures. 3D Print. Addit. Manuf. https://doi.org/10.1089/3dp.2021.0008

Wan, H., Ohtaki, H., Kotosaka, S., Hu, G., 2004. A study of negative Poisson's ratios in auxetic honeycombs based on a large deflection model. Eur. J. Mech. - ASolids 23, 95–106. https://doi.org/10.1016/j.euromechsol.2003.10.006

Wang, M.Y., Wang, X., Guo, D., 2003. A level set method for structural topology optimization. Comput. Methods Appl. Mech. Eng. 192, 227–246. https://doi.org/10.1016/S0045-7825(02)00559-5

Wiberg, A., Persson, J., Ölvander, J., 2019. Design for additive manufacturing – a review of available design methods and software. Rapid Prototyp. J. 25, 1080–1094. https://doi.org/10.1108/RPJ-10-2018-0262

Wong, K.V., Hernandez, A., 2012. A Review of Additive Manufacturing. ISRN Mech. Eng. 2012, 1–10. https://doi.org/10.5402/2012/208760

Wu, J., Wang, C.C.L., Zhang, X., Westermann, R., 2016. Self-supporting rhombic infill structures for additive manufacturing. Comput.-Aided Des. 80, 32–42. https://doi.org/10.1016/j.cad.2016.07.006

Wu, W., Hu, W., Qian, G., Liao, H., Xu, X., Berto, F., 2019. Mechanical design and multifunctional applications of chiral mechanical metamaterials: A review. Mater. Des. 180, 107950.

Zapf, H., Bendig, N., Möller, M., Emmelmann, C., 2017. Design recommendations for laser metal deposition of thin wall structures in Ti–Al6–V4, in: LiM-Lasers in Manufacturing Conference, München.

Zener, C.M., Siegel, S., 1949. Elasticity and Anelasticity of Metals. J. Phys. Colloid Chem. 53, 1468–1468. https://doi.org/10.1021/j150474a017

Zhang, Y., Jarosinski, W., Jung, Y.-G., Zhang, J., 2018. Additive manufacturing processes and equipment, in: Additive Manufacturing. Elsevier, pp. 39–51. https://doi.org/10.1016/B978-0-12-812155-9.00002-5

Zhu, J., Zhou, H., Wang, C., Zhou, L., Yuan, S., Zhang, W., 2021. A review of topology optimization for additive manufacturing: Status and challenges. Chin. J. Aeronaut. 34, 91–110. https://doi.org/10.1016/j.cja.2020.09.020